Bell Aerospace Company DIVISION OF textron

POST OFFICE BOX 1 BUFFALO, NEW YORK 14240

SUBMARINE PARAMETER IDENTIFICATION

by

G.L. Perreault, T.L. Roess, F.D. Powell

Report No. 9500-920237
June 1972

This Research was Carried Out Under the
Naval Ship Systems Command
General Hydromechanics Research Program
Subproject SR 009-01-01
Administered by the Naval Ship Research and Development Center, via
Office of Naval Research
Contract Number N00014-71-C-0162

UNCLASSIFIED
Security Classification

DOCUMENT CONTROL DATA - R & D

(Security classification of title, body of abstract and indexing annotation must be entered when the overall report is classified)

1. ORIGINATING ACTIVITY (Corporate author)	2a. REPORT SECURITY CLASSIFICATION
Bell Aerospace Corporation P.O. Box 1, Buffalo, N.Y. 14240	Unclassified 2b. GROUP –

3. REPORT TITLE

Submarine Parameter Identification

4. DESCRIPTIVE NOTES (Type of report and inclusive dates)

Final Report, Jan. 1971, June 1972

5. AUTHOR(S) (First name, middle initial, last name)

Gerald L. Perrault, Theodore L. Roess, Frederic D. Powell

6. REPORT DATE	7a. TOTAL NO. OF PAGES	7b. NO. OF REFS
June 1972	117	6

8a. CONTRACT OR GRANT NO.	9a. ORIGINATOR'S REPORT NUMBER(S)
N00014-71-C-0162 b. PROJECT NO. SR 009-01-01 c. d.	BAC 9500-920237 9b. OTHER REPORT NO(S) (Any other numbers that may be assigned this report) –

10. DISTRIBUTION STATEMENT

Approved for Public Release;
Distribution Unlimited

11. SUPPLEMENTARY NOTES	12. SPONSORING MILITARY ACTIVITY
–	Naval Ship Research and Development Center (1505) Bethesda, Maryland 20034

13. ABSTRACT

Research was conducted to determine the feasibility of adaptively identifying the values of the hydrodynamic parameters of a submarine or model from submerged free-flight trajectory data. The modified Kalman filter approach which was used was based on the equation-error parameter identification principle instead of the more conventional response error method, resulting in a relatively modest computational requirement. If the controls are driven by appropriate pseudo-random noise sequences, it is possible to determine almost all the parameters to good accuracy from a five minute trajectory sample which is contaminated by realistic additive noise plus bias. Several configurations of suitable instruments for measuring the trajectory are described and the algorithms for processing the trajectory data are discussed.

DD FORM 1 NOV 65 1473

UNCLASSIFIED
Security Classification

Bell Aerospace Company DIVISION OF textron

POST OFFICE BOX 1 BUFFALO, NEW YORK 14240

SUBMARINE PARAMETER IDENTIFICATION

by

G.L. Perreault, T.L. Roess, F.D. Powell

Report No. 9500-920237

June 1972

This Research was Carried Out Under the
Naval Ship Systems Command
General Hydromechanics Research Program
Subproject SR 009-01-01
Administered by the Naval Ship Research and Development Center, via
Office of Naval Research
Contract Number N00014-71-C-0162

CONTENTS

ILLUSTRATIONS

TABLES

ABSTRACT

Research was conducted to determine the feasibility of adaptively identifying the values of the hydrodynamic parameters of a submarine or model from submerged free-flight trajectory data. The extended Kalman filter approach which was used was based on the equation-error parameter identification principle instead of the more conventional response error method, resulting in a relatively modest computational requirement. If the controls are driven by appropriate pseudo-random noise sequences, it is possible to determine almost all the parameters to good accuracy from a five minute trajectory sample which is contaminated by realistic additive noise plus bias. Several configurations of suitable instruments for measuring the trajectory are described and the algorithms for processing the trajectory data are discussed.

I. INTRODUCTION

PURPOSE AND SCOPE

The purpose and scope of this research effort may be briefly defined:

Purpose: Immediate

To demonstrate the feasibility of identifying the values of the hydrodynamic parameters of a submarine or model from free-flight data.

Ultimate

To construct and provide to the U.S. Navy an instrumentation package and a data-processing method which are capable of identifying submarine or model parameters in an operational environment.

Scope: The scope of the research reported herein was limited to the immediate purpose, noted above. The research consisted, broadly, of:

a. analytical study to adapt to this purpose the parameter-identifying procedures which we had developed,

b. to evaluate their performance by digital simulation, and

c. to indicate configurations of instruments which could provide the essential input signals.

BACKGROUND

The system parameters identification problem has been treated by many researchers over the years from various points of view. The work of Kalman[2] has sparked a revolution in the development of solutions for state estimation problems. In this report the theory is extended to parameter identification in a manner that is inverted from standard applications. Generally the equations of motion form the process upon which measurements are made. The technique advanced here interprets the equation of motion as the measurements, and the error structure of the true measurements as the process; this method is related to the Equation-Error Adaptive Identification technique.

One of the more significant elements of this program was, in a sense, completed before the study began. This was the decision that the identification method should be based on the equation error rather than the response error adaptive parameter identifier technique. The motivation for this choice is outlined. The equation-error method permits decoupling of each of the six equations of motion from the others; the response error method, related to conventional Kalman filters, does not. This fact enables the equation error identifier to be far simpler in its computational complexity. We briefly consider the relative complexity of the two systems. Neglect in each case the problems of noise and bias in the instruments, and assume that all signals may be measured.

Each of the six coupled nonlinear equations of motion has 25 (or more) unknown parameters. A response-error model must therefore be a nonlinear coupled net of dynamical order of six. In addition, there are required 150 nonlinear coupled nets to calculate gradients plus 150 nonlinear

coupled algorithm nets to calculate the parameters. All these nets are dynamically coupled and nonlinear, so that the total system is of dynamical order of 306 (or more). The problems of feasibility, of computability, of stability, and of uniqueness of solution can only be imagined. On the other hand, if the equation error method is chosen, each of the six equations may be treated separately from the others; one linear model without dynamics can be formed for each equation, and the 25 signals required to estimate the gradient are available directly from each error net. The parameter estimating algorithms require 25 integrators. Six separate linear problems of dynamical order of 25 therefore result. Uniqueness and the effects of noise may be precalculated.

In view of the relative computational complexity of the response-error approach, and the relatively advanced state of the art of inertial sensors, it was concluded that this study should be restricted to the problem of developing and modifying an equation-error technique to be applicable to the problem. The result is therefore an equation-error Kalman combination which is an extension of the Kalman principles in a novel and unconventional direction.

An appendix provides a detailed heuristic explanation of the computational procedure for those who wish to use the method, or to understand the mathematical techniques. It is not essential for those who wish to appreciate the results of this research which are presented in Sections VI through XI.

II. CONCLUSIONS

1. It is feasible to estimate the entire set of hydrodynamic parameters of a submarine from free-flight data with state-of-the-art instrumentation and an algorithmic procedure which combines an adaptive equation-error parameter identification procedure with Kalman state estimation. This approach results in relatively modest computational requirements.

2. Errors of parameter identification in the presence of instrumentation noise range from a few percent for parameters which strongly influence the submarine trajectory to 100% for those which negligibly influence the trajectory and thus can be obscured by noise.

3. Successful parameter identification requires excitation not only of the bow and stern planes and rudder but also requires blowing ballast and changing speed.

4. The state estimation and parameter identification algorithms are capable of estimating the bias on the signals from the various sensors. In addition, they can be extended to enable estimation of nonstationary parameters and bias. These algorithms are thus capable of very wide application through the entire area of the physical sciences.

5. The combination of parameter identification and state estimation techniques yields an extended Kalman filter. The problems of instability frequently observed in extended Kalman filters have been fully resolved in this approach; it is believed that this method may, therefore, have a significant influence on the practical application of extended Kalman filters and on the direction of their development.

III. RECOMMENDATIONS

1. Much more efficient computational procedures can and should be developed; those used in this project were selected to ensure feasibility, rather than to achieve efficiency.

2. The present parameter identification and state estimation algorithms should be extended, minimizing the uncertainties of the submarine mass and inertias, the center-of-gravity and center of buoyancy locations, to correcting errors due to nonconstant error sources, such as sensor drift and Schuler loop phenomena, and to considering the implications of uncertainty of the ballast state.

3. The design of a specific parameter identification equipment should now be considered.

ORGANIZATION OF THE REPORT

It is assumed that the reader has some familiarity with vector-matrix notation and discrete Kalman filtering theory. The report begins by introducing notations and conventions to facilitate presentation of the basic ideas (Section IV). An estimation problem for which a solution can be advanced is then briefly formulated in Section V. Section VI develops the theoretical bases for the computer algorithm by first expressing the submarine estimation problem in the notational framework of Kalman filtering theory. The general algorithm is then presented and discussed in terms of its stability and convergence.

Section VII provides the philosophical motivation for submarine parameter identification simulation studies; these are summarized in Sections VIII and IX.

Methods by which the dynamic trajectory variables defining the motion of the vehicle can be instrumented are presented and discussed in Section X. The remaining sections (XI and XII) present normalized plots of the computer algorithm's convergence to the solutions for the hydrodynamic coefficients.

IV. EQUATIONS OF MOTION

To facilitate presentation of the basic ideas, vector notations will be employed to express the general equations of a submarine.

Detailed expressions for the force-moment equations which characterize the motion of a submarine are given in [1] and will not be completely reproduced here. It will suffice to represent them in the following form:

$$f_i(x_d) = c_i^T \Gamma_i(x_d, \delta) + h_i, \; i = 1, 2, \ldots 6$$

where,

- i is the equation number designating the axial, lateral, normal, roll, pitch, and yaw, force and moment equations respectively,
- x_d is the dynamic state vector whose elements are the components of vehicle velocity, acceleration, angular rates and angular acceleration in body fixed coordinates respectively,
- c_i is a vector whose elements are the hydrodynamic parameters for equation i,
- δ is a vector denoting the deflections of the control surfaces,
- h_i designates the thrust and weight-blown effects plus other force-moment phenomena that act on the submarine,
- $\Gamma_i(x_d, \delta)$ denotes a function vector for equation i whose elements couple the hydrodynamic parameters into the equations of motion,
- $f_i(x_d)$ represents the mass or moment of inertia terms, accordingly,
- T superscript T implies "Transpose".

To illustrate the notation a shorter form of the axial force equation (i = 1) will be written out in detail:

$$f_1(x_d) = m(\dot{u} - vr + wq)$$

$$h_1 = F_x - \Sigma\, w_j \sin\theta$$

$$x_d^T = (u, v, w, \dot{u}, \dot{v}, \dot{w}, p, q, r, \dot{p}, \dot{q}, \dot{r})$$

where u, v, w, $\dot{u}$, $\dot{v}$, $\dot{w}$, are the longitudinal, lateral and normal velocity and acceleration components respectively;

p, q, r, $\dot{p}$, $\dot{q}$, $\dot{r}$ are the roll, pitch and yaw angular rates and angular accelerations respectively; the second term in h_1 denotes the effect of the weights blown from the ballast tanks,

F_x - thrust from propeller rpm

m - mass of vehicle

θ - pitch angle

The hydrodynamic coefficient vector (c_i) for this equation is given by:

$$c_1^T = (x_{qq}, x_{rr}, x_{rp}, x_{\dot{u}}, x_{vr}, x_{wq}, x_{uu}, x_{vv}, x_{ww}, x_{\delta r \delta r}, x_{\delta s \delta s}, x_{\delta b \delta b})$$

where δ_s, δ_b and δ_r denote stern, bow and rudder surface deflections. The Γ_1 vector is correspondingly given by

$$\Gamma_1^T = (q^2, r^2, rp, \dot{u}, vr, wq, u^2, v^2, w^2, u^2\,\delta r^2, u^2\,\delta s^2, u^2\,\delta b^2)$$

The remaining equations (i = 2, 3, 4, 5, 6) can be similarly written out. It is not necessary explicitly to represent time dependency of the parameters in this notation since time can always be introduced as a state of the system.

V. PROBLEM FORMULATION

The utlimate goal is to determine the quality and quantity of instrumentation required to estimate the hydrodynamic coefficient vectors, c_j, from a sequence of control surface deflections over a given time interval. The immediate objective of this work is to develop a data-processing method that will aid in the achievement of this goal. Note that the control inputs (δ) are initially specified as arbitrary. It is of course desirable that they be sufficiently random such that the signals which form the coefficient of each parameter be linearily independent of the signals for all other parameters in the system. An additional reason for randomness of the control sequence will be explained later in relation to the convergence and performance of the proposed coefficient estimation algorithm.

The system states which define the motion of a submarine are such that they can be readily obtained by instrumentation; e.g., gyros and accelerometers can be placed on board which directly measure $\dot{u}$, $\dot{v}$, $\dot{w}$, p, q, and r. Gravity and earth's spin rate are of course subtracted from the respective instrument outputs. If the initial attitude of the vehicle is established, u, v, w can then be obtained by what is equivalent to a strapdown inertial navigation mechanization, while $\dot{p}$, $\dot{q}$ and $\dot{r}$ can be directly instrumented or obtained from the gyro outputs.

The essential issue here is that estimates of the dynamic states can be made without imposing (as part of the problem) the constraints of the force-moment equations. Any instrument employed to measure a variable is essentially a biased estimator; e.g., an accelerometer is a biased estimator of acceleration or a gyro is a biased estimator of attitude rate. For any vehicle employing inertial navigation the standard mechanizations are biased estimators of the dynamic states.

VI. ESTIMATION ALGORITHM

The hydrodynamic parameter identification problem can be treated by the methods outlined in Appendix A. The technique is to obtain a priori estimates of the dynamic variables (kinematic part of the problem) by conventional methods (discussed in Section X), and then incorporate the constraints of the force-moment equations as nonlinear measurements on an error system whose states consist of vector $\tilde{x}_d$ augmented with the $\tilde{c}_i$, i = 1, 2, . . . 6, error vectors. The resultant error state vector $\tilde{x}$ is now given by

$$\tilde{x}^T = (\tilde{x}_d^T, \tilde{c}_1^T, \tilde{c}_2^T, \ldots \tilde{c}_6^T).$$

The vector x will denote the true values for the respective elements.

If it is assumed that the hydrodynamic coefficients are constant ($\dot{c}_i = 0$), then the error dynamics is reduced to specifying the function for $\dot{\tilde{x}}_d$. The simplest case is the assumption of noise-free, linear, time-invariant dynamics for $\tilde{x}_d$,

$$\dot{\tilde{x}}_d = F \tilde{x}_d \qquad (1)$$

where,

$$F = \begin{bmatrix} 0&0&0&1&0&0&0&0&0&0&0&0 \\ 0&0&0&0&1&0&0&0&0&0&0&0 \\ 0&0&0&0&0&1&0&0&0&0&0&0 \\ 0&0&0&0&0&0&0&0&0&0&0&0 \\ 0&0&0&0&0&0&0&0&0&0&0&0 \\ 0&0&0&0&0&0&0&0&0&0&0&0 \\ 0&0&0&0&0&0&0&0&0&1&0&0 \\ 0&0&0&0&0&0&0&0&0&0&1&0 \\ 0&0&0&0&0&0&0&0&0&0&0&1 \\ 0&0&0&0&0&0&0&0&0&0&0&0 \\ 0&0&0&0&0&0&0&0&0&0&0&0 \\ 0&0&0&0&0&0&0&0&0&0&0&0 \end{bmatrix}.$$

This is valid for instances where the duration of the parameter estimation interval is short. Where this does not apply, a higher degree of freedom for $\tilde{x}_d$ is obtained by making $\tilde{u}$, $\tilde{v}$, $\tilde{w}$, $\tilde{p}$, $\tilde{q}$ and $\tilde{r}$ random correlated processes. The augmented system error dynamics can now be summarized,

$$\dot{\tilde{x}} = \left[\begin{array}{c|c} F & 0 \\ \hline 0 & 0 \end{array}\right] \tilde{x}.$$

The measurements on this system are the force-moment equations and are given by,

$$y_i = c_i^T \Gamma_i (x_d, \delta) + h_i - f_i (x_d), \quad i = 1, 2, \ldots, 6$$

where y_i is identically zero. When estimated quantities for c_i and x_d are substituted in y_i the expressions become $\hat{y}_i$.

Therefore, $\tilde{y}_i$, the error of estimation of y_i, is given by,

$$\tilde{y}_i = y_i - \hat{y}_i = -\hat{y}_i.$$

Expanding y_i about $\hat{x}_d$ and $\hat{c}_i$ and setting equal to $\hat{y}_i$,

$$\hat{y}_i = \hat{c}_i^T \left[\Gamma_i(\hat{x}_d, \delta), \hat{x}_d\right]\tilde{x}_d - \left[f_i(\hat{x}_d), \hat{x}_d\right]^T \tilde{x}_d + \Gamma_i^T(\hat{x}_d, \delta)\,\tilde{c}_i \qquad (2)$$

+ higher order terms.

where $, \hat{x}_d$ denotes vector partial differentiation with respect to $\hat{x}_d$. These expressions can be summarized in the following form:

$$\tilde{z} = -\begin{bmatrix} \hat{y}_1 \\ \hat{y}_2 \\ \cdot \\ \cdot \\ \cdot \\ \hat{y}_6 \end{bmatrix} \approx M(x)\,\tilde{x} + \nu \qquad (3)$$

where M(x) is a 6xn matrix which is a function of x, and the vector ν is introduced as white measurement noise. Obviously this assumption is not correct – but is necessary in order to apply Kalman filtering theory[2]. Since the elements of M are functions of the states it becomes necessary to incorporate multiple iterations into any computational algorithm. A major practical problem is the dimension (n) of $\tilde{x}$. The number of coefficients for a typical vehicle can easily exceed 100. For this reason the estimation of x is partitioned into six separate Kalman filtering problems which share the covariance matrix for $\tilde{x}_d$,

$$P_{\tilde{x}_d} = E\left\{\tilde{x}_d\,\tilde{x}_d^T\right\}.$$

The six partitioned error state systems are given by,

$$\begin{bmatrix} \tilde{x}_d \\ \tilde{c}_1 \end{bmatrix}, \begin{bmatrix} \tilde{x}_d \\ \tilde{c}_2 \end{bmatrix}, \ldots \begin{bmatrix} \tilde{x}_d \\ \tilde{c}_6 \end{bmatrix}.$$

Let P_i denote the error covariance matrix for system i. A computational algorithm which successively applies the discrete Kalman filtering equations can now be formulated. It will be assumed that the initial estimates for $\hat{x}_d$ have been obtained at discrete points in time (t_k) and are stored into an array. It is further hypothesized that convergence of the algorithm may be sensitive to the order in which the error systems are processed. Therefore, the equation-measurement processing sequence is initially specified.

In developing the following procedure it was assumed that little or no information on the c_i coefficients is available other than their initial variance; i.e., the initial estimates for $\hat{c}_i$ are zero and the covariance matrix is diagonal and its elements are equal to the initial variances. This situation tends to invalidate the approximations implicit in equation 3; i.e., the higher order terms of equation 2 are not insignificant. If the partial derivative terms (coupling the $\tilde{x}_d$ states) are initially

evaluated, and an attempt is made on the first pass accurately to balance the force or moment measurement equation, then divergence of the extended Kalman filter is guaranteed. To prevent this condition from occurring, the procedure is first to process the set of measurements $\hat{y}(t_k)$ with a large value for Q_i, where $Q_i = E\{ v_i v_i \}$, and on successive passes over the same equations introduce the $\tilde{x}_d$ state terms by evaluating the respective partial derivatives. On these additional passes the value of Q_i is reduced. Q_i is the noise covariance matrix, and in this case is a scaler.

The important issue is to obtain from P_i a matrix $P_{\tilde{x}_d}$ which accurately reflects the state of uncertainty in $\hat{x}_d$. The resulting estimates for $\tilde{x}_d$ obtained from a particular equation are then used to update the values for $\hat{x}_d$. The starting covariance for $P_{\tilde{x}_d}$ in the next system P_j, $i \neq j$, is obtained from P_i. For the deterministic error dynamics postulated by equation 1, transferring the terminal $P_{\tilde{x}_d}$ to initial time presents no problem; but for a more general stochastic error structure it is necessary to construct multiple point smoothing into the algorithm. The remaining equation-measurements are processed in a similar manner. The primary motivation for this procedure is that the six equations of motion, processed sequentially, can provide sufficient observability for $\tilde{x}_d$ so that improved estimates of c_i are obtained if the force-moment equations are reprocessed.

The basic algorithm then is a sequence of multiple sweeps on six error state systems where the measurement on each system consist of the corresponding force or moment equation. After each of the six systems has been multiple-iterated once, the computations are repeated with fewer individual sweeps since the greatest convergence will occur during the initial sweeps. From simulations of this algorithm it was established that only one additional sweep through each system was required to obtain the parameter vectors c_i.

Convergence of this technique is directly related to obtaining unbiased estimates for c_i on the first pass, where the value of Q_i is large. From this it is asserted that the sequence of control surface deflections should be as random as possible in an attempt to whiten the higher order terms of equation 2, thereby making valid the assumptions of the discrete Kalman filter.

The major source of instability in this algorithm is the process of updating estimates with the successive sweeps. This may account for the instability noted at present in all applications of extended Kalman filtering. It was discovered that false-observability was created if the corrections to the c_i obtained from the current sweep were used in that sweep to compute the partials coupling the $\tilde{x}_d$ state into the measurement. This is obvious when it is considered that the c_i vectors are constant; to introduce the convergence dynamics of the c_i vectors into the measurement structure is a gross modeling error. This may be the reason why some researchers have concluded that the extended Kalman filter is unstable or very sensitive; and have resorted to least-squares methods which inherently avoid this observability distortion.

This difficulty is avoided by simply using the end results from the previous sweep in evaluating the partials on the current sweep.

The logical flow diagram presented as Figure 1 shows the interrelationships of the various sweeps, iterations and updating procedures.

A separate subroutine (YWIG) was constructed into the program for the computation of $\tilde{y}_i$ (Figure 1). This made the computation of the partials (numerically) convenient by calling YWIG for two different values of a particular dynamic variable - differencing the result and dividing this by the difference between the two values of the dynamic variable.

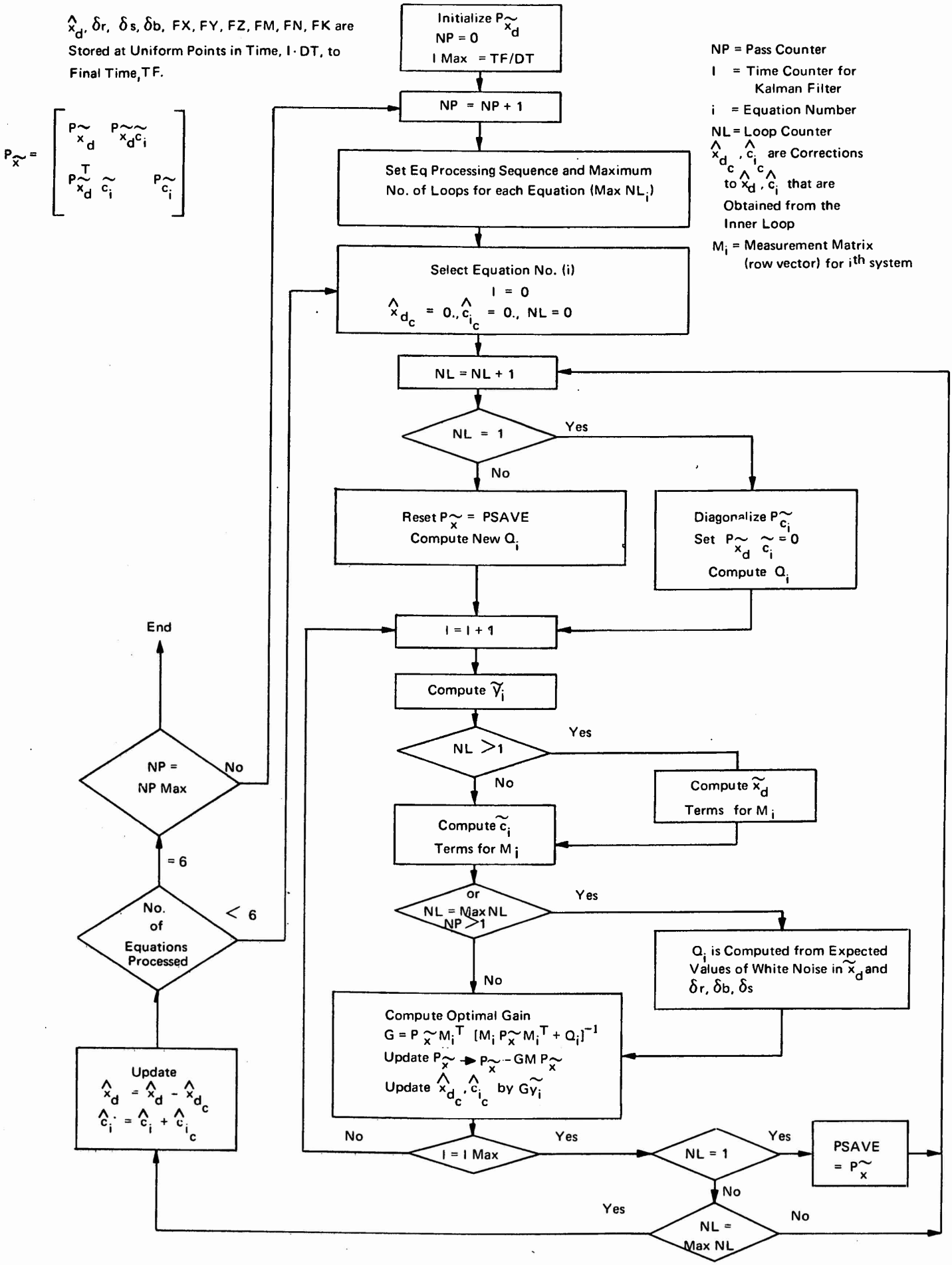

Figure 1. Flow Diagram for Hydrodynamic Coefficient Estimation Algorithm

VII. INTRODUCTION TO SIMULATIONS

The approach taken by BAC to evaluate this algorithm was to initially solve the simplest problem possible. This is the case where all the states $\tilde{x}_d$ are constant, i.e., F=0. The main reason for doing this is that the time varying problem would require greater programming and larger execution time. It was felt that under the limited funding, a realistic and useful goal would first be established. Also, if a simplified version of the problem could not be solved then it would be economically wasteful to expend effort developing sophisticated processing algorithms which had no chance of success. This simplified problem may turn out to be the best way in which the real world submarine identification problem can be approached. The real situation is often characterized by the occurrence of events that are unexpected, i.e., no matter what the assumed mathematical model for the submarine is, there is a significant probability that it is not quite correct. If some hydrodynamic coefficients are not constant, how then should they be modeled? Are they functions of depth, speed, etc.? Higher degrees of freedom can be built into an algorithm by assuming random correlated (stochastic) modeling for any coefficient(s); this places a much greater decision making requirement on the program operator as to where a higher degree of freedom is needed. This is a difficult area because it is conceivable that at some level of freedom nothing is gained, i.e., submarine coefficients can be obtained to fit any set of random signals.

These considerations make the method outlined above attractive as a means of attacking the real world problem. It follows that it would be more useful and practical to break up an hour of submarine trajectory data into short separate intervals and process the data as though it was from different submarines, rather than have a complex time-varying identification algorithm to process the data as taken from one submarine. This general approach had been taken in reducing flight data on BAC Hipernas inertial navigators and was found to be the most beneficial. To this goal then, it is hoped that the following simulations will contribute significantly.

VIII. SIMULATIONS

The following are results from simulations of a typical submerged vehicle with zero initial conditions – except for u = 50 ft/sec. The control surface commands are basic pseudo random sequences with a 5 sec pulse interval. The thrust is such that u is decreased to 20 ft/sec over a 10-minute flight time. Salient features of the resultant trajectory are shown in Figure 2. The sequential Kalman filter computation interval is six seconds; processing of data was performed for a five minute flight. It required five minutes of computing time on an IBM 360/65 to compute a trajectory and estimate the parameters and bias values. The number of states for each error system and the order in which they were processed are:

Axial Force System	24
Rolling Moment System	25
Pitching Moment System	28
Normal Force System	28
Lateral Force System	27
Yaw Moment System	26.

These values include the 12 dynamic states, $\tilde{x}_d$. It might be argued that the order of these separate systems should be lower since, for each system, some of the x_d variables are not directly involved. However, the algorithm advanced here does couple the errors of these variables (in the error covariance matrix) as the systems are sequentially processed and the covariance, for the $\tilde{x}_d$, from processing a given system is used to start the processing of the following system.

The dynamic states (x_d) were generated for the true coefficients with the submarine simulation program and submarine parameter data supplied to BAC by NSRDC [3]. The hydrodynamic coefficient estimation program was written to operate on a two dimension array that consist of sampled values of the following dynamic variables at discrete points in time,

$u, v, w, \dot{u}, \dot{v}, \dot{w}, p, q, r, \dot{p}, \dot{q}, \dot{r}, \delta r, \delta s, \delta b,$

PRMNI, FX, FY, FZ, FM, FN, FK

The first 12 variables are the dynamic variables (x_d) that define the motion of the vehicle; δr, δs, δb are the control surface deflections; PRMNI is $(n' - 1)$ where n' is the ratio of ordered speed to current axial velocity. In the set of hydrodynamic coefficients supplied to BAC, the parameters associated with PRMNI were zero, therefore at this time estimation of these terms have not been investigated.

The remaining terms in the above array are defined as follows:

$$FX = -\Sigma W_i \sin\theta + FXP$$
$$FY = \Sigma W_i \sin\phi \cos\theta + FYS$$
$$FZ = \Sigma W_i \cos\theta \cos\phi + FZS$$
$$FM = B(Z_B) \sin\theta - \Sigma W_i X_{Ti} \cos\theta \cos\phi + QYS$$
$$FN = \Sigma W_i X_{Ti} \cos\theta \sin\phi + QZS$$
$$FK = B(Z_B) \cos\theta \sin\phi + QXS$$

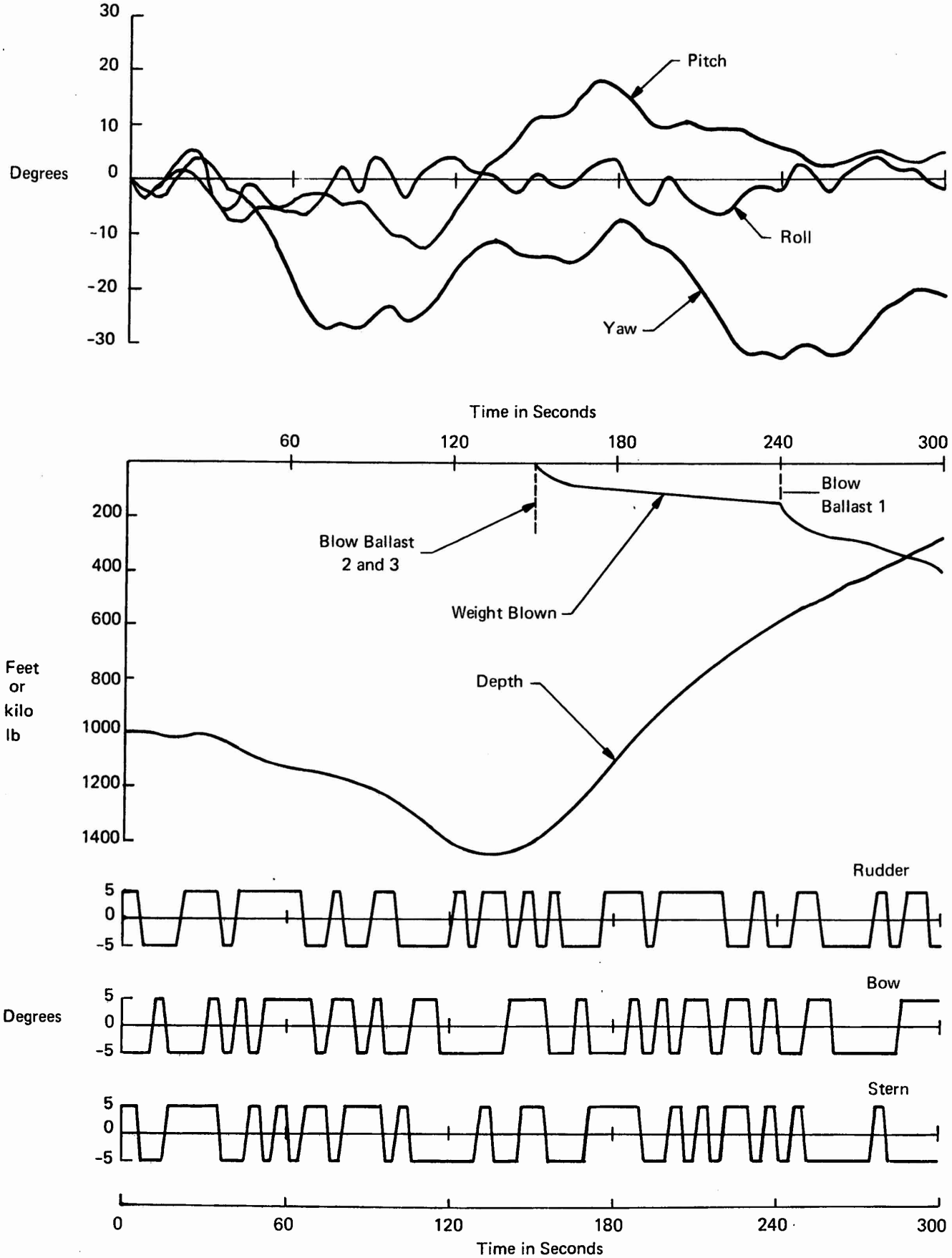

Figure 2. Trajectory Data and Control Surface Deflections for Parameter Estimation Simulations

The S terms here are sea state effects which the simulation program sets equal to zero; θ and ϕ are pitch and roll of the submarine. As a first step in the development of the program it was felt that identification of the parameters should be investigated with knowledge of Z_B, θ, ϕ, FXP and ΣW_i (sum of weights blown). It is recognized that any real world situation has errors in these terms – also errors in knowledge of the CG exist. The program is structured such that extending the degrees of freedom to include these errors is a trivial matter.

Before the data outlined above is reduced (estimating the hydrodynamic coefficients) the variables are first corrupted by bias and random errors.

The results presented in tables 1 through 7 are for one set of bias errors; these are given in Table 7. Table 7 also shows how well the bias errors were estimated (by the algorithm) for two levels of white noise, (1) zero and (2) as follows:

Δu =	0.01 ft/sec	$\Delta \delta s$ =	0.0005 rad
Δv =	0.005 ft/sec	$\Delta \dot{u}$ =	0.0003 ft/sec^2
Δw =	0.005 ft/sec	$\Delta \dot{v}$ =	0.0003 ft/sec^2
Δp =	$0.5(10)^{-5}$ rad/sec	$\Delta \dot{w}$ =	0.0003 ft/sec^2
Δq =	$0.5(10)^{-5}$ rad/sec	$\Delta \dot{p}$ =	$0.2(10)^{-5}$ rad/sec^2
Δr =	$0.5(10)^{-5}$ rad/sec	$\Delta \dot{q}$ =	$0.2(10)^{-5}$ rad/sec^2
$\Delta \delta r$ =	0.0005 rad	$\Delta \dot{r}$ =	$0.2(10)^{-5}$ rad/sec^2
$\Delta \delta b$ =	0.0005 rad		

These random errors were added to the trajectory variables as independent-uniformly distributed processes. Tables 1 through 6 summarize the accuracies obtained for the dimensionless hydrodynamic coefficients associated with each force/moment equation. Those hydrodynamic parameters that do not appear in the table were given to BAC by NSRDC as zero and therefore not made a part of this study. The program is coded for the n′ coefficients and additional ones can readily be added.

The convergence dynamics for every coefficient estimated is of interest because it readily identifies the observability structure of the parameters. This information can be used to ascertain whether or not a particular coefficient would be observable if it were not constant over the estimation time interval. For this reason normalized plots of the convergence to each coefficient is provided at the end of this report. Of particular significance is the convergence sequence depicted in the plots and the corresponding noise levels, Q_i, which control the gains in the Kalman filter. The form of Q_i and the operational details of the computer algorithms looping pattern are summarized below.

1. Each system-equation was first iterated five times in the following equation number sequence, 1-4-5-3-2-6. The end covariance from the first sweep was stored and used for initializing the succeeding sweeps.

2. Estimates of $\tilde{x}_d$, which are obtained starting with the second sweep, are reset to zero before starting the succeeding sweeps. After the final sweep on an equation-system, the estimates are used to update the array of $\hat{x}_d(t_k)$. This array is, at the start of the algorithm, the sum of the true dynamic variables (x_d) plus the bias and random elements described above.

3. As in estimating the $\tilde{x}_d$ variables, corrections to the hydrodynamic coefficients are obtained from any sweep, and at the final time of each sweep the estimates are used to update the respective coefficient array. This is necessary to avoid introducing the convergence dynamics into the measurement structure.

TABLE 1
SUMMARY OF AXIAL FORCE
DIMENSIONLESS COEFFICIENT ESTIMATION

		Estimated Values With Bias		% Estimated (Based Upon Covariance)	
Parameter	True Value	No White Noise	White Noise	No White Noise	With White Noise
X_{qq}	$-1.7(10)^{-4}$	$-1.695(10)^{-4}$	$-1.619(10)^{-4}$	96.23	56.23
X_{rr}	$-8.6(10)^{-5}$	$-9.553(10)^{-5}$	$-2.737(10)^{-5}$	47.42*	1.45
X_{rp}	$2.7(10)^{-4}$	$2.702(10)^{-4}$	$2.744(10)^{-4}$	98.71	83.09
$X_{\dot{u}}$	$-1.42(10)^{-4}$	$-1.392(10)^{-4}$	$0.1562(10)^{-4}$	91.94	29.94
X_{vr}	$1.1(10)^{-2}$	$1.093(10)^{-2}$	$1.072(10)^{-2}$	97.38*	91.56*
X_{wq}	$-7.46(10)^{-3}$	$-7.455(10)^{-3}$	$-7.209(10)^{-3}$	99.70	97.05
X_{uu}	0.	–	–	–	–
X_{vv}	$6.5(10)^{-3}$	$6.388(10)^{-3}$	$6.025(10)^{-3}$	92.58*	60.42*
X_{ww}	$1.92(10)^{-3}$	$1.929(10)^{-3}$	$2.174(10)^{-3}$	99.02	89.56
$X_{\delta r\delta r}$	$-2.89(10)^{-3}$	$-2.887(10)^{-3}$	$-2.826(10)^{-3}$	99.53	94.28
$X_{\delta s\delta s}$	$-2.46(10)^{-3}$	$-2.458(10)^{-3}$	$-2.428(10)^{-3}$	99.27	90.34
$X_{\delta b\delta b}$	$-2.59(10)^{-3}$	$-2.585(10)^{-3}$	$-2.370(10)^{-3}$	99.49	93.43

TABLE 2
SUMMARY OF LATERAL FORCE
DIMENSIONLESS COEFFICIENT ESTIMATION

		Estimated Values With Bias		% Estimated) (Based Upon Covariance)	
Parameter	True Value	No White Noise	White Noise	No White Noise	With White Noise
$Y_{p\|p\|}$	0.	–	–	–	–
Y_{pq}	$1.7(10)^{-4}$	$1.694(10)^{-4}$	$0.298(10)^{-4}$	93.68*	56.65
$Y_{\dot{p}}$	$-2.7(10)^{-4}$	$-2.700(10)^{-4}$	$-2.584(10)^{-4}$	99.82	97.86
$Y_{\dot{r}}$	$8.6(10)^{-5}$	$8.539(10)^{-5}$	$-7.903(10)^{-5}$	87.85*	24.61
$Y_{\dot{v}}$	$-1.1(10)^{-2}$	$-1.100(10)^{-2}$	$-0.995(10)^{-2}$	99.67	96.06
$Y_{v\|r\|}$	$-7.3(10)^{-3}$	$-7.299(10)^{-3}$	$-6.464(10)^{-3}$	99.32	91.67
Y_{wp}	$7.46(10)^{-3}$	$7.457(10)^{-3}$	$6.613(10)^{-3}$	99.61	95.29
Y_r	$3.57(10)^{-3}$	$3.569(10)^{-3}$	$3.227(10)^{-3}$	98.93*	92.48
$Y_{\|r\|\delta r}$	$-1.3(10)^{-3}$	$-1.299(10)^{-3}$	$-0.9307(10)^{-3}$	98.69	88.22
Y_p	$-6.74(10)^{-4}$	$-6.740(10)^{-4}$	$-6.832(10)^{-4}$	99.62	96.86
Y_{uu}	0.	–	–	–	–
$Y_{v\|v\|}$	-0.06	-0.05998	-0.05271	99.46	95.64
Y_v	-0.0213	-0.02130	-0.02161	99.56	96.34
$Y_{\delta r}$	-0.00652	-0.006517	-0.005578	99.38	95.84
Y_{wv}	-0.066	-0.06598	-0.05919	99.66	96.81
$Y_{\|w\|}$	0.	–	–	–	–
Y_{ww}	0.	–	–	–	–
Y_{vs}	-0.02075	–	–	–	–

TABLE 3
SUMMARY OF NORMAL FORCE
DIMENSIONLESS COEFFICIENT ESTIMATION

		Estimated Values With Bias		% Estimated (Based Upon Covariance)	
Parameter	True Value	No White Noise	White Noise	No White Noise	With White Noise
Z_{rr}	-0.00178	-0.001782	-0.001794	96.24*	82.47*
Z_{rp}	$-5.33(10)^{-4}$	$-5.332(10)^{-4}$	$-3.164(10)^{-4}$	97.98	77.83
$Z_{\dot{q}}$	$-1.7(10)^{-4}$	$-1.699(10)^{-4}$	$-1.559(10)^{-4}$	98.99	88.94
$Z_{\dot{w}}$	-0.00746	-0.00746	-0.007418	99.96	99.56
Z_{vr}	0.00203	0.002015	0.00151	78.39*	7.71*
$Z_{w\|q\|}$	0.0062	0.0062	0.006356	99.69	96.22
Z_q	-0.0044	-0.0044	-0.004364	99.87	98.65
$Z_{\|q\|\delta s}$	0.	–	–	–	–
Z_{vp}	-0.0068	-0.0068	-0.006043	99.46	94.62
$Z_{\Delta vp}$	0.	–	–	–	–
Z_{uu}	$-1.11(10)^{-4}$	$-1.11(10)^{-4}$	$-1.121(10)^{-4}$	99.85	98.00
Z_{vv}	0.066	0.06598	0.06442	98.86*	94.68
$Z_{w\|w\|}$	-0.03184	-0.03184	-0.03165	99.83	97.95
Z_w	-0.01059	-0.01059	-0.0106	99.93	99.24
$Z_{\delta s}$	-0.00542	-0.00542	-0.00534	99.91	98.95
$Z_{\delta b}$	-0.00267	-0.00267	-0.002665	99.95	99.39
$Z_{\|w\|}$	0.	–	–	–	–
Z_{ww}	0.	–	–	–	–
Z_{vs}	-0.02075	–	–	–	–

TABLE 4.
SUMMARY OF ROLL MOMENT
DIMENSIONLESS COEFFICIENT ESTIMATION

		Estimated Values With Bias		% Estimation (Based Upon Covariance)	
Parameter	True Value	No White Noise	White Noise	No White Noise	With White Noise
$K_{p\|p\|}$	$-3.4(10)^{-6}$	$-3.398(10)^{-6}$	$-3.828(10)^{-6}$	98.72	78.14
K_{qr}	$-1.02(10)^{-4}$	$-1.02(10)^{-4}$	$-1.028(10)^{-4}$	99.93	98.90
$K_{\dot{p}}$	$-3.3(10)^{-6}$	$-3.3(10)^{-6}$	$-3.194(10)^{-6}$	99.90	98.29
$K_{\dot{r}}$	$-1.44(10)^{-5}$	$-1.44(10)^{-5}$	$-1.487(10)^{-5}$	99.88	97.94
$K_{\dot{v}}$	$-2.7(10)^{-4}$	$-2.70(10)^{-4}$	$-2.623(10)^{-4}$	99.91	98.49
K_{wp}	$2.7(10)^{-4}$	$2.7(10)^{-4}$	$2.629(10)^{-4}$	99.92	98.66
K_r	0.	—	—	—	—
K_p	$-3.6(10)^{-5}$	$-3.6(10)^{-5}$	$-3.582(10)^{-5}$	99.96	99.41
K_{uu}	0.	—	—	—	—
$K_{v\|v\|}$	$-1.037(10)^{-3}$	$-1.037(10)^{-3}$	$-0.9744(10)^{-3}$	99.85	97.50
K_v	$-3.87(10)^{-4}$	$-3.871(10)^{-4}$	$-3.845(10)^{-4}$	99.96	99.28
$K_{\delta r}$	$6.4(10)^{-5}$	$6.4(10)^{-5}$	$5.993(10)^{-5}$	99.79	96.45
K_{wv}	$3.54(10)^{-4}$	$3.539(10)^{-4}$	$3.931(10)^{-4}$	99.63	93.72

TABLE 5
SUMMARY OF PITCH MOMENT DIMENSIONLESS
COEFFICIENT ESTIMATION

		Estimated Values With Bias		% Estimation (Based Upon Covariance)	
Parameter	True Value	No White Noise	White Noise	No White Noise	With White Noise
M_{rr}	-0.00112	-0.001121	-0.0009485	99.92	77.70*
M_{rp}	$9.92(10)^{-5}$	$9.944(10)^{-5}$	$13.11(10)^{-5}$	99.87	58.62
$M_{\dot{q}}$	$-3.9(10)^{-4}$	$-3.9(10)^{-4}$	$-3.76(10)^{-4}$	99.99	98.17
$M_{\Delta rp}$	0	–	–	–	–
$M_{\dot{w}}$	$-1.73(10)^{-4}$	$-1.73(10)^{-4}$	$-1.645(10)^{-4}$	99.97	94.18
M_{vr}	-0.00362	-0.003626	-0.003081	99.84	55.19*
$M_{\|w\|q}$	-0.0022	-0.0022	-0.002241	99.98	94.79
M_q	-0.00255	-0.00255	-0.002504	99.99	99.16
$M_{\|q\|\delta s}$	0	–	–	–	–
M_{vp}	$8.44(10)^{-4}$	$8.447(10)^{-4}$	$10.50(10)^{-4}$	99.94	84.32
M_{uu}	$4.2(10)^{-5}$	$4.2(10)^{-5}$	$4.275(10)^{-5}$	99.96	98.13
M_{vv}	0.0146	0.01459	0.01427	99.93	80.79*
$M_{w\|w\|}$	-0.00473	-0.004732	0.005042	99.98	94.88
M_w	0.0032	0.0032	0.003177	99.99	99.10
$M_{\delta s}$	-0.00258	-0.00258	-0.002529	99.99	99.13
$M_{\delta b}$	$5.2(10)^{-4}$	$5.2(10)^{-4}$	$5.086(10)^{-4}$	99.99	98.97
$M_{\|w\|}$	0	–	–	–	–
M_{ww}	0	–	–	–	–

TABLE 6
SUMMARY OF YAW MOMENT
DIMENSIONLESS COEFFICIENT ESTIMATION

Parameter	True Value	Estimated Values With Bias		% Estimated (Based Upon Covariance)	
		No White Noise	White Noise	No White Noise	With White Noise
N_{pq}	$-3.87(10)^{-4}$	$-3.872(10)^{-4}$	$-0.538(10)^{-4}$	99.95	89.92*
$N_{\dot{p}}$	$-7.2(10)^{-6}$	$-7.184(10)^{-6}$	$-6.59(10)^{-6}$	99.92	83.09
$N_{\dot{r}}$	$-4.92(10)^{-4}$	$-4.922(10)^{-4}$	$-1.426(10)^{-4}$	99.95	91.60*
$N_{\dot{v}}$	$3.12(10)^{-4}$	$3.131(10)^{-4}$	$0.888(10)^{-4}$	99.86	71.55
$N_{\|v\|r}$	$-4.45(10)^{-3}$	$-4.450(10)^{-3}$	$-3.073(10)^{-3}$	99.97	93.42
N_{wp}	$-1.73(10)^{-4}$	$-1.739(10)^{-4}$	$-0.424(10)^{-4}$	99.79	57.13
N_r	$-3.2(10)^{-3}$	$-3.200(10)^{-3}$	$-1.986(10)^{-3}$	99.97	95.50*
$N_{\|r\|\delta r}$	$1.3(10)^{-3}$	$1.300(10)^{-3}$	$0.819(10)^{-3}$	99.97	95.01
N_p	$-2.2(10)^{-4}$	$-2.200(10)^{-4}$	$-1.445(10)^{-4}$	99.98	95.50*
N_{uu}	0.	-	-	-	-
$N_{v\|v\|}$	0.0135	0.01351	0.00681	99.96	92.66
N_v	-0.00713	-0.007130	-0.00448	99.97	95.30*
$N_{\delta r}$	-0.00333	-0.003331	-0.00204	99.97	95.45*
N_{wv}	0.0146	0.01461	0.00901	99.97	95.01

TABLE 7
ESTIMATION OF BIAS ERRORS

Parameter	True Bias Value	Estimated Values With		% Estimated (Based Upon Covariance)	
		No White Noise	White Noise	No White Noise	With White Noise
Δ_u ft/sec	3.0	3.000	2.939	99.98	96.22
Δ_v ft/sec	0.3	0.3001	0.303	99.99	99.32
Δ_w ft/sec	0.3	0.3002	0.2994	99.96	96.14
$\Delta_{\dot{u}}$ ft/sec^2	0.0032	0.00316	0.00203	97.48	70.4
$\Delta_{\dot{v}}$ ft/sec^2	0.0032	0.00320	0.00318	99.58	92.43
$\Delta_{\dot{w}}$ ft/sec^2	0.0032	0.00318	0.00287	96.84	57.50
Δ_p rad/sec	$0.5(10)^{-4}$	$0.504(10)^{-4}$	$0.237(10)^{-4}$	98.39	36.68
Δ_q rad/sec	$0.5(10)^{-4}$	$0.483(10)^{-4}$	$-0.066(10)^{-4}$	95.89	20.47
Δ_r rad/sec	$0.5(10)^{-4}$	$0.496(10)^{-4}$	$0.295(10)^{-4}$	99.65	82.4
$\Delta_{\dot{p}}$ rad/sec^2	$0.2(10)^{-5}$	$0.068(10)^{-5}$	$-0.007(10)^{-5}$	45.20	0.11
$\Delta_{\dot{q}}$ rad/sec^2	$0.2(10)^{-5}$	$0.237(10)^{-5}$	$-0.006(10)^{-6}$	79.26	0.40
$\Delta_{\dot{r}}$ rad/sec^2	$0.2(10)^{-5}$	$0.205(10)^{-5}$	$-0.055(10)^{-5}$	97.03	3.06

4. Initialization of the covariance matrix for a given system-equation consist of diagonalizing the covariance matrix for $\tilde{c}_i$ and zeroing the off-diagonal elements between $\tilde{x}_d$ and $\tilde{c}_i$. This is done only for the first sweep; succeeding sweeps are initialized by setting the covariance of the equation-system equal to that obtained from the end of the initial sweep (where Q_i was high). The covariance for $\tilde{x}_d$ is initialized as diagonal and is not altered when sweeps on a new equation-system are initiated.

5. The measurement noise levels on the initial five sweeps were computed as follows:

$$Q_i = R_i^2 \, (SR_i)^2 \qquad \text{for first sweep}$$

$$Q_i = \left[R_i + (R_i SR_i) \left(1 - \frac{I}{5}\right)^2 \right]^2 \qquad \text{for } I = 2, 3, 4$$

where I is the sweep number and SR_i is a dimensionless gain factor introduced to set the level of Q_i. The fifth sweep is made adaptive with respect to noise by computing Q_i from an inputed array reflecting the expected values of the white noise errors in $\hat{x}_d$, and the sensitivity functions coupling the bias errors into the measurement. The selection of Q_i sequence is somewhat aribtrary; the particular choice made here is based upon the intuitive notion that the algorithm should converge (most naturally) on a parabolic type trajectory.

6. After processing each system five times, one additional sweep is made through each system with Q_i computed as in the final loop of the first sequence of sweeps. The values of R_i and SR_i used in the simulations are given below,

No White Noise	White Noise
R_1 = 300 lb , SR_1 = 50	R_1 = 300 lb , SR_1 = 50
R_2 = 300 lb , SR_2 = 50	R_2 =1000 lb , SR_2 = 200
R_3 = 300 lb , SR_3 = 50	R_3 = 600 lb , SR_3 = 200
R_4 = 3000 ft-lb, SR_4 = 50	R_4 =30,000 lb, SR_4 = 50
R_5 = 3000 ft-lb, SR_5 =100	R_5 =30,000 lb, SR_5 = 100
R_6 = 3000 ft-lb, SR_6 =100	R_6 =100,000 ft-lb, SR_6 = 100

It should be mentioned that these values were arrived at by a closed loop operation between the computer program developer and the computer output. The degree to which this is necessary is directly related to the degree of ignorance in the apriori estimates of the hydrodynamic coefficients. Instability or a biased performance of the algorithms will be experienced if these values are underestimated. This occurs for two reasons: (1) the white noise corrupted dynamic variables are used in constructing the measurement matrix, and if Q_i is too low false observability will be generated in the covariance matrix, (2) the measurement error, $\tilde{y}_i$, cannot be forced to zero or to the level of white noise without being able to compute reasonably accurate partial derivatives that couple the bias errors into the equation-measurement. It should be emphasized that considerable latitude does exist in the selection R_i and SR_i, and as a general rule it is safe to select them on the high side. This flexibility results from the form of Q_i, which varies Q_i through a large dynamic range, and from the adaptive feature described in step 5 above that optimizes the value of Q_i on the fifth sweep, and when the equation-systems are reprocessed on the final pass.

It was mentioned in step 4 above that the starting covariance matrix for $\tilde{c}_i$ is diagonal; for this study the value of these diagonal elements were obtained by squaring twice the value of the hydrodynamic coefficients supplied to BAC by NSRDC. Correspondingly, the initial estimates of all coefficients were set at zero. This was done to establish a very conservative apriori knowledge requirement for starting the algorithm.

IX. DISCUSSION OF RESULTS

The results in Tables 1-7 for the no white noise case were obtained with the gains of the Kalman filter (on the final sweep) computed for a measurement noise level of 100 lb for the force equations and 500 ft-lb for the moment equation. Therefore, the final covariance matrix reflects this level of error and the estimates will be better than the columns designated "% Estimated" (in the tables) indicate. These columns are computed as follows:

$$\% \text{ Estimated} = \left(1 - \sqrt{\frac{P_{jj}\ (t_f)}{P_{jj}\ (t_o)}} \right) (100)$$

where $P_{j\,j}$ ( ) denotes the respective diagonal element of the covariance matrix for a coefficient at the time indicated.

The degree to which a particular coefficient can be estimated (observability) is related to two physical situations; the effect of a coefficient in the equation-measurement may be (1) equivalent to a linear combination of other coefficients or (2) at a level that is within the measurement noise. It is of interest then to determine the nature of an observability problem associated with any parameter. This information is available from the off-diagonal elements of the final covariance matrix. The correlation between two variables are obtained from the following expression,

$$\text{cor}_{i\,j} = \frac{P_{ij}}{\sqrt{P_{ii}\ P_{jj}}}$$

where $P_{i\,j}$ is the i′ th row and j ′ th column off-diagonal element of the covariance matrix. Variables that are in combination with a correlation greater than 0.9 are designated by an asterisk (*) in Tables 1 through 6. For coefficients where the "% Estimated" does not indicated good estimation, and the variable is not correlated with another variable, it can be inferred that this coefficient does not contribute significantly to the submarine trajectory.

A situation that can occur is that some variables are redundant unless the level of random error is zero or very small. This is illustrated by the pitch equation results for parameters M_{rr}, M_{vr} and M_{vv}. A similar effect between variables X_{rr}, X_{vr} and X_{vv} exist for the axial force equations. But in this case the correlation for X_{rr} did not develop in the white noise case. This indicates that the influence of the X_{rr} term on the submarine is very small. To obtain a quantitative measure of the influence of these terms, Table 8 gives the nominal influence of the white noise variables on the balancing of each equation. The term nominal is used here because the effect is of course variable along the submarine trajectory.

In Tables 2 and 3, Y_{vs} and Z_{vs} are sinusoidal hydrodynamic effects at the vortex shedding frequence (ω). The value of ω supplied to BAC by NSRDC was zero, therefore these term did not excite the system and consequently are not estimated.

---

* In effect, an asterisk indicates that the functions which form the coefficients of the marked parameters become correlated at the level of the parameter value indicated, thus preventing further convergence.

TABLE 8
EFFECT OF WHITE NOISE ERRORS
ON DYNAMIC EQUATIONS

Equation Number	Effect of $\tilde{x}_d$ (White)	Effect of Errors in Control (White)
1 (Axial)	190 lbs	1200 lbs
2 (Lateral)	900 lbs	900 lbs
3 (Normal)	700 lbs	900 lbs
4 (Roll)	750 lbs	3500 ft - lbs
5 (Pitch)	50,000 ft - lbs	150,000 ft - lbs
6 (Yaw)	80,000 ft - lbs	150,000 ft - lbs

An important issue of submarine parameter identification is featured in the results (white noise case) for the yaw coefficients. It is noted that some coefficients are not estimated within the expected accuracy indicated (Table 6). The question immediately arises is the algorithm failing for the level of noise employed, or is the submarine yaw equation non-unique. The test was to simulate the submarine with the incorrect coefficients and compare the resulting trajectory variables with the true ones. This was done and the two trajectories matched to within 0.1 percent; thus indicating that the submarine was non-unique. It is ascertained that the reason for this occurrence is related to the requirement the submarine must blow weight to allow a unique solution for the yaw equation. This requirement is also true for the lateral and normal force equations. The basic problem is that the inertia terms are similar to some hydrodynamic coefficients, e.g., the yaw equation is

$$I_z \dot{r} + (I_y - I_x)\ pq - \sum_j w_j x_{t_j} \cos\theta \sin\phi$$

$$= \left(\frac{\rho}{2} \ell^5 N_{\dot{r}}\right) \dot{r} + \left(\frac{\rho}{2} \ell^5 N_{pq}\right)\ pq$$

$$+ \text{other coefficients}$$

Without blowing weight, estimation of the coefficients must come from the information contained in the left hand side of this equation. But the left hand side is embedded into the coefficient side since $\dot{r}$ and pq appear on both sides thereby unscaling the equation.

Therefore the submarine must blow weight in order to be unique. What is happening, in the results of Table 6, is that the selected level of noise is starting to mask the equation's observability for the weight-blowing profile depicted in Figure 1. This situation in the equations also forced the computer program to be executed in double precision. Note also that the processing sequence for the equation-systems list first those equations that do not require mass changes to be observable. Instability of the algorithm was experienced for sequences that processed the lateral and normal force equation before the pitch and roll equations.

This relationship between uniqueness, weight blown and noise level is an area requiring further investigation along with those listed in the introduction to simulations section. Another simulation was made with the white noise a factor of ten higher than those listed previously. In this case estimates for Equation 2 were degraded along with Equation 6. However, the estimates were able to reproduce the true submarine trajectory reasonably well.

An area that remains to be investigated is the true nature of the errors obtained in the dynamic variables $\hat{x}_d$ from the various instrumentation methods to be discussed in the following section; and how this affects the algorithm as constituted. The immediate area of concern is the cross coupling that will be obtained between the dynamic variables due to the non-orthogonality of the instruments or their mountings. Some comfort is gained in that the white noise level (Q_i) can always be increased in the Kalman filter such that unmodeled errors reside well within this level. This generally assures a stable computation with some loss of optimality.

X. NAVIGATION AND MOTION MEASUREMENT INSTRUMENTATION

The submarine parameter identification program is dependent on motion measurement data of high resolution over several minutes of maneuvering flight time. Medium to high accuracy data are required within a restricted frequency spectrum of the submarine motion during the maneuvers. The complexity of the on-board motion measurement instrumentation is partly a function of the availability and accuracy of various navigation equipments. Several options are outlined, including an inertial platform navigator, and an inertial strap-down navigator.

A possible solution to the instrumentation problem is a low cost inertial navigator with a vertical channel slaved to pressure depth. The navigator North and East Schuler axes are damped by the ship's EM log resolved by pitch and azimuth through a MK 19 gyro compass. The azimuth gyro of the navigator is aligned and drift corrected by feeding back a comparison of platform azimuth with the MK 19 azimuth.

If the submarine is traveling at reasonably constant depth, heading, and speed for approximately one hour the inertial navigator can become aligned, leveled, and referenced to the average local ocean currents. Before starting maneuvers the inertial navigator is uncoupled from the EM log and the gyro compass. The navigator has less dynamic error than the other equipment, for accelerating maneuvers over short periods of time.

The submarine performs the maneuvers based on pseudo-random pulse sequences applied to the bow plane, stern plane and rudder. Control biases are added to the random pulse sequence to avoid excessive pitch angles and depths. The control surface deflections must be very accurately measured but need not necessarily be accurately controlled. Manual inputs obtained by following a panel meter display are satisfactory.

After several minutes of maneuvering, the submarine returns to its original depth, heading, and speed. At this time the velocity outputs of the navigator are recorded and compared with the EM log and gyro compass to obtain an estimate of the Schuler error build up.

Assuming the ocean currents are constant, the inertial platform measurements during the maneuvers are with respect to the water mass. This is desirable because the basic equations are hydrodynamic.

The platform errors are mainly at the Schuler frequency (a period of 84 minutes) of about 0.00125 rad/sec. The recommended pseudo pulse sequence has a minimum frequency of about 0.02 rad/sec and a maximum significant frequency of about 0.6 rad/sec. The Schuler errors of the platform can be separated in the frequency domain from the measured motion of the submarine during the pseudo-random maneuver. This insures that the Schuler cycle can be estimated and corrected in order to remove ramps and bias caused by the Schuler oscillation during the maneuver.

A significant instrumentation problem involves converting the navigator outputs in terms of earth fixed coordinates, North, East and vertical velocity and roll, pitch and yaw, to body coordinates of u, v, w, p, q, r and derivatives thereof. The method of accomplishing this is shown in Figure 3. The coordinate transformation represented by Figure 3 must be accomplished with an inaccuracy of less than 0.1% preferably 0.05%.

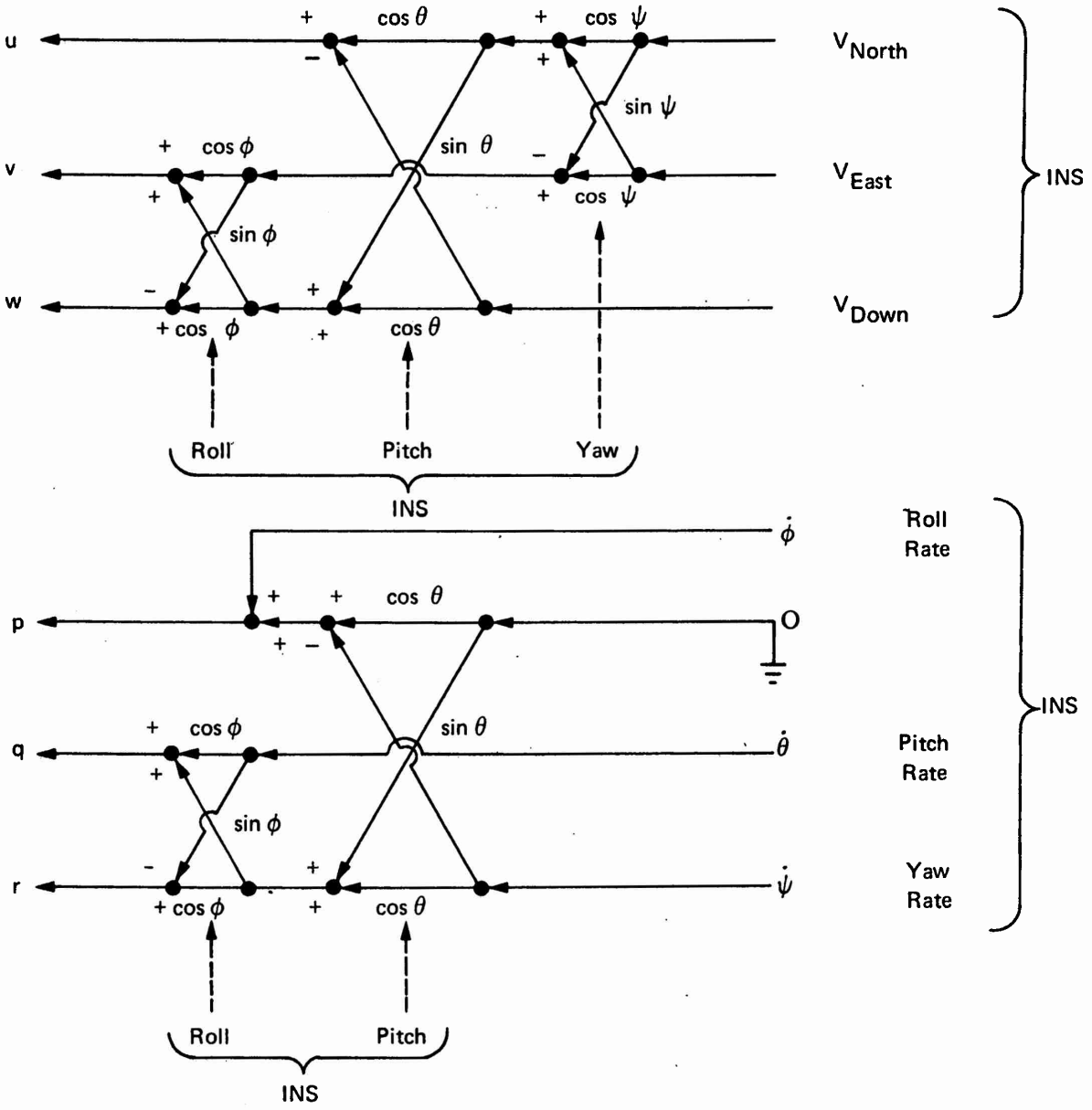

Figure 3. Transformed INS Measurements

The derivatives can be obtained by a combination of processing and smoothing of the basic quantities in such a way that they are in juxtaposition with each other, i.e., lagged equivalently in time or processed by equivalent spectral windows, such that the smoothed quantity is the integral of the smoothed derivative.

A possible alternative to the standard platform type inertial navigator is the strap down inertial navigator. The strap down instrumentation is attractive because the basic measurements are already in the body axes coordinate system. The requirements of coordinate transformations through roll, pitch and yaw still exist however, since the strap down system must be pseudo leveled with respect to the gravity vector. Figure 4 shows how a typical vertical gyro may be simulated by body mounted accelerometers and rate gyros. In order to understand Figure 4 the following equations are helpful.

1) $$\begin{vmatrix} p \\ q \\ r \end{vmatrix} = \begin{vmatrix} & & \\ & R & \\ & & \end{vmatrix} \begin{vmatrix} \dot{\phi} \\ \dot{\theta} \\ \dot{\psi} \end{vmatrix}$$

2) $$\begin{vmatrix} \dot{\phi} \\ \dot{\theta} \\ \dot{\psi} \end{vmatrix} = \begin{vmatrix} & & \\ & R^{-1} & \\ & & \end{vmatrix} \begin{vmatrix} p \\ q \\ r \end{vmatrix}$$

3) $$\begin{vmatrix} & & \\ & R & \\ & & \end{vmatrix} = \begin{vmatrix} 1 & 0 & -\sin\theta \\ 0 & \cos\phi & \cos\theta \sin\phi \\ 0 & -\sin\phi & \cos\theta \cos\phi \end{vmatrix}$$

4) $$\begin{vmatrix} & & \\ & R^{-1} & \\ & & \end{vmatrix} = \begin{vmatrix} 1 & \sin\phi \tan\theta & \cos\phi \tan\theta \\ 0 & \cos\phi & -\sin\phi \\ 0 & -\sin\phi \sec\theta & \cos\phi \sec\theta \end{vmatrix}$$

5) $$a_x = g_x + a_u$$
$$a_y = g_y + a_v$$
$$a_z = g_z + a_w$$

6) $$a_u = \dot{u} + qw - rv$$
$$a_v = \dot{v} + ru - pw$$
$$a_w = \dot{w} + pv - qu$$

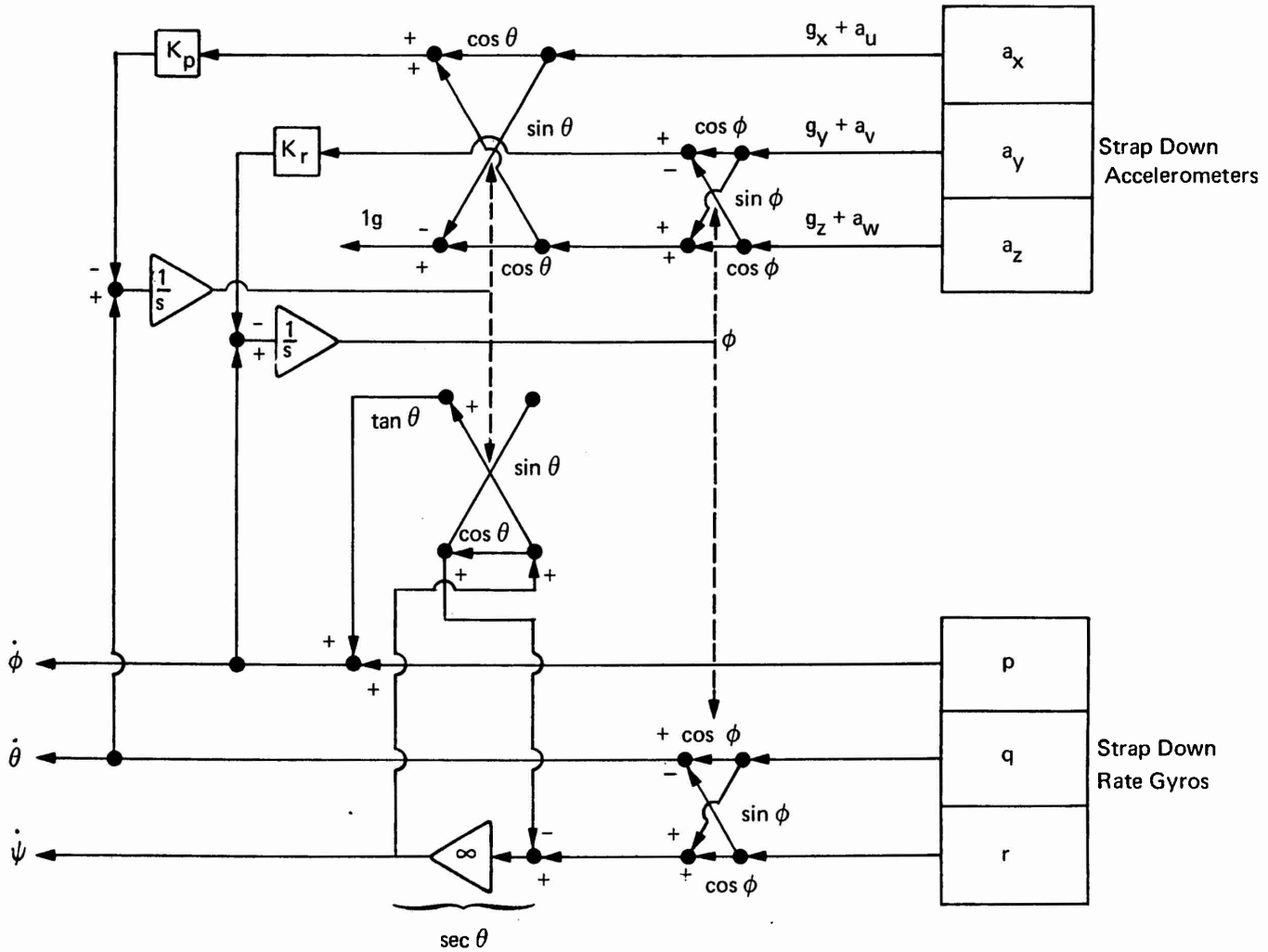

Figure 4. Strap Down Vertical Gyro Simulation with Pendulum Erection

The vertical gyro simulation as shown is capable of a nominal roll and pitch measurement similar to that of an actual gyro. It is reasonably accurate under normal cruise conditions. The gyro leveling loops closed by gain K_p and K_r may be momentarily removed in which case the gyro simulated is a free gyro. The roll axis gain K_r is typically removed during turns. If the rate gyro and accelerometer outputs are encoded for transmission into a digital computer, the mechanization shown becomes strictly computational. A simulated free vertical gyro during maneuvers may be corrected for earth rate and motion over the earth. In this case the simulation begins to resemble a strap down inertial system.

The next step in strap-down motion measurement instrumentation is to indicate the body axis velocity computations. Figure 5 shows a method of instrumenting u, v, and w where u is continually compared with the EM log. The u, v, and w components are then resolved through roll and pitch, integrated and compared with depth. Errors between computed depth and actual depth are used to correct u, v , and w and the gravity computation. Other outputs such as V_{North} and V_{East} can be compared with SINS. V_{North} and V_{East} can be integrated in terms of Latitude and Longitude and these can be compared with outputs from Omega or SINS etc. The total mechanization of Figures 4 and 5 can be computational. The gains K_p, K_r, K_1, K_2, K_3, and K_4 can be based on a covariance computation as per the optimal Kalman filter.

p, q, r and $\dot{p}$, $\dot{q}$, $\dot{r}$ can be obtained with good accuracy by using a rate integrating gyro with feedback between pickoff and torquer. Inaccuracies occur due to scale factor, misalignment, drift of the non-g, g and g^2 type, output axis coupling, earth rate, motion over the earth, and coneing. Nearly all these effects can be compensated by careful measurement of the appropriate gyro characteristics before installation and mechanizing the necessary computational feedbacks between the gyros,accelerometers and other motion measuring equipment. Of course the gyro parameters are random and vary a certain amount from minute to minute, day to day, or turn-on to turn-on, consequently the compensation is never perfect. Lack of compensation, mount vibration, bearing rumble and rotor RPM variations can be considered as gyro noise. Figure 6 avoids these complications but shows the basic p and $\dot{p}$ mechanization. The computation can be made accurate from 0 to 50 Hz (with corrections). Additional filtering (not shown) to eliminate ship's vibration and noise is desirable to prevent aliasing of the data before any digital processing is attempted. The same filters, if required, should be used on the accelerometers. The filters should have negligible phase shift or attenuation from zero to 0.5 Hertz. (This may not be adequate for model submarines).

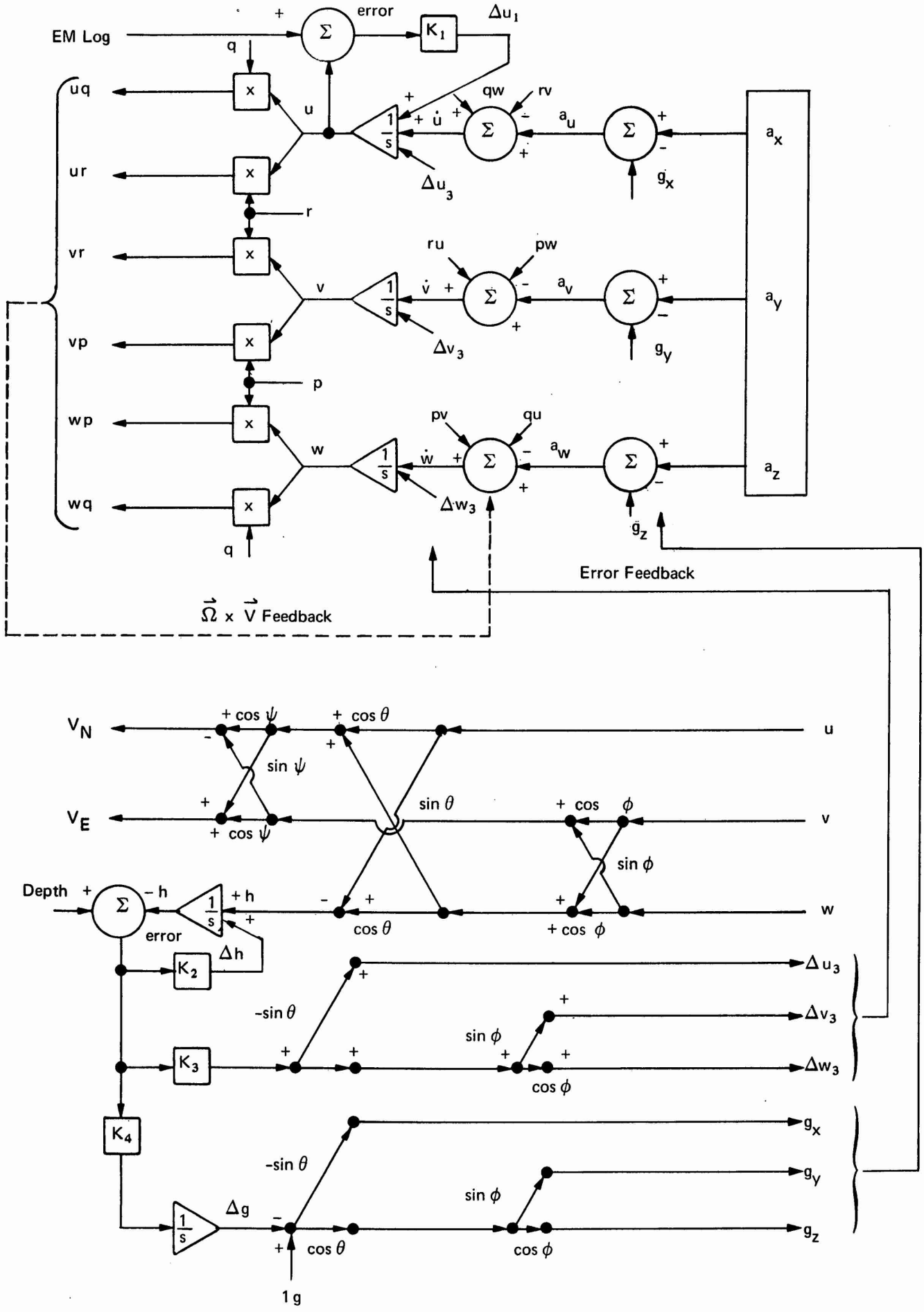

Figure 5. Velocity Computations

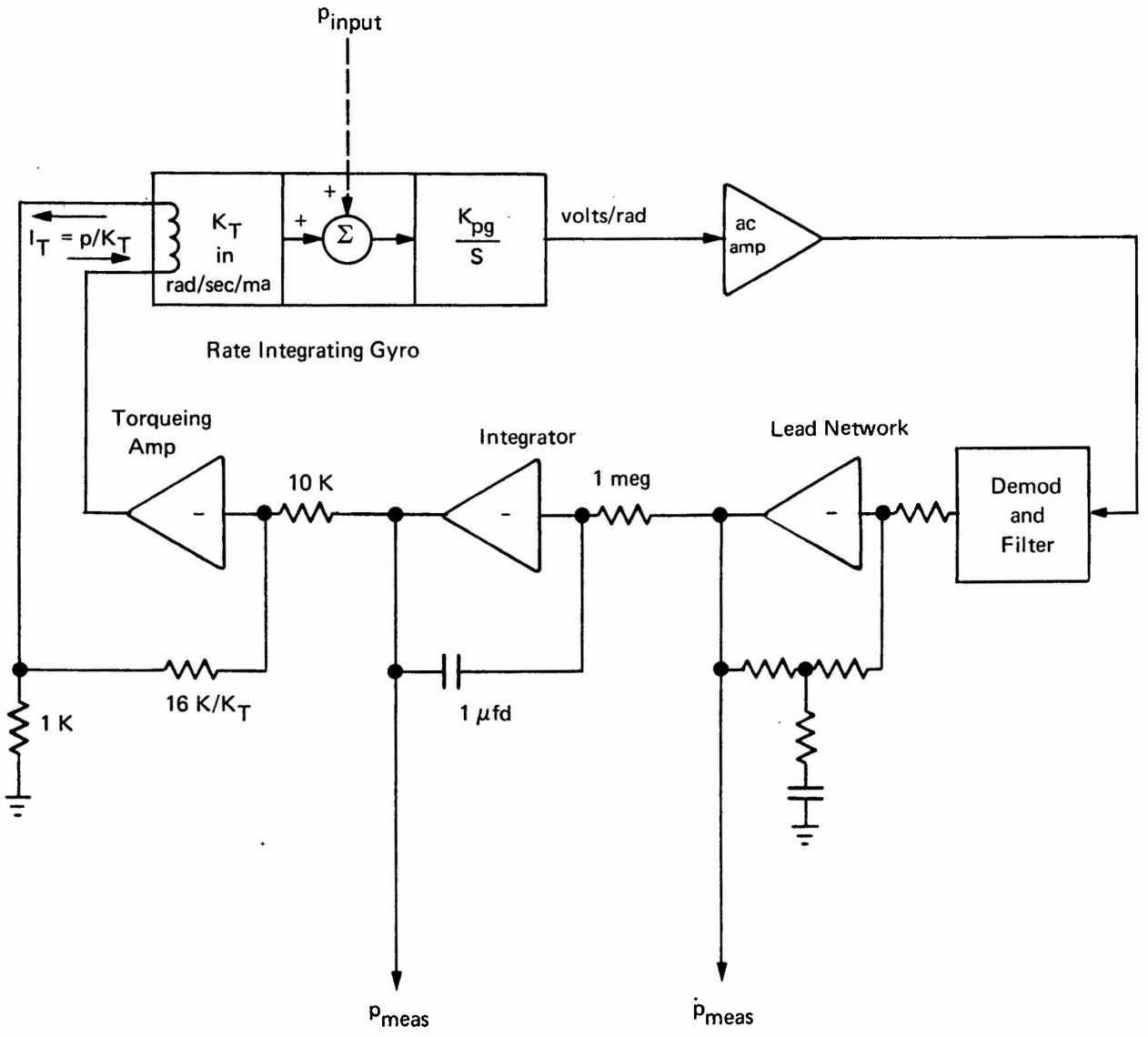

Figure 6. Basic p and $\dot{p}$ Measurement

XI. NOISE FREE PARAMETER ESTIMATE TRAJECTORIES

This section contains typical trajectories of the estimates of the parameters, or coefficients, under the data processing algorithms described in Section VI. The parameter trajectories shown in this section are computed with the assumption of sensor bias, but no sensor noise. The sequence is:

Axial Force Parameters
Rolling Moment Parameters
Pitching Moment Parameters
Normal Force Parameters
Lateral Force Parameters
Yawing Moment Parameters

All trajectories of the estimates have been normalized so that correct estimation yields an ordinate of unity.

A common format is used throughout; the entire set of data is processed twice. On the first pass, five loops are conducted through each equation from time equal to zero and 300 seconds. On the second pass only one loop is conducted. This corresponds to a maximum NP of 2 where NL equals 5 for NP = 1 and NL equals 1 for NP = 2 in Figure 1. The plots for the hydrodynamic coefficients show the entire estimation history in the algorithm of Figure 1.

Since estimates for the bias errors (in the dynamic state variables) are obtained from all the loops of every equation, a different format is employed in the plots of these quantities. Only the estimation response from the final loop for a given NP is shown in these figures.

As the digital plot machine does not provide subscripts, it is necessary to interpret:
XQQ = X_{qq}, etc.

It should be emphasized that the notation used in the plots are, in some cases, not the same as Tables 1 through 6. The subscripting of the hydrodynamic parameters in the tables is that of Reference 3, which is, for some parameters, overly abbreviated. The actual nature of the hydrodynamic effect is therefore obscured. For this reason the notation used in the plot figures has been modified so that the true nature of the hydrodynamic effect is indicated. The presentation of the parameters in the plots is in the same order as that of the tables.

The phenomena of rapid fluctuation observed in the yaw curves near the beginning of pass 2 is not readily understood, since one would not expect it to occur. It should be pointed out that on pass 2 the covariance matrix for the parameters is restarted and the measurement noise level is significantly lowered. Therefore the Kalman gains are "wide-open" to allow large deviations. Note also that the roll and pitch angular acceleration rate errors are not estimated at the time that the estimates of the parameters dip. These may account for the dip that the estimates show in the interval $70<t<150$ seconds. Consider also that unique determination of the yaw coefficients is heavily linked to blowing ballast, which occurs at 150 seconds -- when the rapid convergence occurs. This effect accounts for the convergence to correct values observed at $t>150$ seconds. The covariance matrix for the parameters did show a rapid decrease, so that a rapid fluctuation of the estimates is not unexpected.

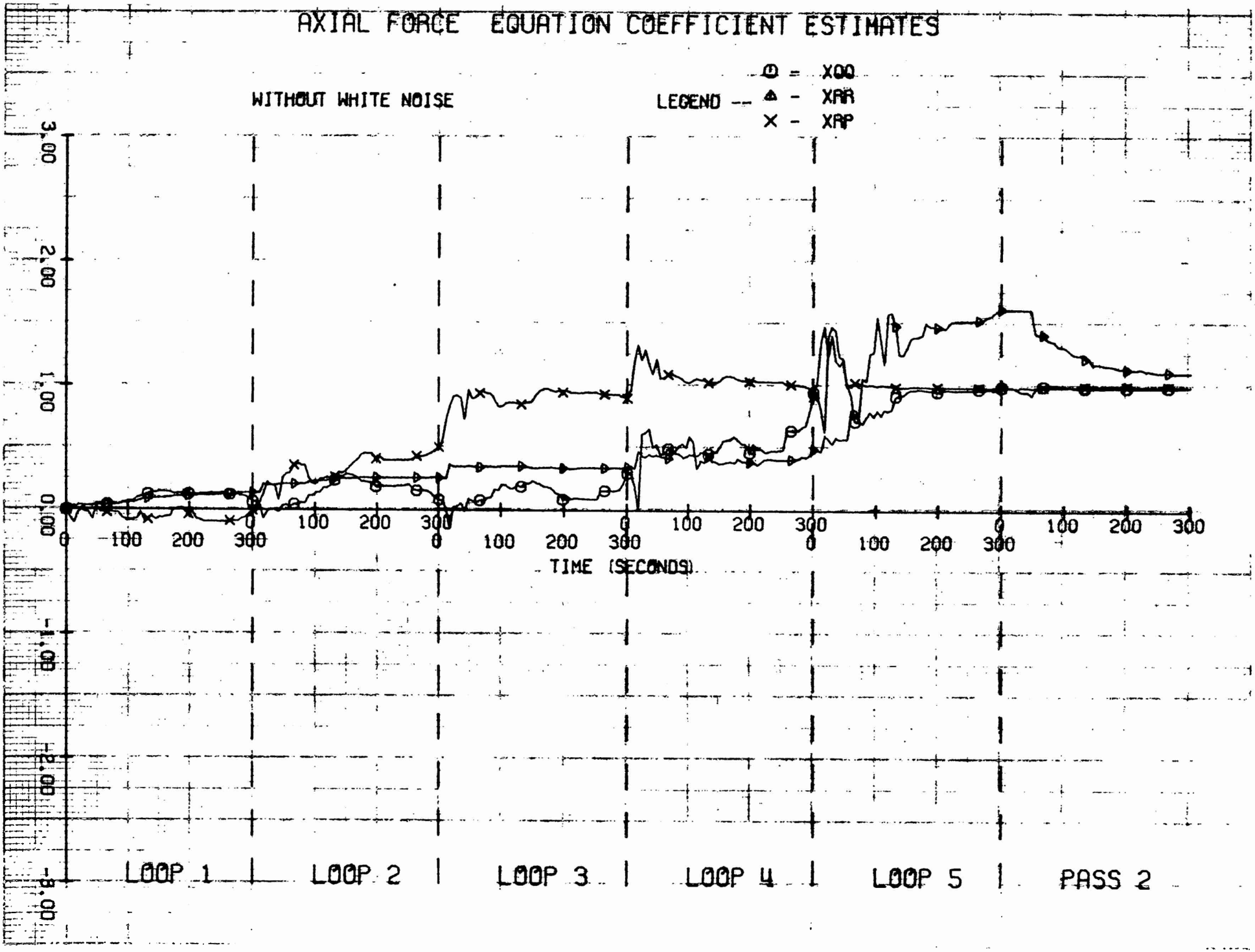
AXIAL FORCE EQUATION COEFFICIENT ESTIMATES
WITHOUT WHITE NOISE
LEGEND -- ① = XQQ
△ - XAA
× - XAP
3.00
2.00
1.00
0.00
-1.00
-2.00
-3.00
0 100 200 300
TIME (SECONDS)
LOOP 1
LOOP 2
LOOP 3
LOOP 4
LOOP 5
PASS 2

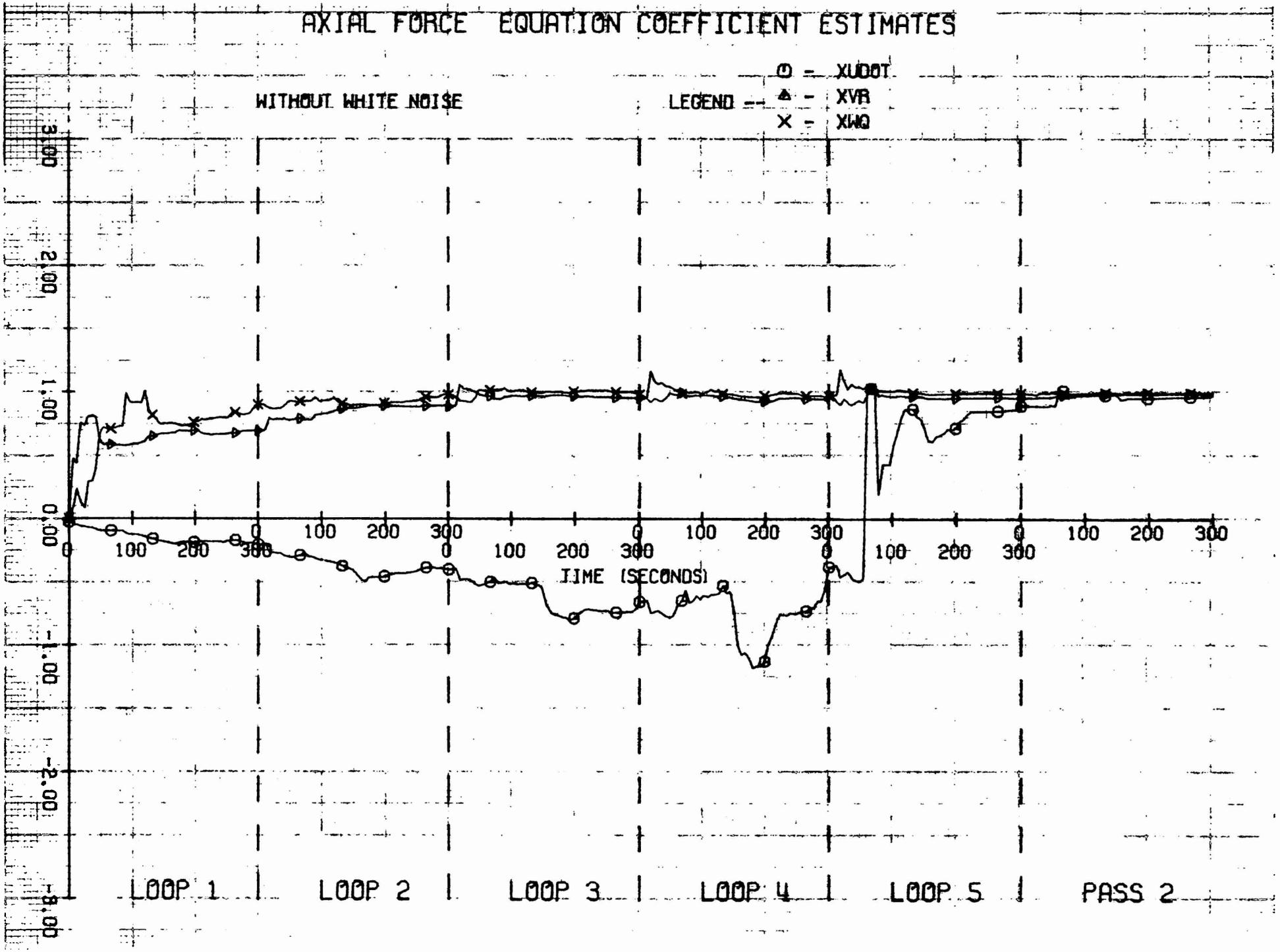
AXIAL FORCE EQUATION COEFFICIENT ESTIMATES
WITHOUT WHITE NOISE
LEGEND -- ⊙ - XUDOT
△ - XVR
X - XWQ
3.00
2.00
1.00
0.00
-1.00
-2.00
-3.00
0
100
200
300
TIME (SECONDS)
LOOP 1
LOOP 2
LOOP 3
LOOP 4
LOOP 5
PASS 2

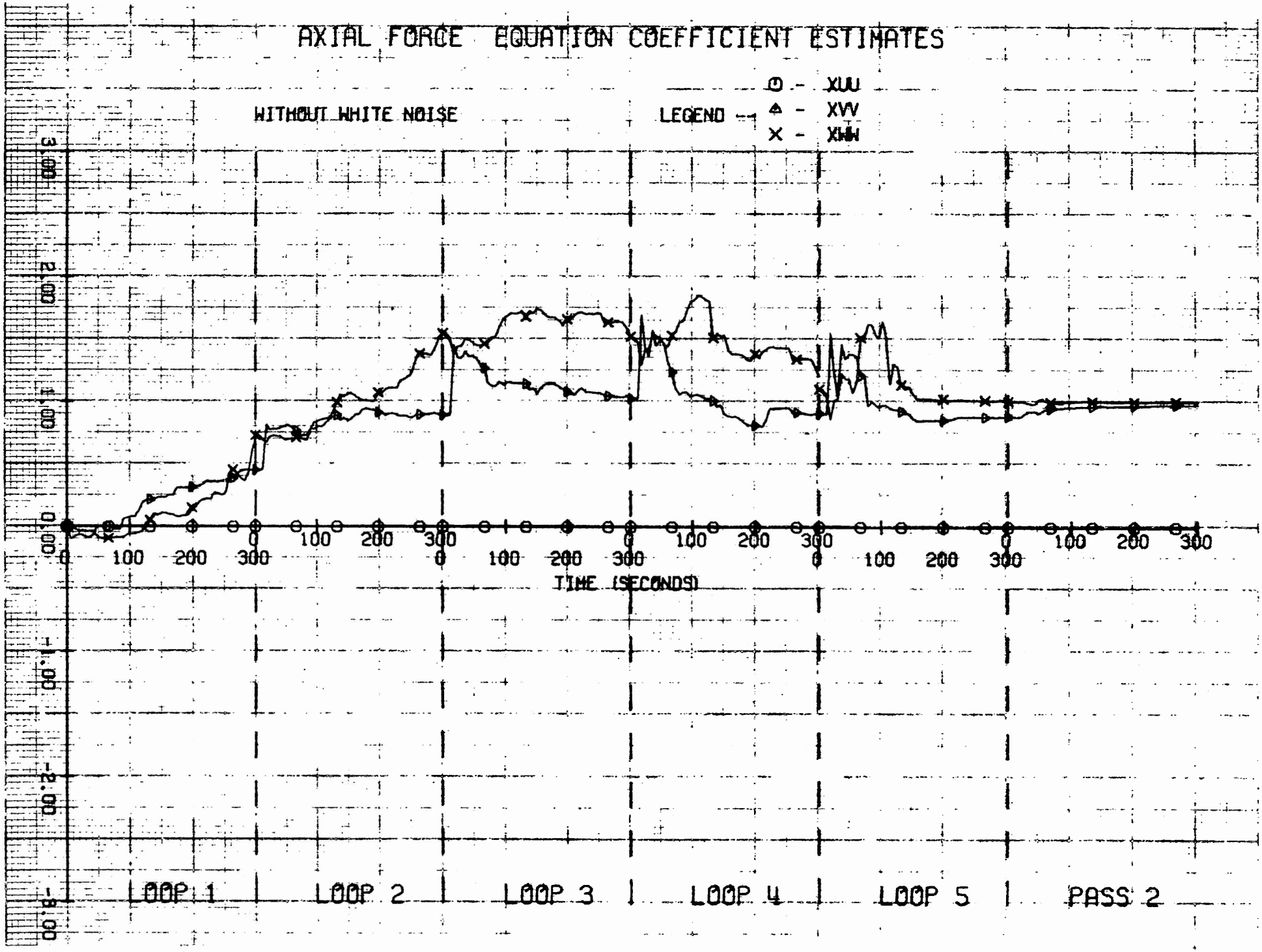
AXIAL FORCE EQUATION COEFFICIENT ESTIMATES
WITHOUT WHITE NOISE
LEGEND --
XUU
XVV
XWW
3.00
2.00
1.00
0.00
-1.00
-2.00
-3.00
0
100
200
300
TIME (SECONDS)
LOOP 1
LOOP 2
LOOP 3
LOOP 4
LOOP 5
PASS 2

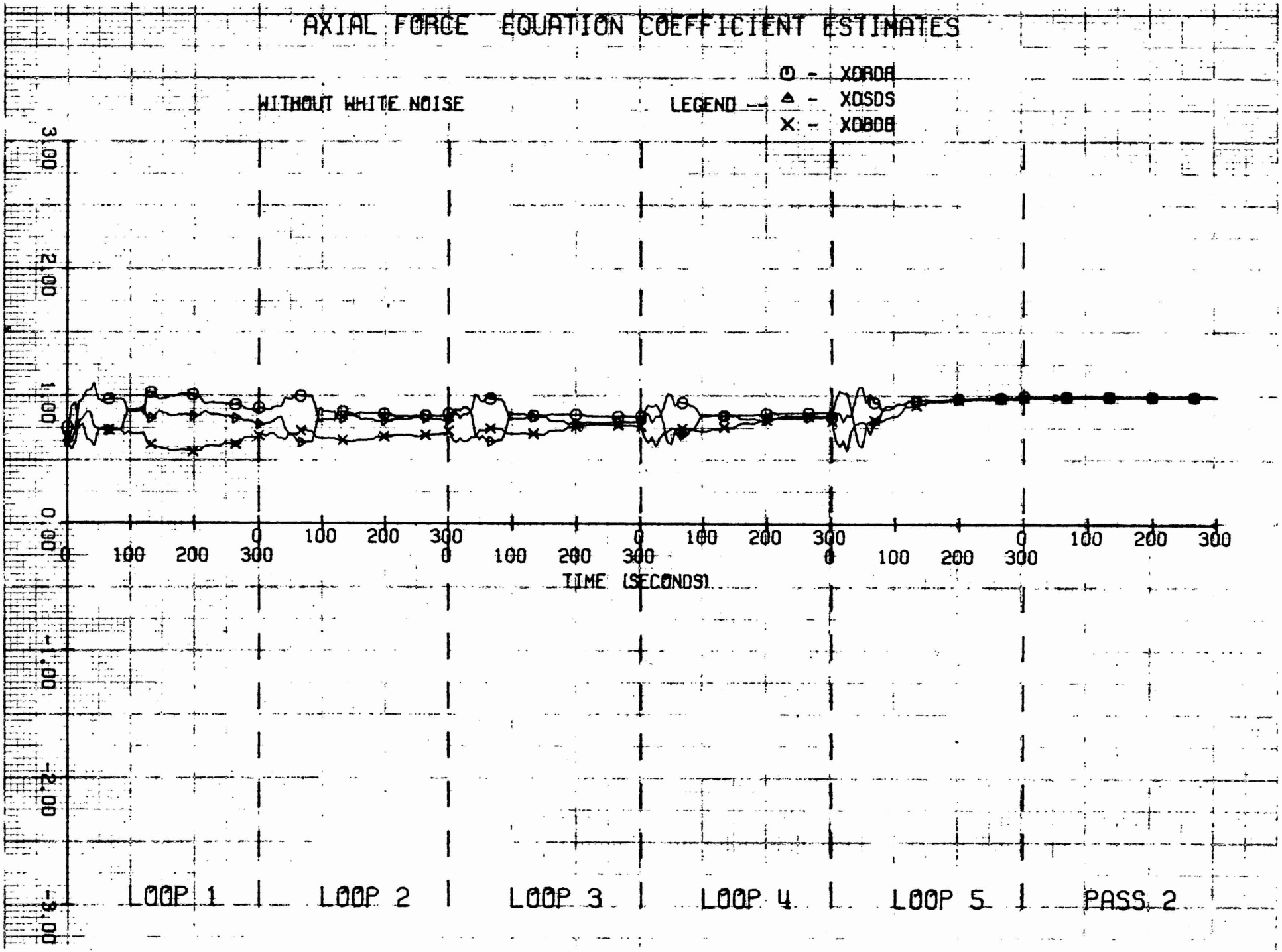
AXIAL FORCE EQUATION COEFFICIENT ESTIMATES
WITHOUT WHITE NOISE
LEGEND
XDRDR
XDSDS
XDBDB
3.00
2.00
1.00
0.00
-1.00
-2.00
-3.00
0
100
200
300
TIME (SECONDS)
LOOP 1
LOOP 2
LOOP 3
LOOP 4
LOOP 5
PASS 2

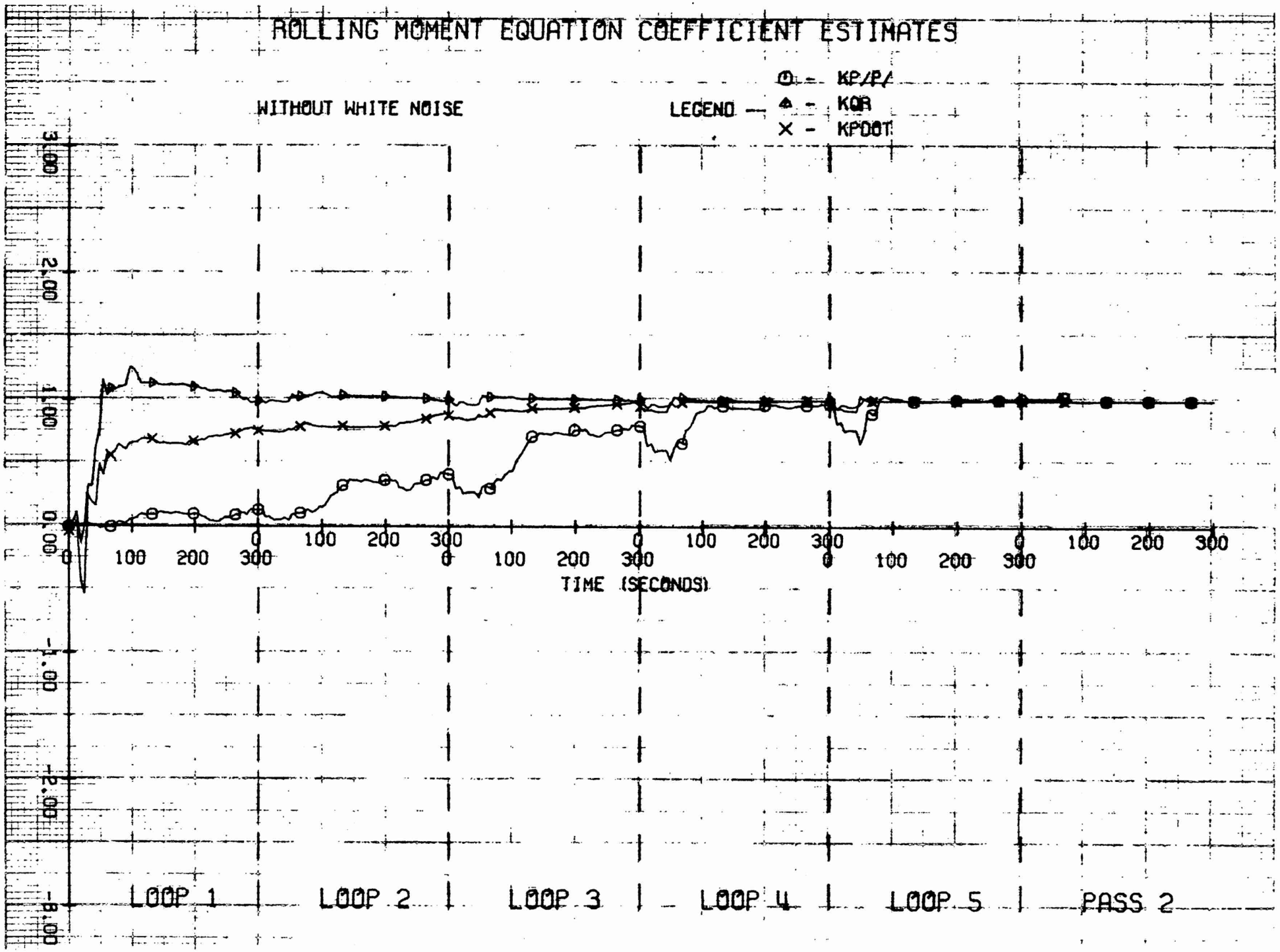
ROLLING MOMENT EQUATION COEFFICIENT ESTIMATES
WITHOUT WHITE NOISE
LEGEND
KP/P/
KQR
KPDOT
3.00
2.00
1.00
0.00
-1.00
-2.00
-3.00
0
100
200
300
TIME (SECONDS)
LOOP 1
LOOP 2
LOOP 3
LOOP 4
LOOP 5
PASS 2

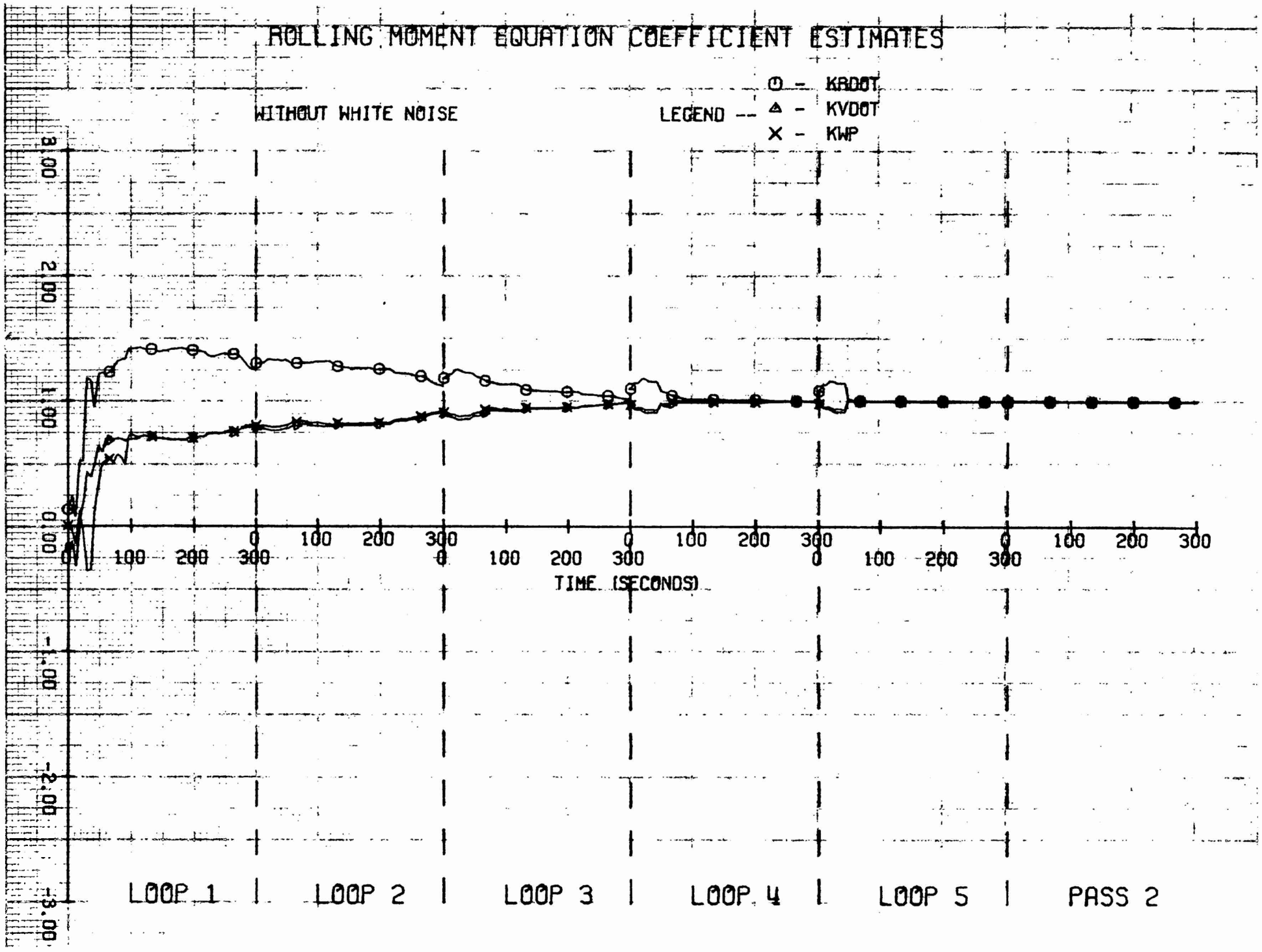
ROLLING MOMENT EQUATION COEFFICIENT ESTIMATES
WITHOUT WHITE NOISE
LEGEND -- ○ - KRDOT
△ - KVDOT
× - KWP
3.00
2.00
1.00
0.00
-1.00
-2.00
-3.00
0
100
200
300
TIME (SECONDS)
LOOP 1
LOOP 2
LOOP 3
LOOP 4
LOOP 5
PASS 2

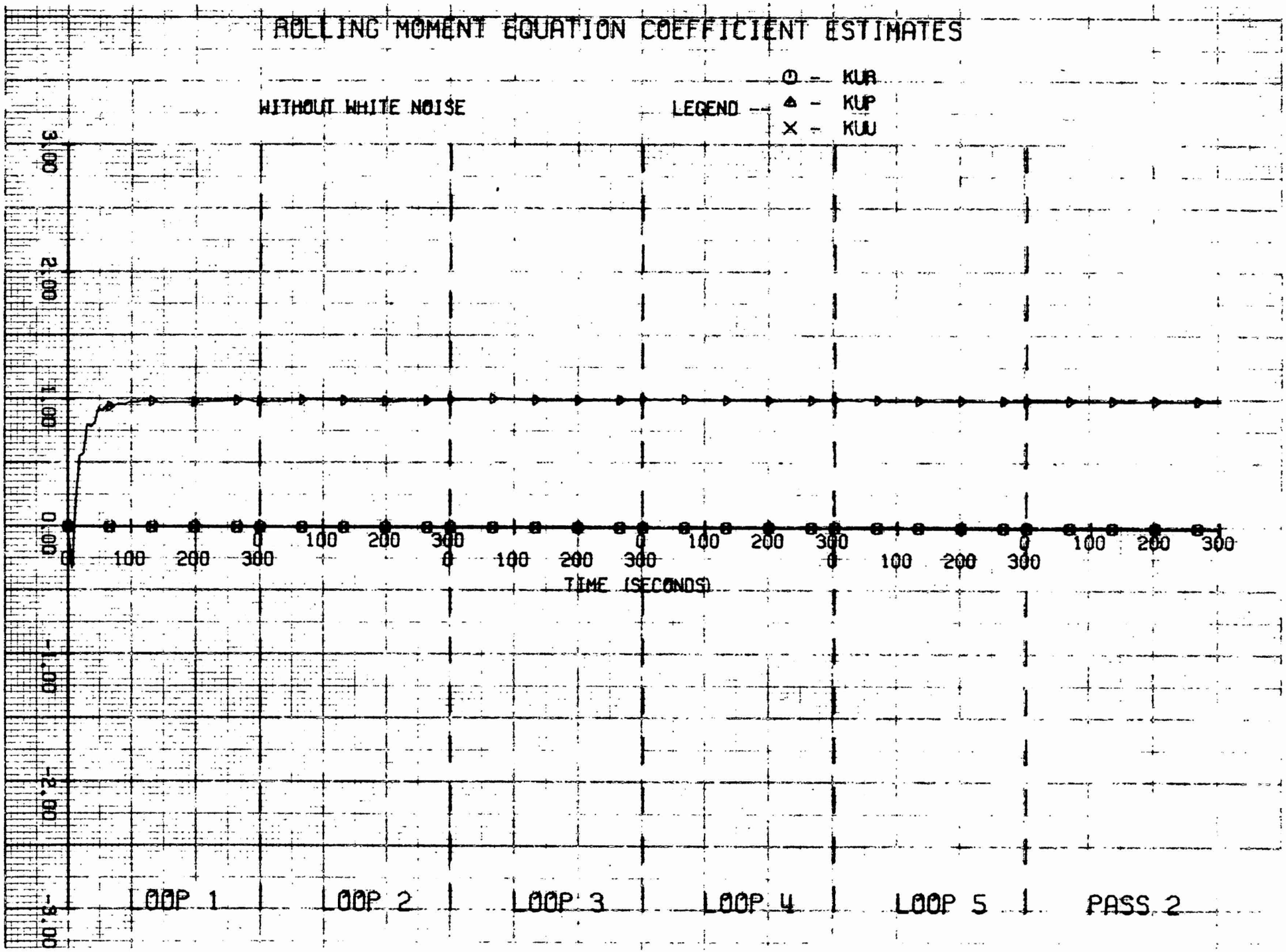
ROLLING MOMENT EQUATION COEFFICIENT ESTIMATES
WITHOUT WHITE NOISE
LEGEND -- ⊙ - KUR
△ - KUP
× - KUU
3.00
2.00
1.00
0.00
-1.00
-2.00
-3.00
0 100 200 300 0 100 200 300 0 100 200 300 0 100 200 300
TIME (SECONDS)
LOOP 1
LOOP 2
LOOP 3
LOOP 4
LOOP 5
PASS 2

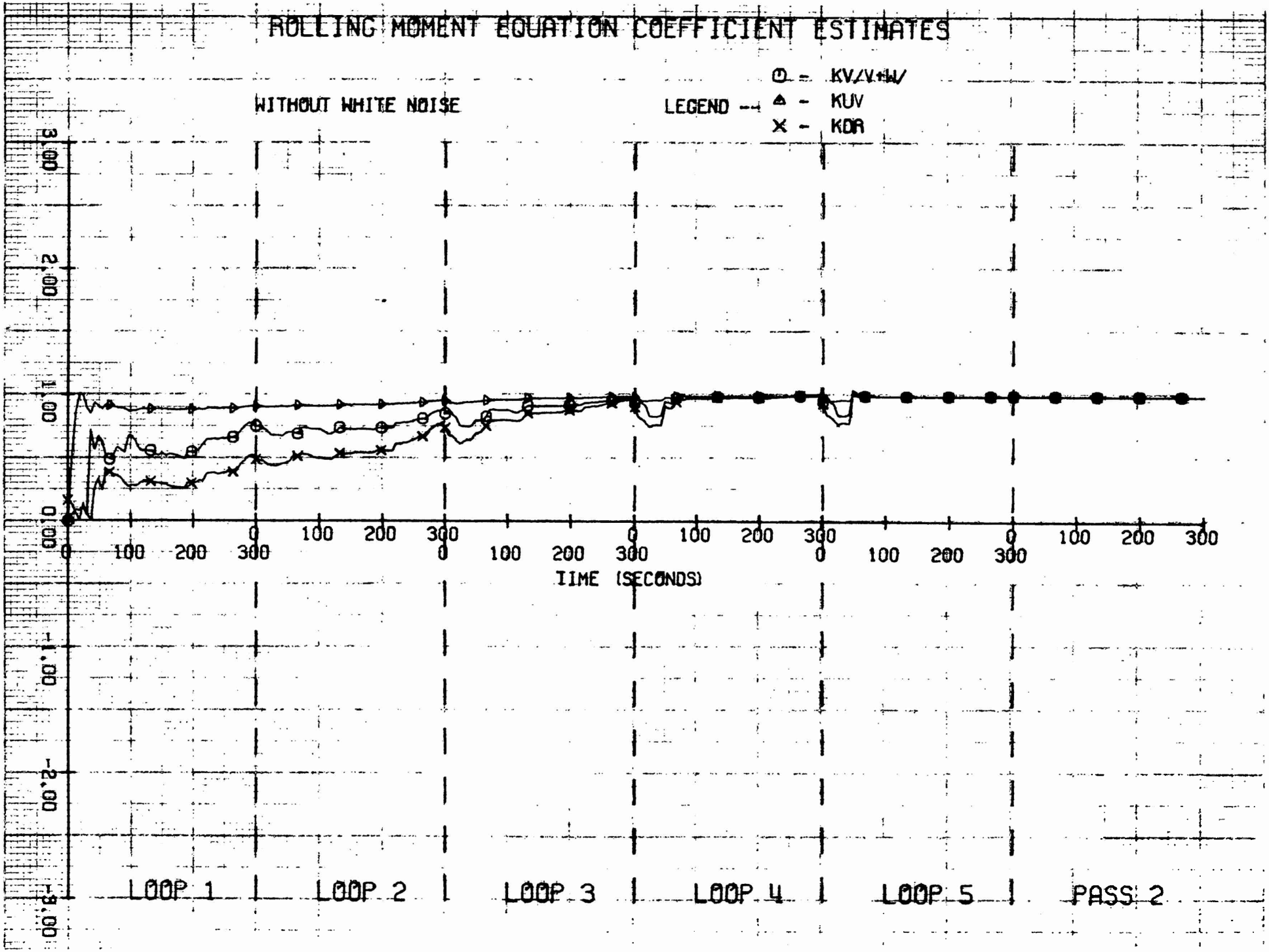
ROLLING MOMENT EQUATION COEFFICIENT ESTIMATES
WITHOUT WHITE NOISE
LEGEND --
KV/V+W/
KUV
KDR
3.00
2.00
1.00
0.00
-1.00
-2.00
-3.00
0
100
200
300
TIME (SECONDS)
LOOP 1
LOOP 2
LOOP 3
LOOP 4
LOOP 5
PASS 2

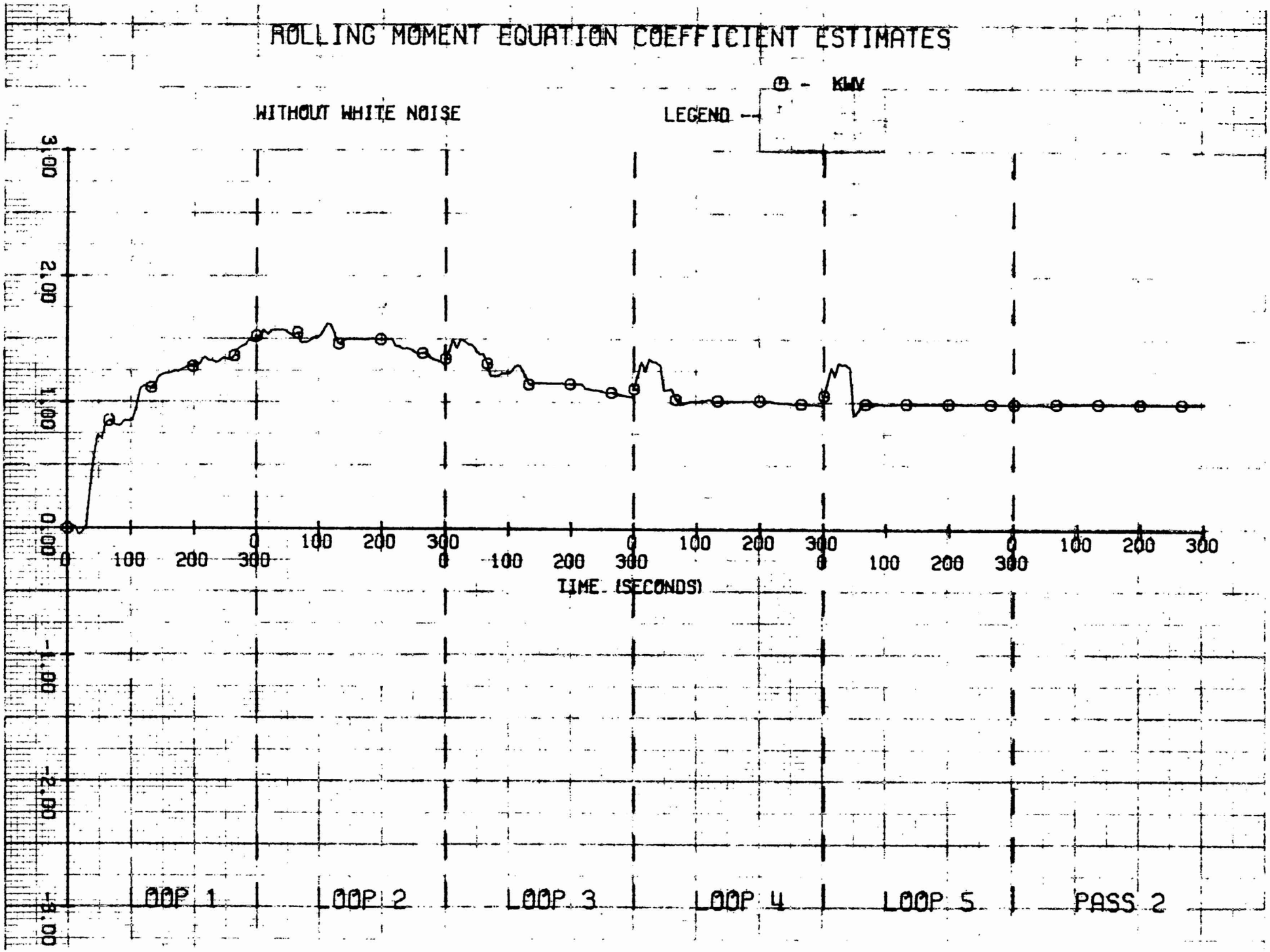
ROLLING MOMENT EQUATION COEFFICIENT ESTIMATES
WITHOUT WHITE NOISE
LEGEND
Ⓐ - KMV
3.00
2.00
1.00
0.00
-1.00
-2.00
-3.00
0
100
200
300
TIME (SECONDS)
LOOP 1
LOOP 2
LOOP 3
LOOP 4
LOOP 5
PASS 2

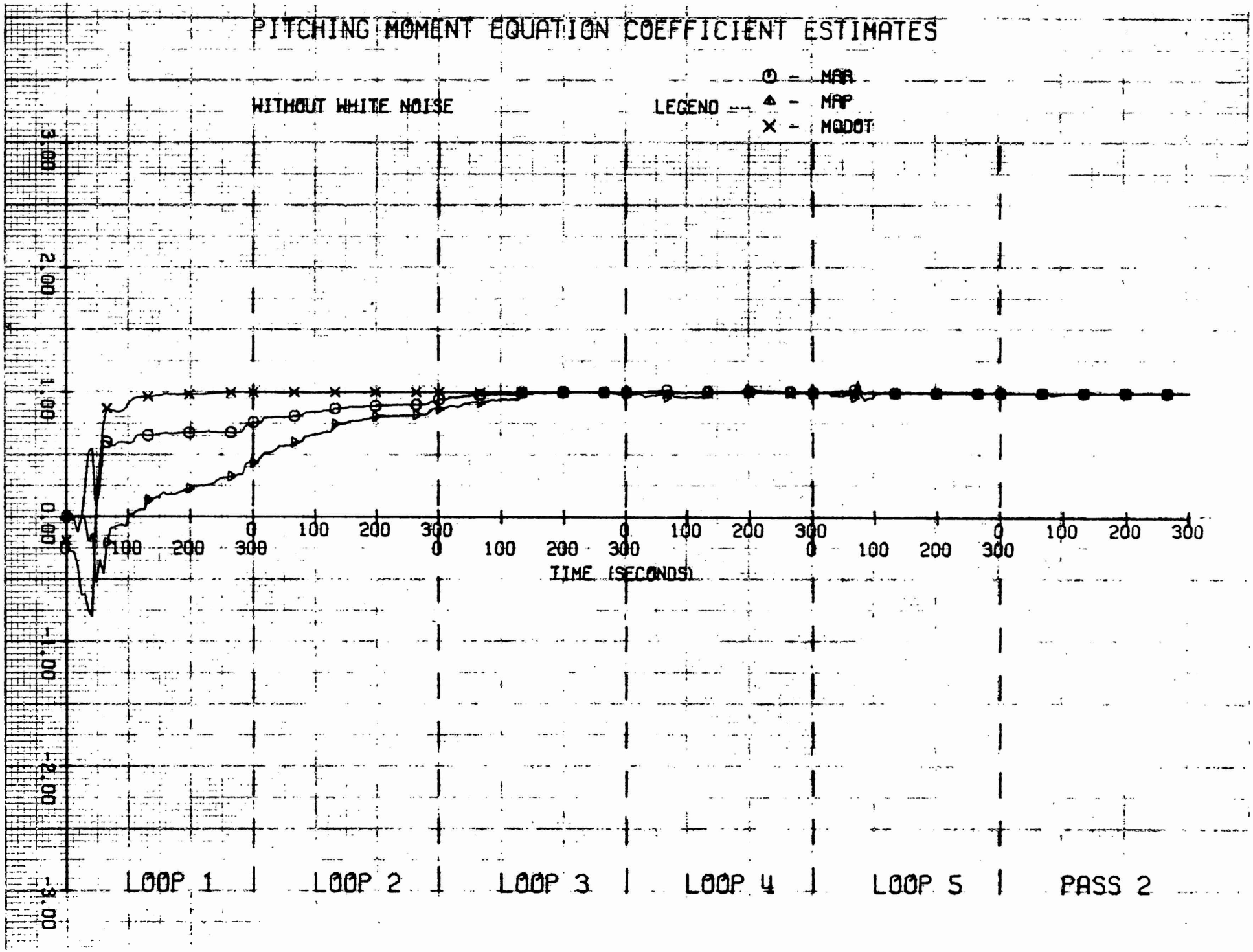
PITCHING MOMENT EQUATION COEFFICIENT ESTIMATES
WITHOUT WHITE NOISE
LEGEND --
- MAR
- MAP
- MQDOT
3.00
2.00
1.00
0.00
-1.00
-2.00
-3.00
0
100
200
300
TIME (SECONDS)
LOOP 1
LOOP 2
LOOP 3
LOOP 4
LOOP 5
PASS 2

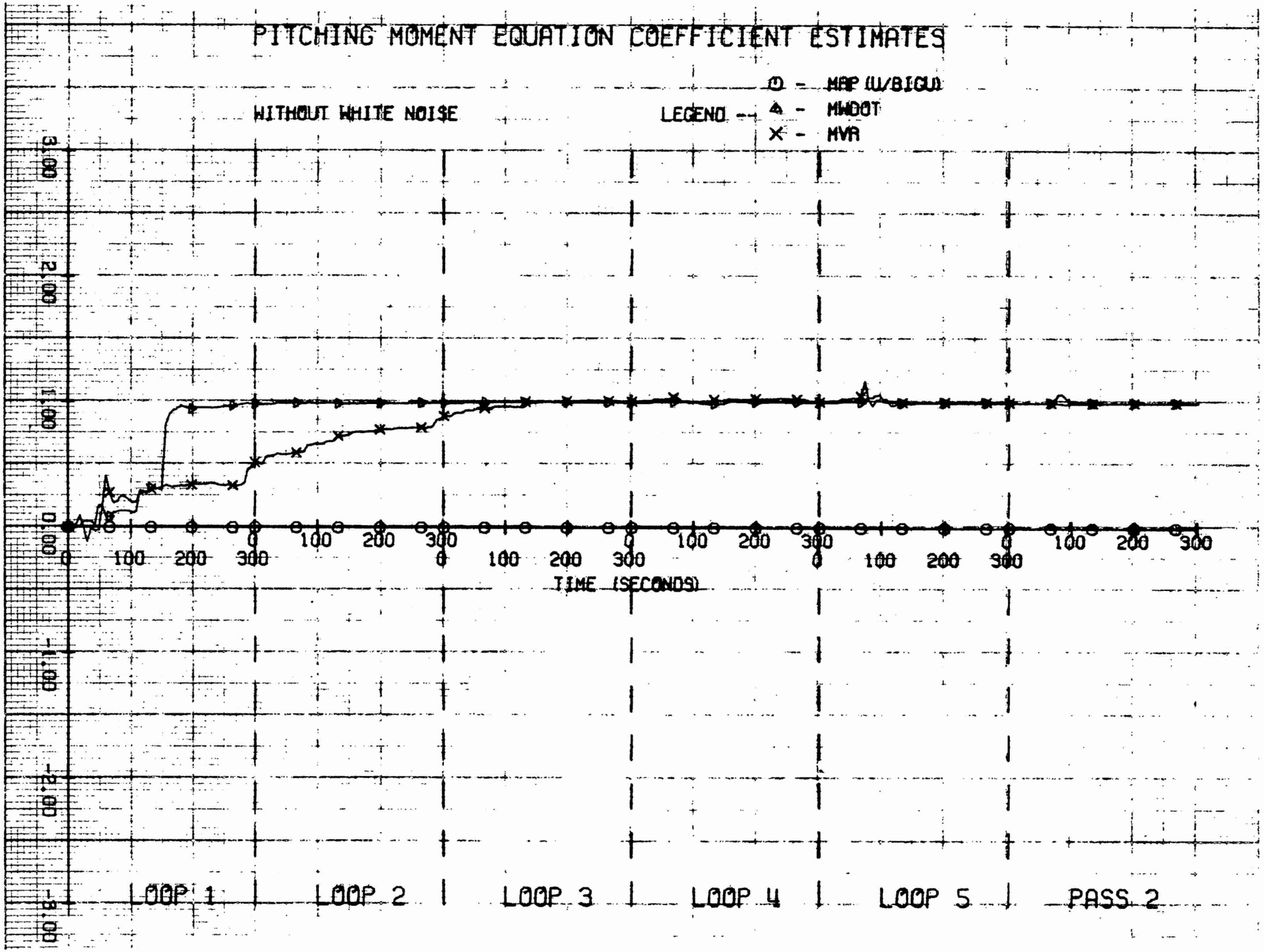
PITCHING MOMENT EQUATION COEFFICIENT ESTIMATES
WITHOUT WHITE NOISE
LEGEND --
MAP (U/BIGU)
MWDOT
MVR
3.00
2.00
1.00
0.00
-1.00
-2.00
-3.00
0
100
200
300
TIME (SECONDS)
LOOP 1
LOOP 2
LOOP 3
LOOP 4
LOOP 5
PASS 2

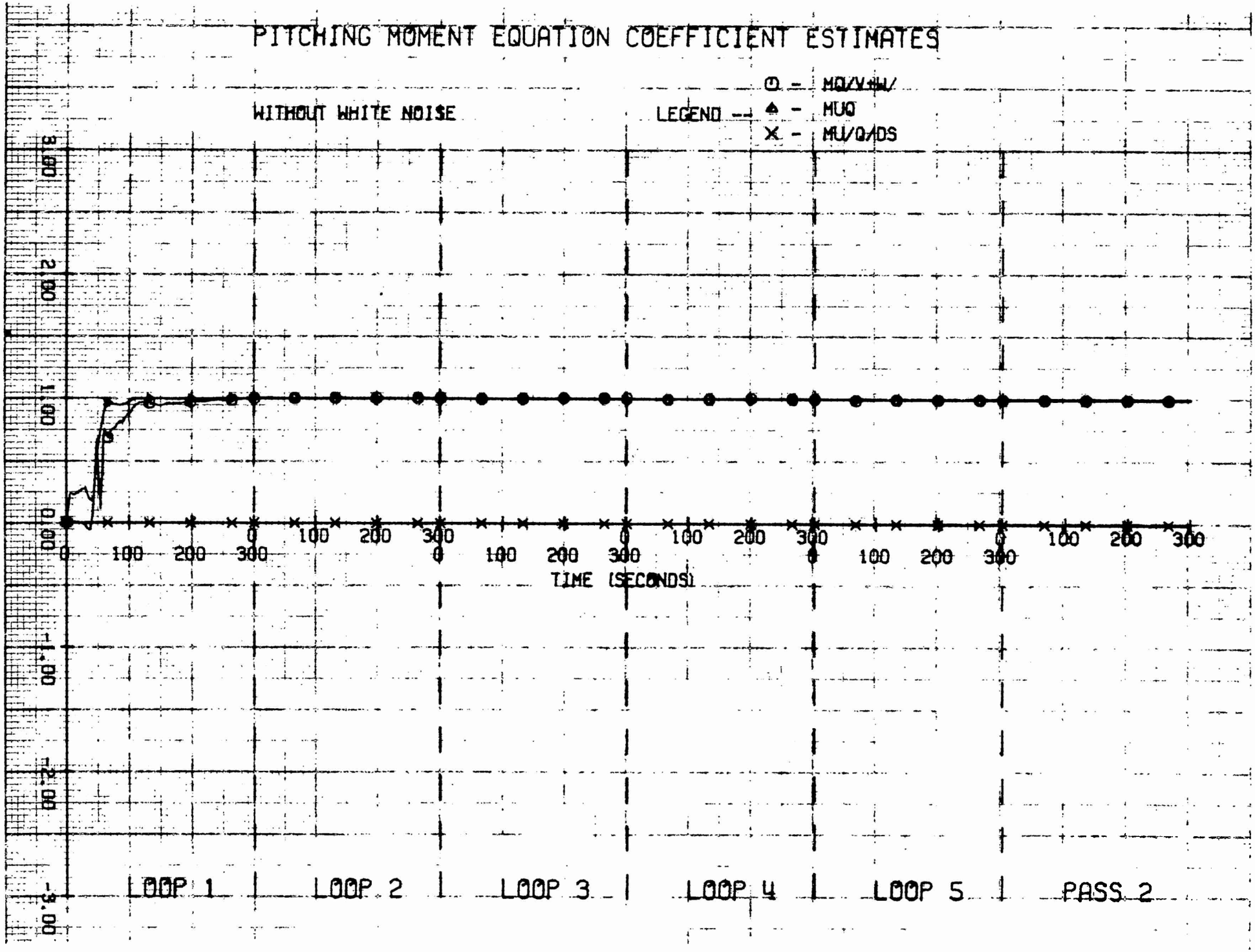
PITCHING MOMENT EQUATION COEFFICIENT ESTIMATES
WITHOUT WHITE NOISE
LEGEND --
MQ/V+W/
MUQ
MU/Q/DS
3.00
2.00
1.00
0.00
-1.00
-2.00
-3.00
0
100
200
300
TIME (SECONDS)
LOOP 1
LOOP 2
LOOP 3
LOOP 4
LOOP 5
PASS 2

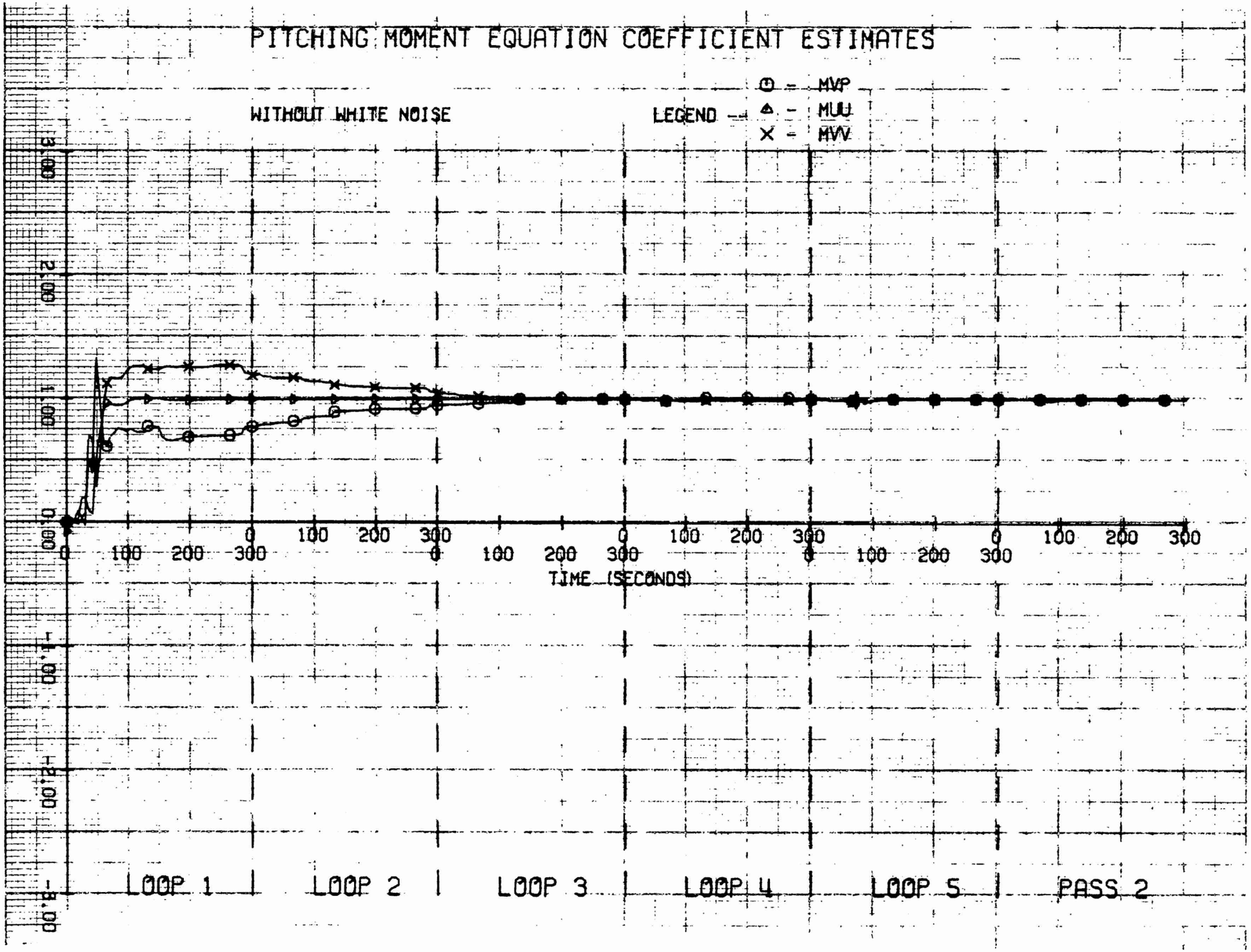
PITCHING MOMENT EQUATION COEFFICIENT ESTIMATES
WITHOUT WHITE NOISE
LEGEND -- MVP
MUU
MVV
3.00
2.00
1.00
0.00
-1.00
-2.00
-3.00
0 100 200 300 0 100 200 300 0 100 200 300 0 100 200 300
TIME (SECONDS)
LOOP 1
LOOP 2
LOOP 3
LOOP 4
LOOP 5
PASS 2

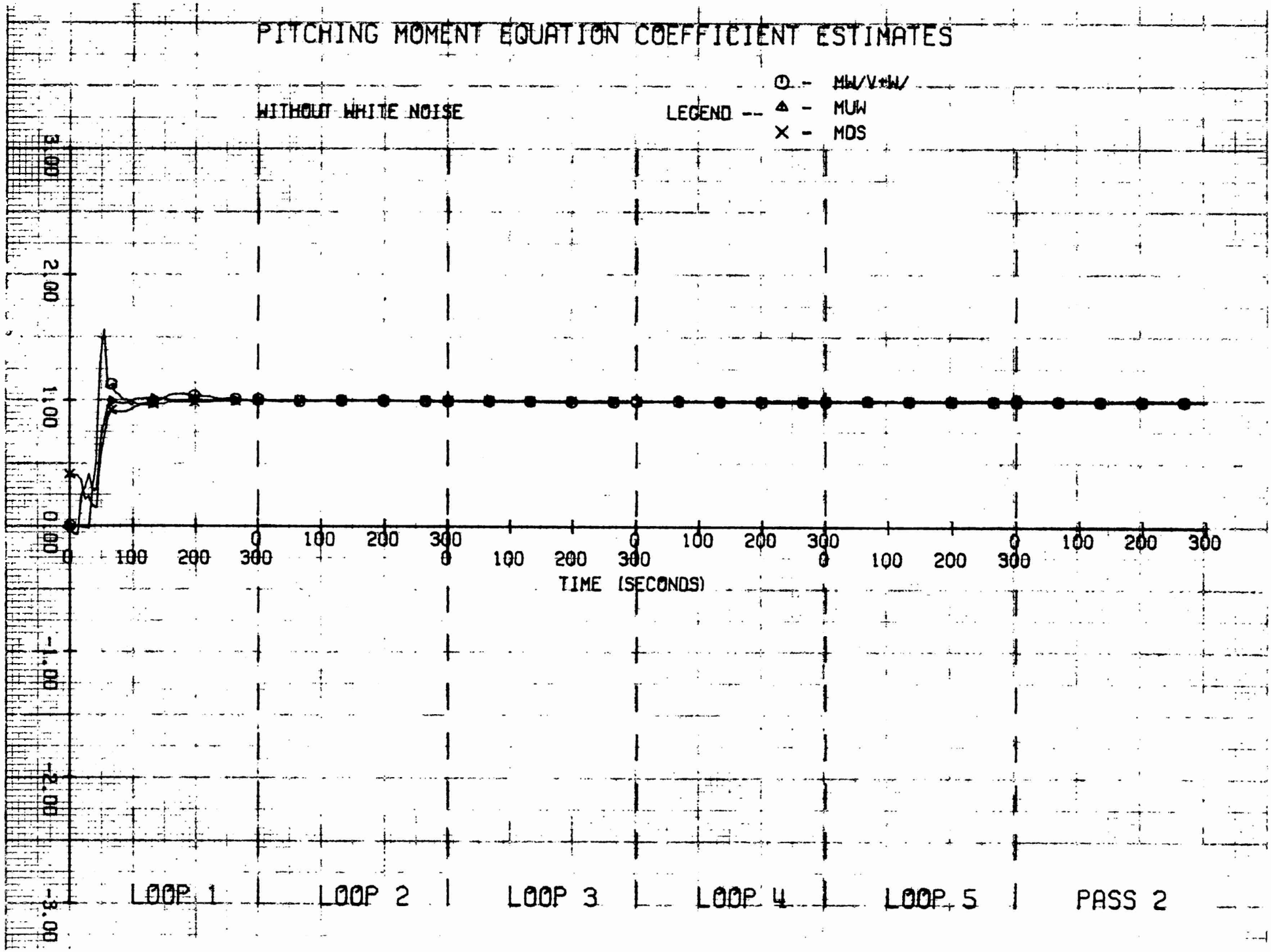
PITCHING MOMENT EQUATION COEFFICIENT ESTIMATES
WITHOUT WHITE NOISE
LEGEND --
⊙ - MW/V+W/
△ - MUW
× - MDS
3.00
2.00
1.00
0.00
-1.00
-2.00
-3.00
0
100
200
300
TIME (SECONDS)
LOOP 1
LOOP 2
LOOP 3
LOOP 4
LOOP 5
PASS 2

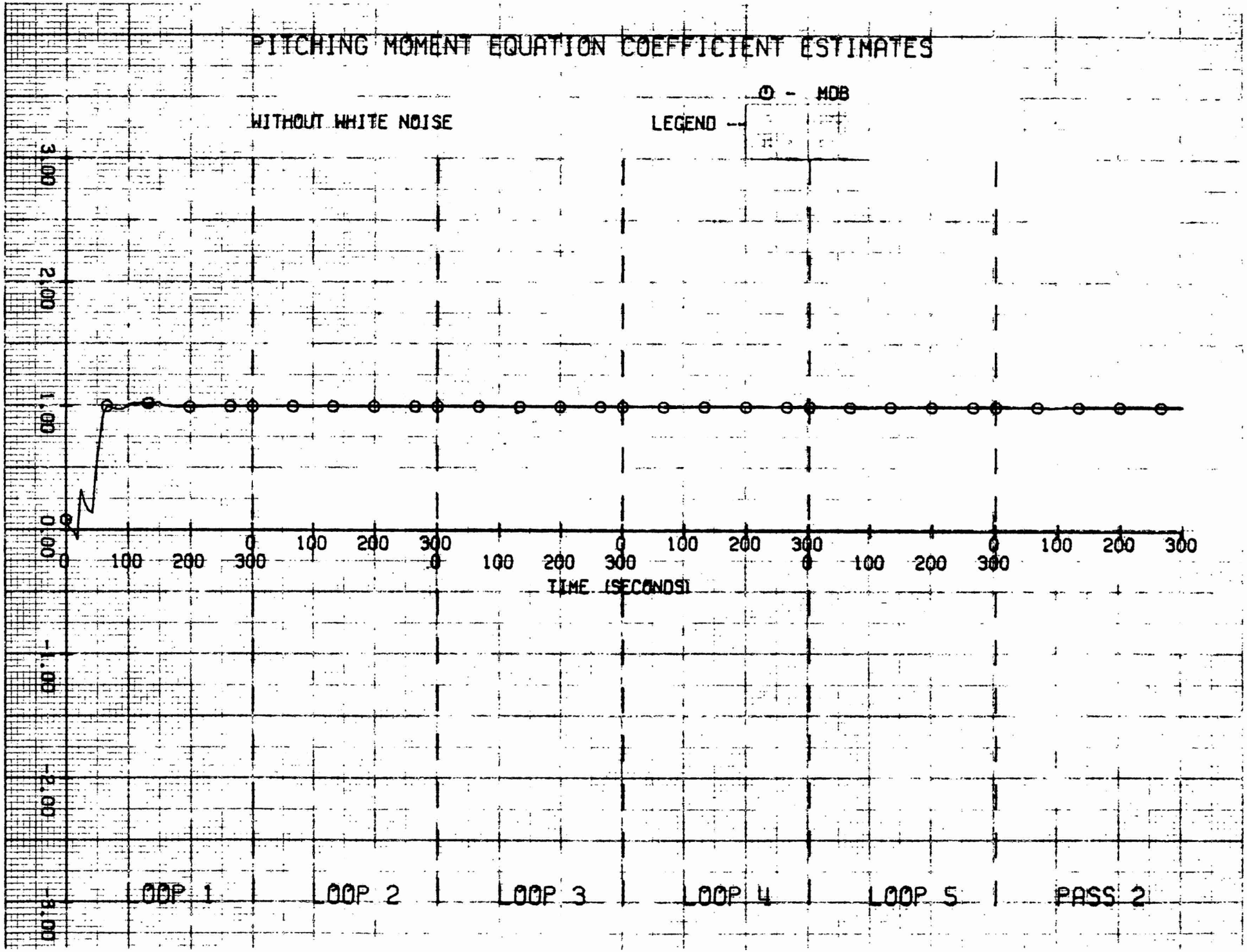
PITCHING MOMENT EQUATION COEFFICIENT ESTIMATES
WITHOUT WHITE NOISE
LEGEND -- ⊙ - MDB
3.00
2.00
1.00
0.00
-1.00
-2.00
-3.00
0
100
200
300
TIME (SECONDS)
LOOP 1
LOOP 2
LOOP 3
LOOP 4
LOOP 5
PASS 2

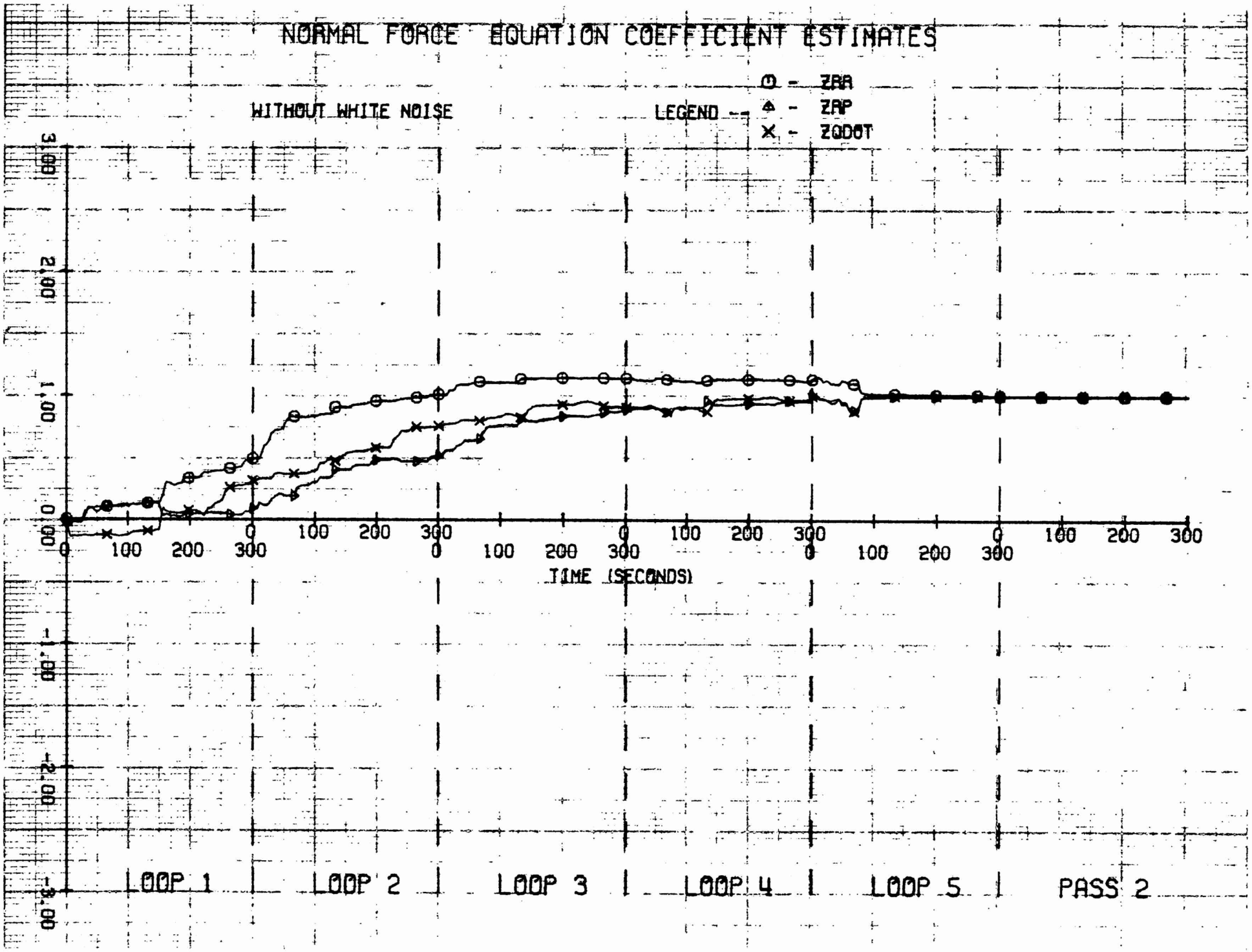
NORMAL FORCE EQUATION COEFFICIENT ESTIMATES
WITHOUT WHITE NOISE
LEGEND --
- ZBA
- ZAP
- ZQDOT
3.00
2.00
1.00
0.00
-1.00
-2.00
-3.00
0
100
200
300
TIME (SECONDS)
LOOP 1
LOOP 2
LOOP 3
LOOP 4
LOOP 5
PASS 2

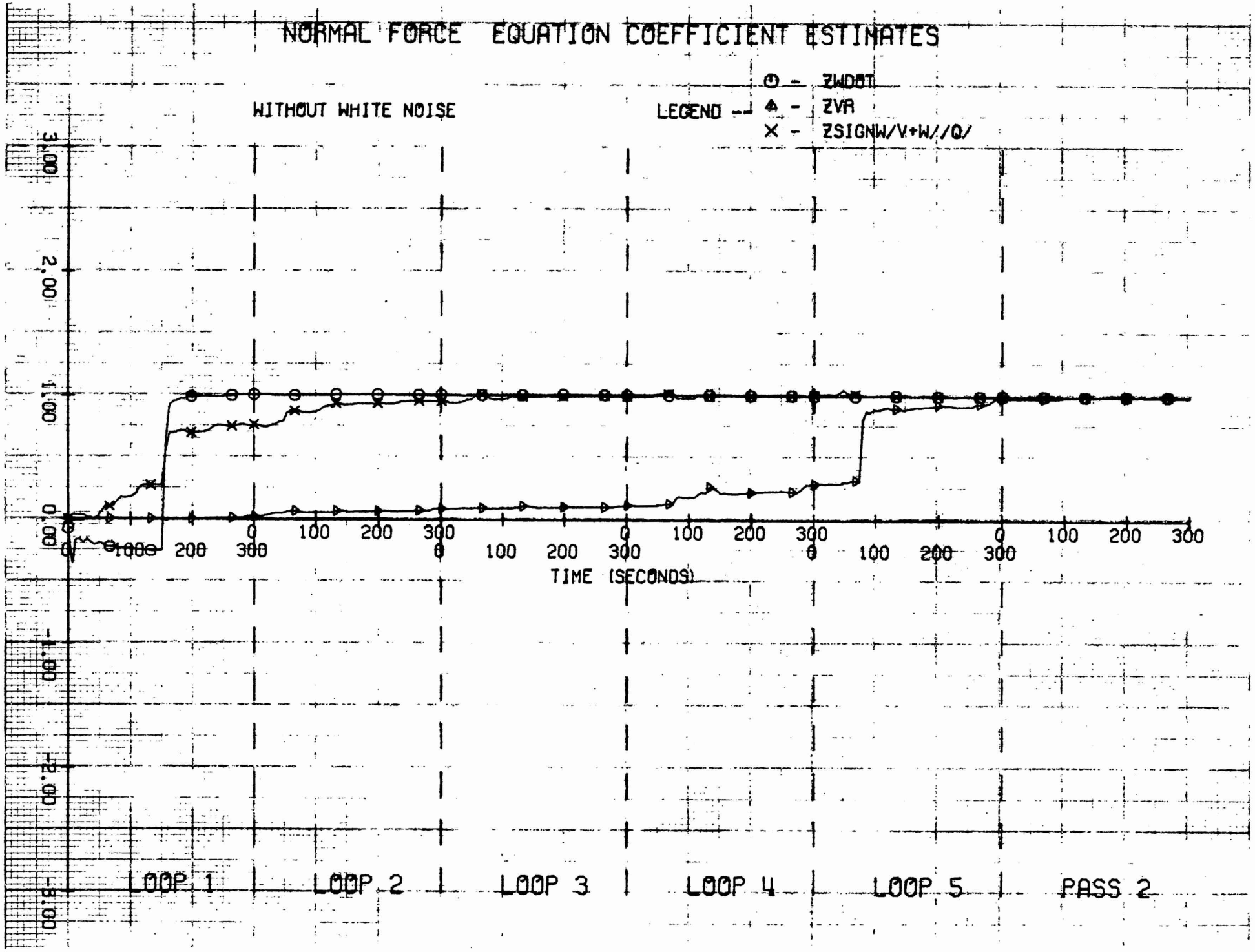
NORMAL FORCE EQUATION COEFFICIENT ESTIMATES
WITHOUT WHITE NOISE
LEGEND --
⊙ - ZWDOT
△ - ZVR
× - ZSIGNW/V+W//Q/
3.00
2.00
1.00
0.00
-1.00
-2.00
-3.00
0
100
200
300
TIME (SECONDS)
LOOP 1
LOOP 2
LOOP 3
LOOP 4
LOOP 5
PASS 2

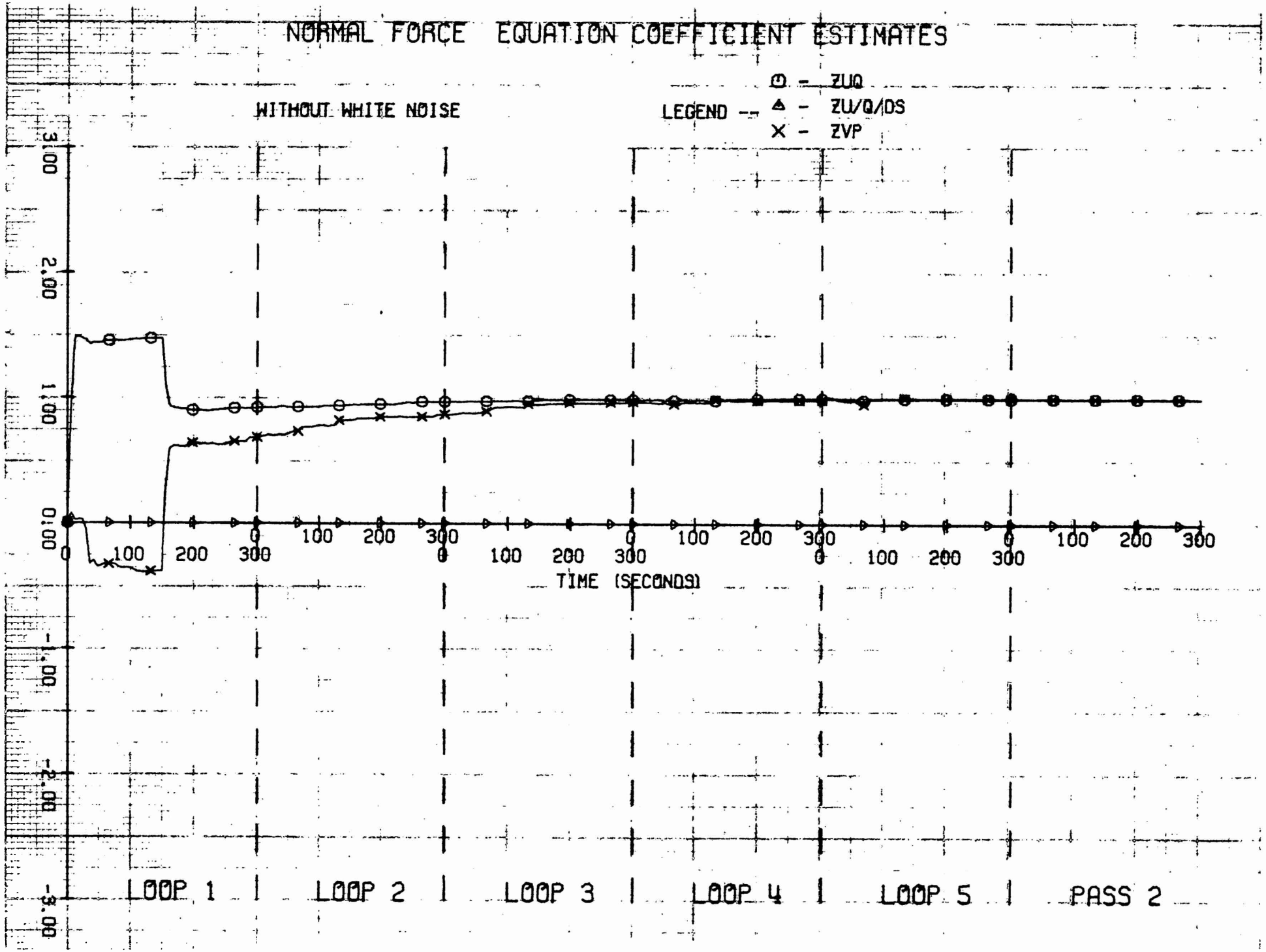
NORMAL FORCE EQUATION COEFFICIENT ESTIMATES
WITHOUT WHITE NOISE
LEGEND --
ZUQ
ZU/Q/DS
ZVP
3.00
2.00
1.00
0.00
-1.00
-2.00
-3.00
0
100
200
300
TIME (SECONDS)
LOOP 1
LOOP 2
LOOP 3
LOOP 4
LOOP 5
PASS 2

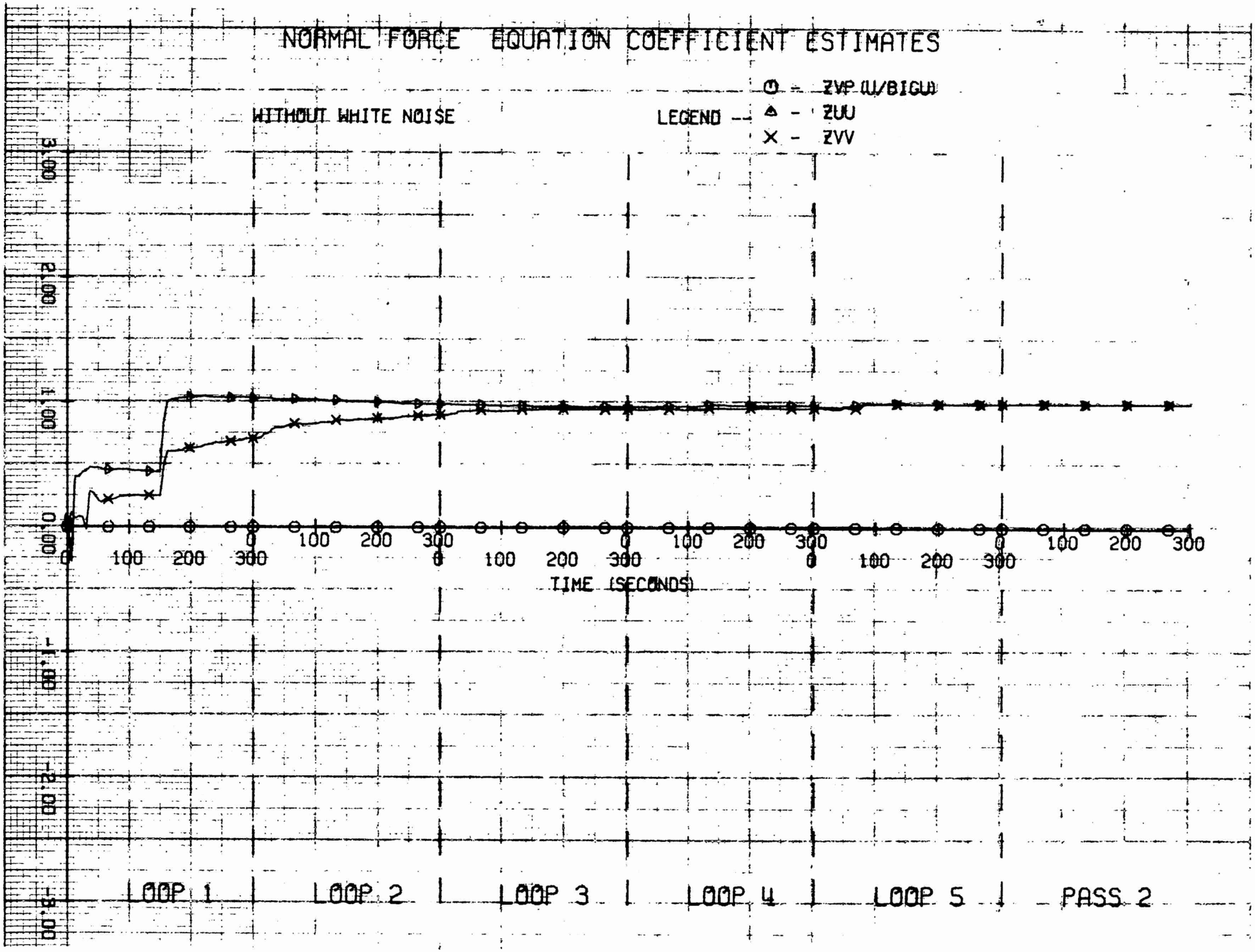
NORMAL FORCE EQUATION COEFFICIENT ESTIMATES
WITHOUT WHITE NOISE
LEGEND --
ZVP (U/BIGU)
ZUU
ZVV
3.00
2.00
1.00
0.00
-1.00
-2.00
-3.00
0
100
200
300
TIME (SECONDS)
LOOP 1
LOOP 2
LOOP 3
LOOP 4
LOOP 5
PASS 2

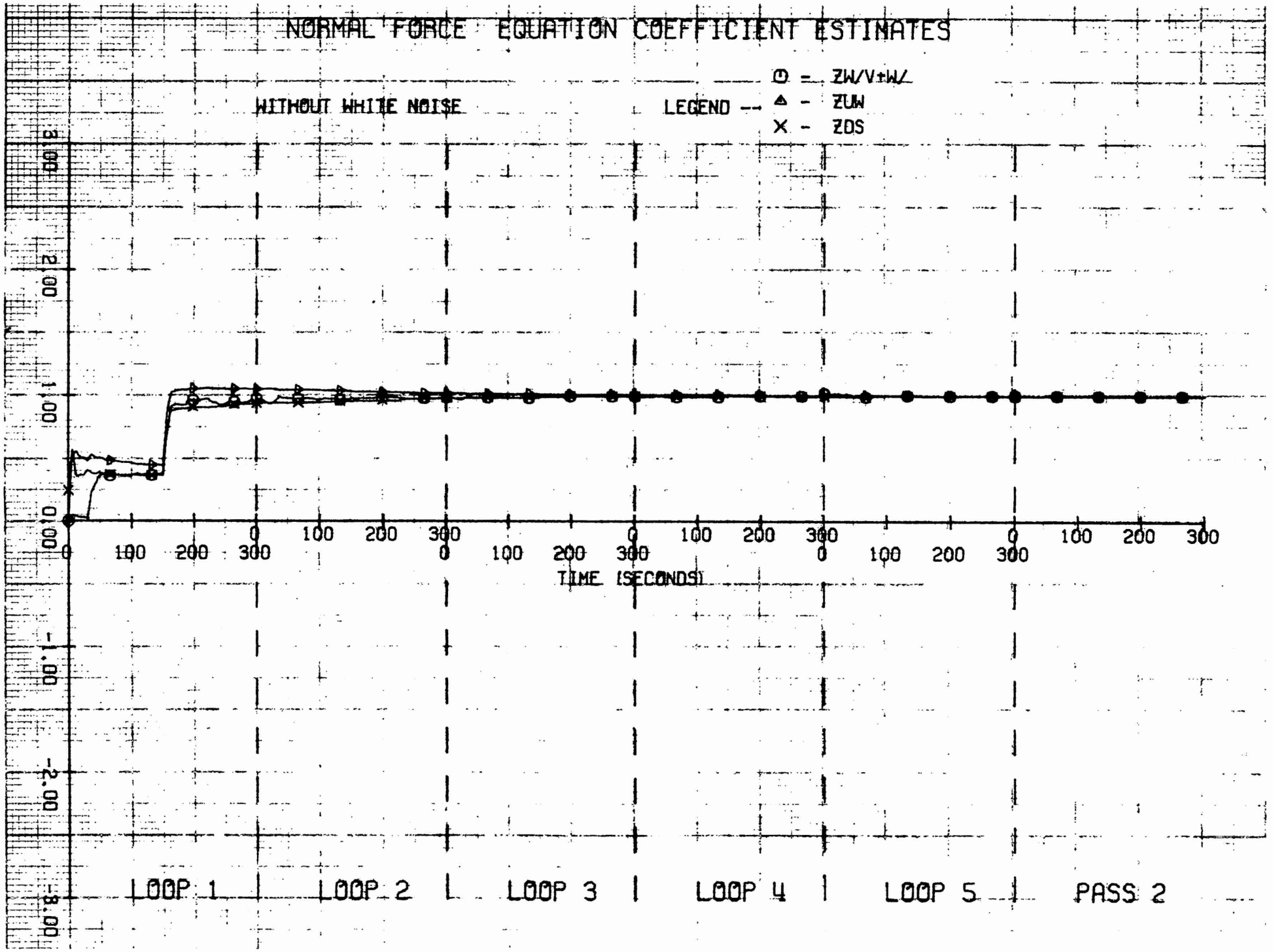
NORMAL FORCE EQUATION COEFFICIENT ESTIMATES
WITHOUT WHITE NOISE
LEGEND --
⊙ = ZW/V+W/
△ - ZUW
X - ZDS
3.00
2.00
1.00
0.00
-1.00
-2.00
-3.00
0
100
200
300
TIME (SECONDS)
LOOP 1
LOOP 2
LOOP 3
LOOP 4
LOOP 5
PASS 2

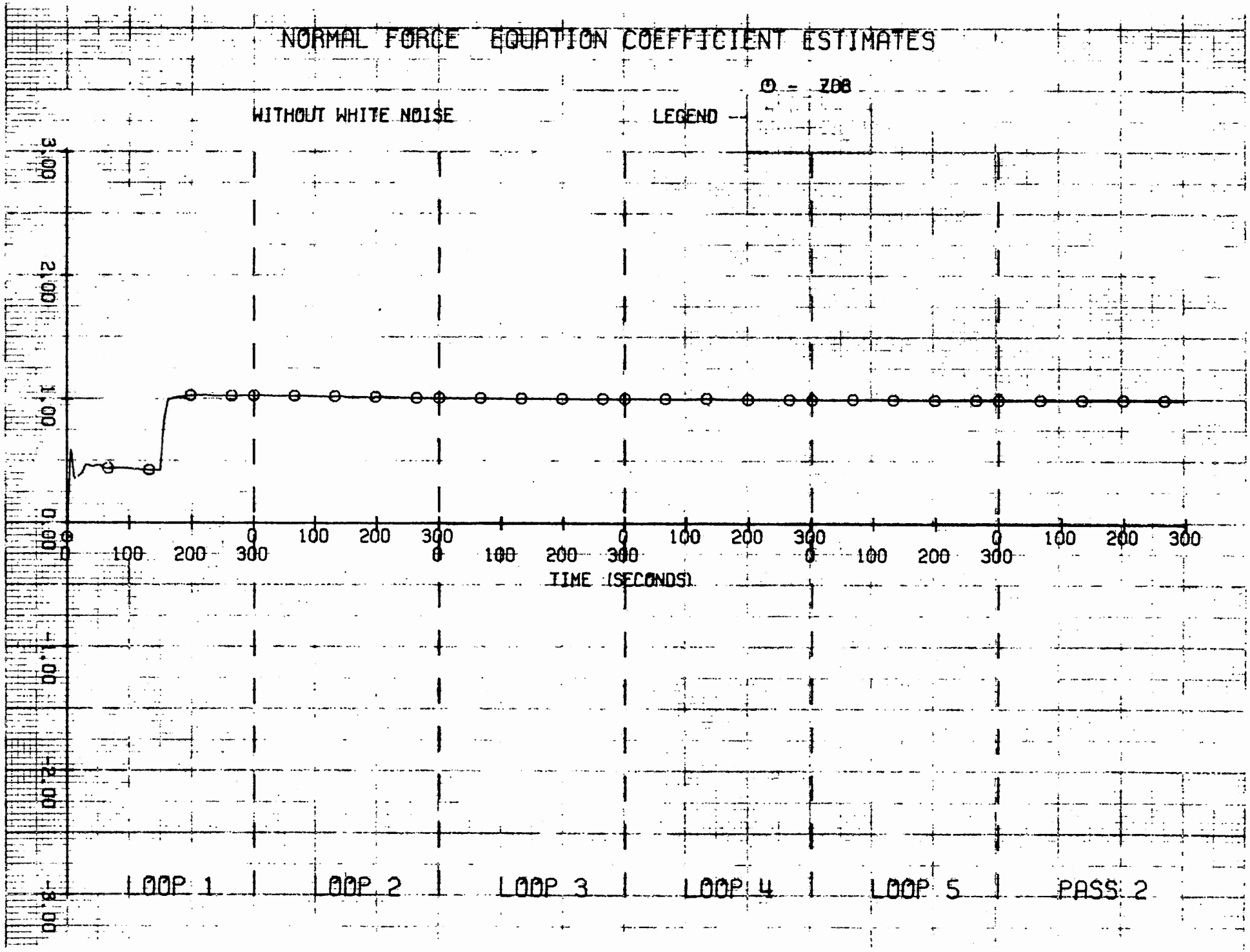
NORMAL FORCE EQUATION COEFFICIENT ESTIMATES
WITHOUT WHITE NOISE
LEGEND
Z08
3.00
2.00
1.00
0.00
-1.00
-2.00
-3.00
0
100
200
300
TIME (SECONDS)
LOOP 1
LOOP 2
LOOP 3
LOOP 4
LOOP 5
PASS 2

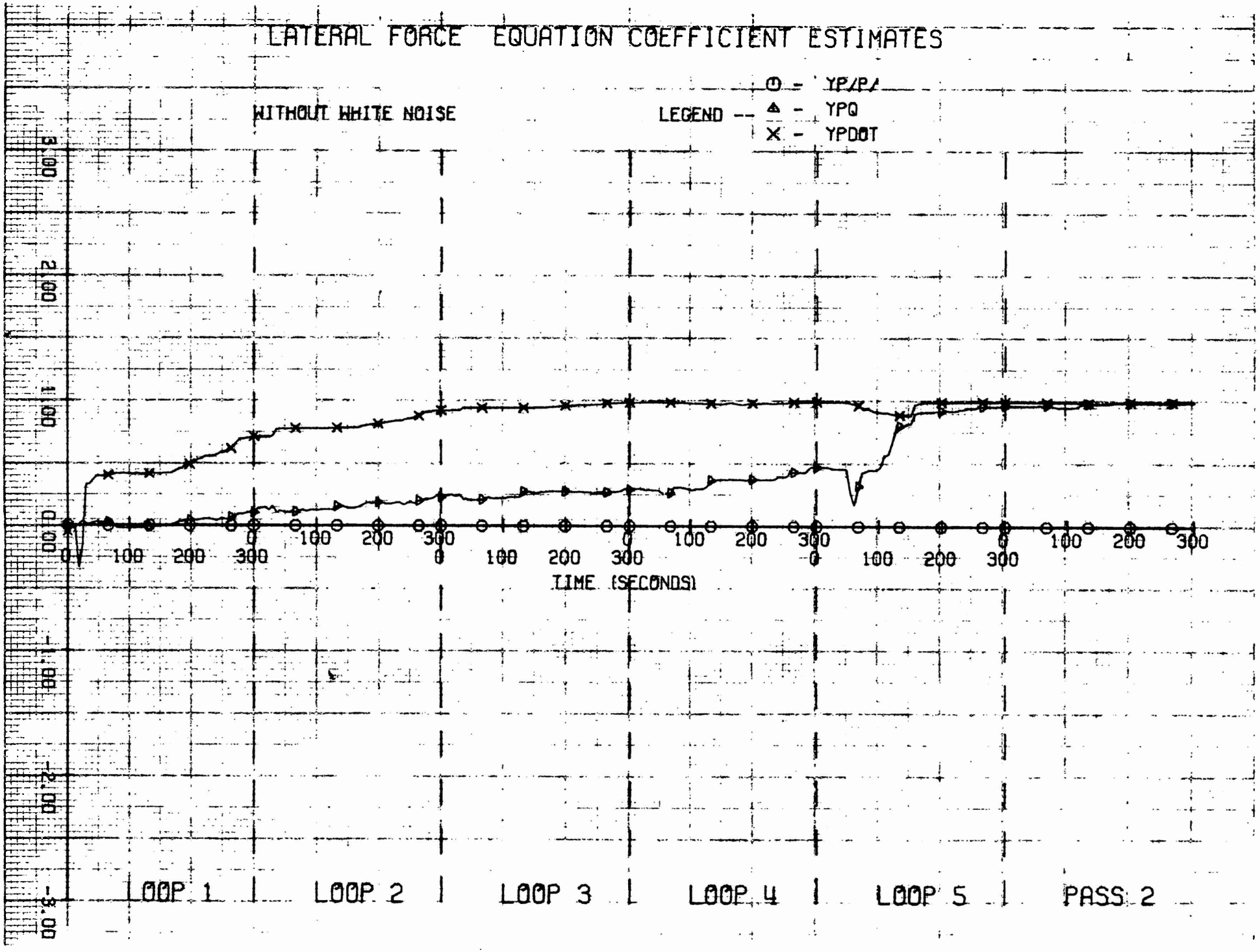
LATERAL FORCE EQUATION COEFFICIENT ESTIMATES
WITHOUT WHITE NOISE
LEGEND -- ⊙ - YP/P/
▲ - YPQ
× - YPDOT
3.00
2.00
1.00
0.00
-1.00
-2.00
-3.00
0
100
200
300
TIME (SECONDS)
LOOP 1
LOOP 2
LOOP 3
LOOP 4
LOOP 5
PASS 2

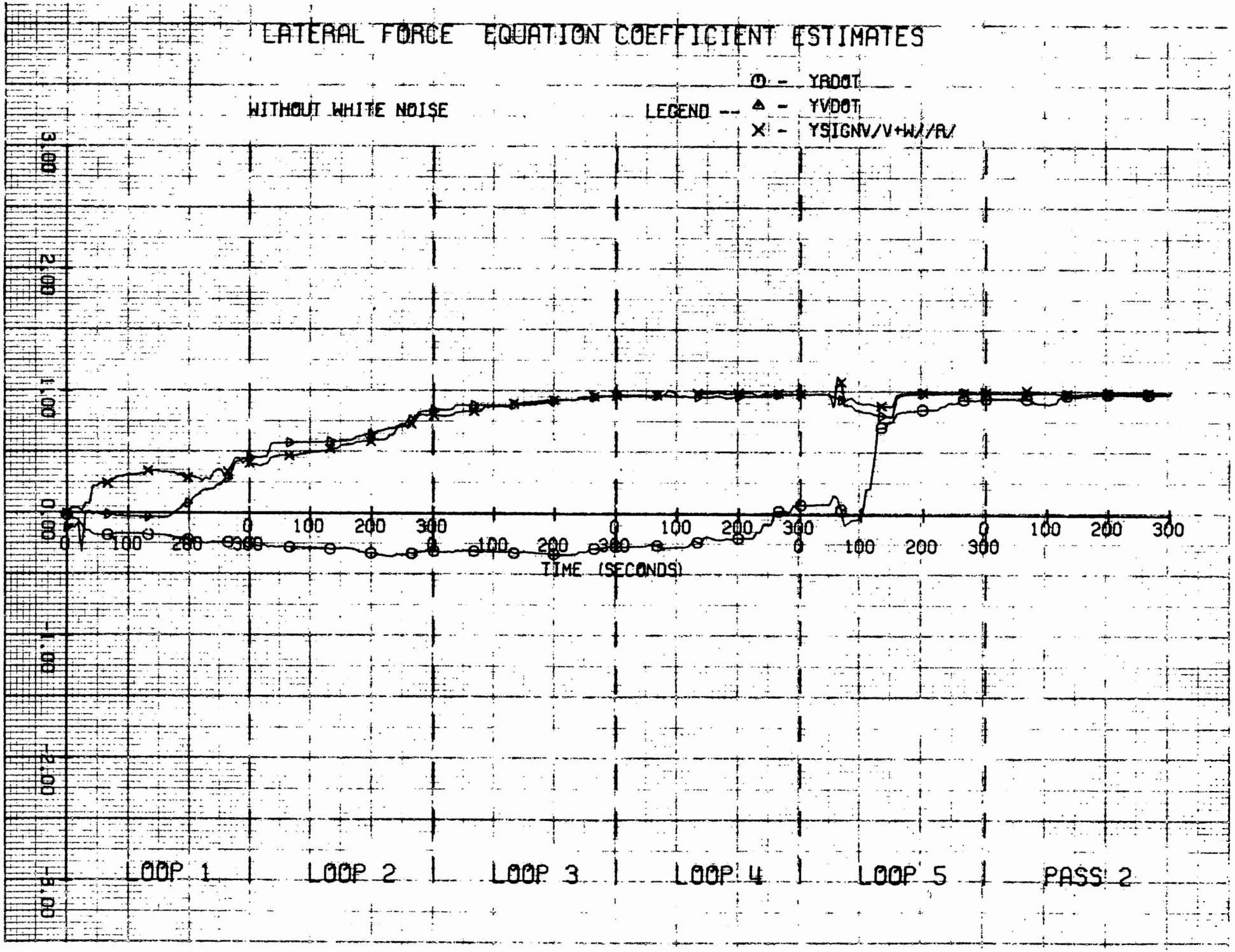
LATERAL FORCE EQUATION COEFFICIENT ESTIMATES
WITHOUT WHITE NOISE
LEGEND --
- YRDOT
- YVDOT
- YSIGNV/V+W/
3.00
2.00
1.00
0.00
-1.00
-2.00
-3.00
0
100
200
300
TIME (SECONDS)
LOOP 1
LOOP 2
LOOP 3
LOOP 4
LOOP 5
PASS 2

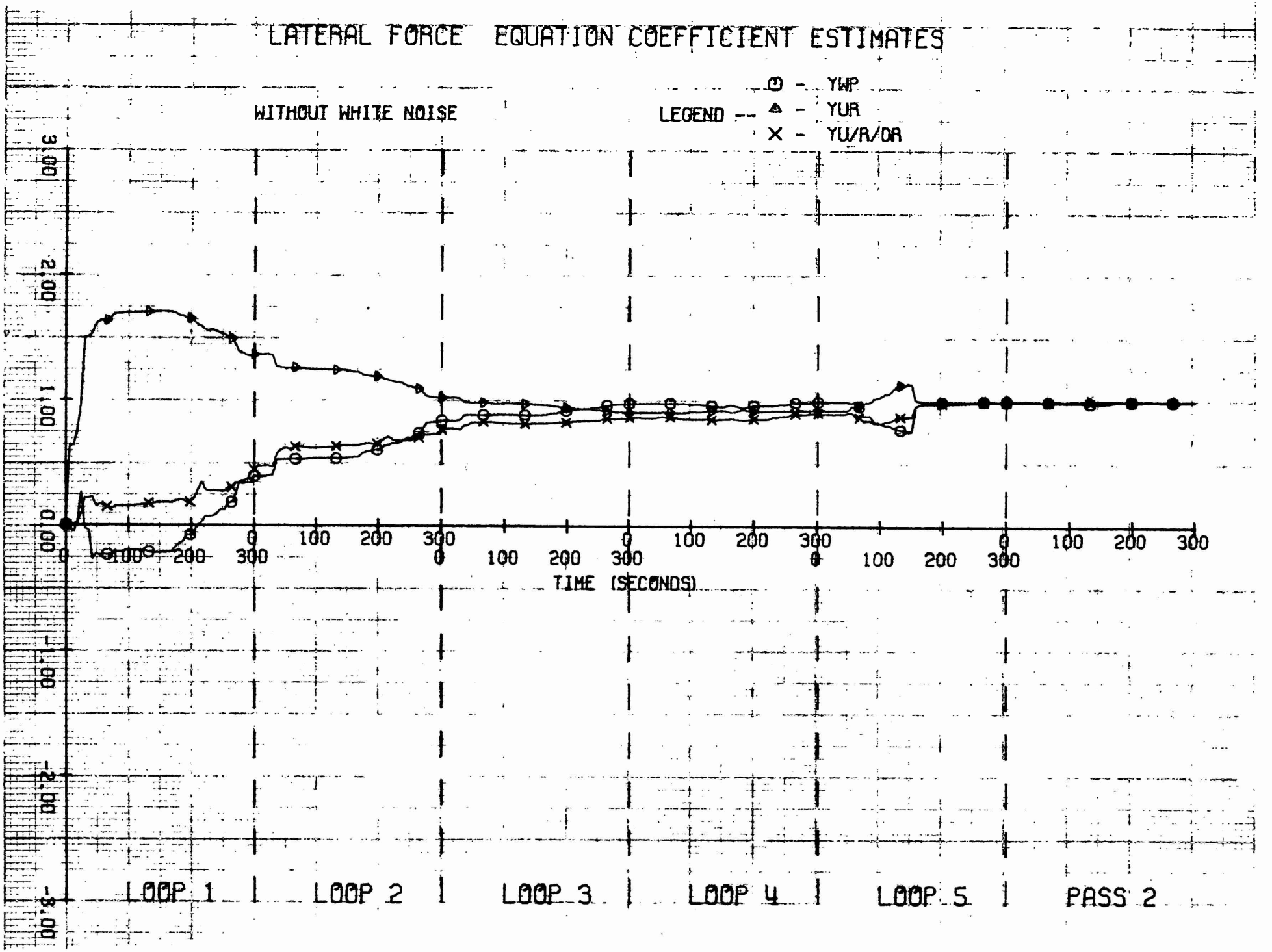
LATERAL FORCE EQUATION COEFFICIENT ESTIMATES
WITHOUT WHITE NOISE
LEGEND -- ⊙ - YWP
△ - YUR
× - YU/R/DR
3.00
2.00
1.00
0.0
-1.00
-2.00
-3.00
0 100 200 300
TIME (SECONDS)
LOOP 1
LOOP 2
LOOP 3
LOOP 4
LOOP 5
PASS 2

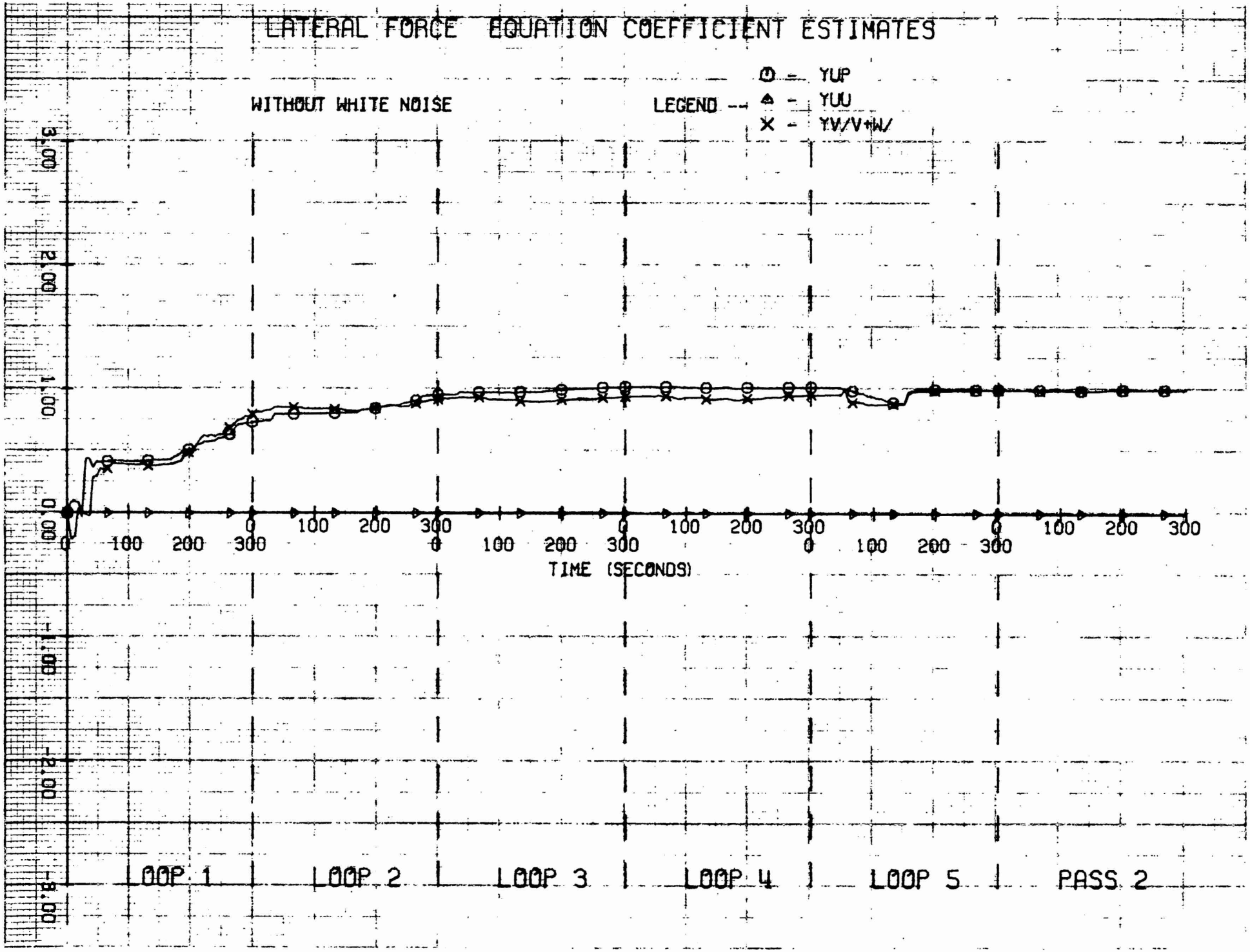
LATERAL FORCE EQUATION COEFFICIENT ESTIMATES
WITHOUT WHITE NOISE
LEGEND -- ⊙ - YUP
△ - YUU
× - YV/V+W/
3.00
2.00
1.00
0.00
-1.00
-2.00
-3.00
0 100 200 300 0 100 200 300 0 100 200 300 0 100 200 300 0 100 200 300
TIME (SECONDS)
LOOP 1
LOOP 2
LOOP 3
LOOP 4
LOOP 5
PASS 2

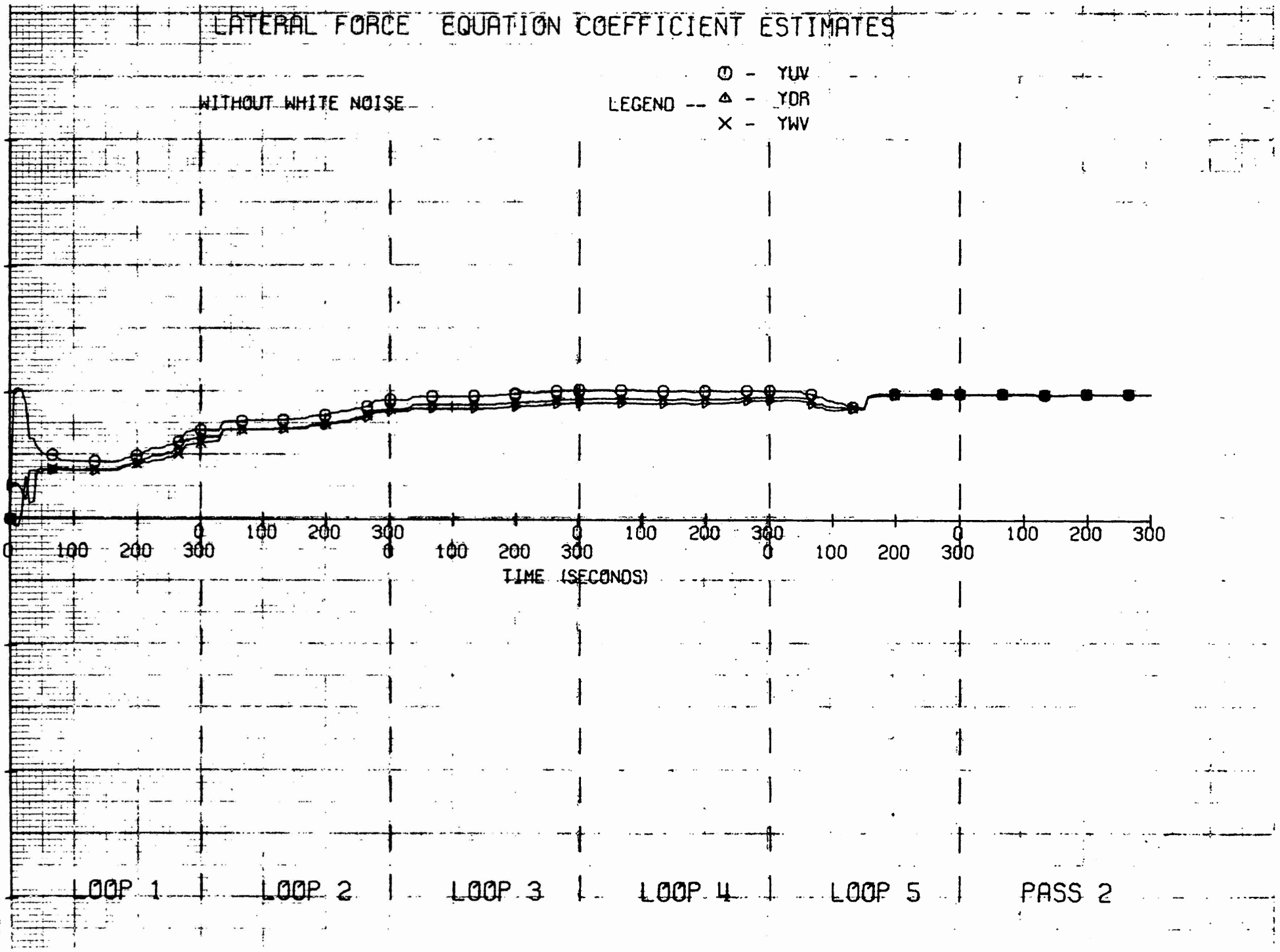
LATERAL FORCE EQUATION COEFFICIENT ESTIMATES
WITHOUT WHITE NOISE
LEGEND -- ⊙ - YUV
△ - YDR
× - YWV
3.00
2.00
1.00
0.00
-1.00
-2.00
-3.00
0 100 200 300 0 100 200 300 0 100 200 300 0 100 200 300
TIME (SECONDS)
LOOP 1
LOOP 2
LOOP 3
LOOP 4
LOOP 5
PASS 2

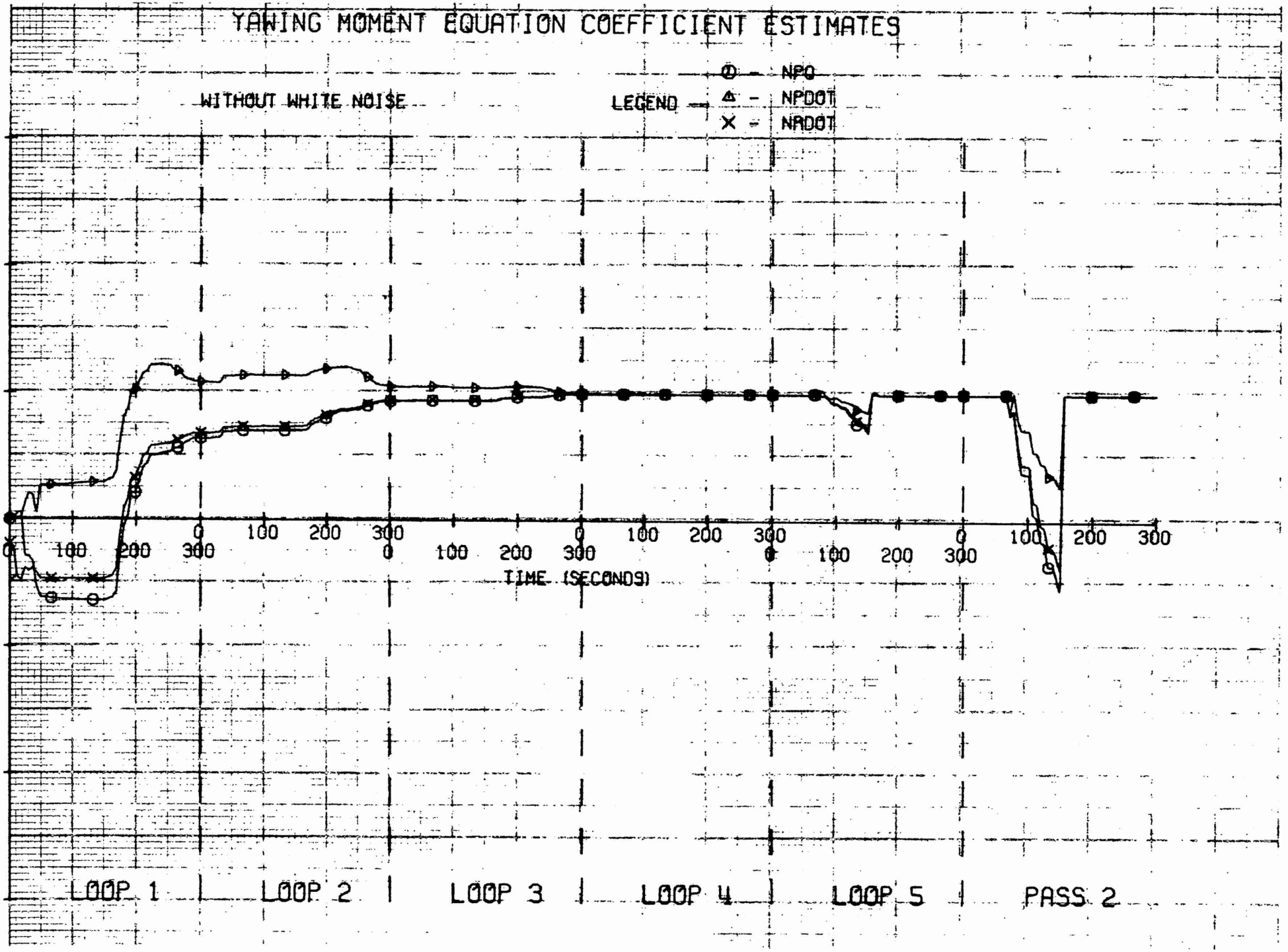
YAWING MOMENT EQUATION COEFFICIENT ESTIMATES
WITHOUT WHITE NOISE
LEGEND
NPQ
NPDOT
NRDOT
3.00
2.00
1.00
0.00
-1.00
-2.00
-3.00
0
100
200
300
TIME (SECONDS)
LOOP 1
LOOP 2
LOOP 3
LOOP 4
LOOP 5
PASS 2

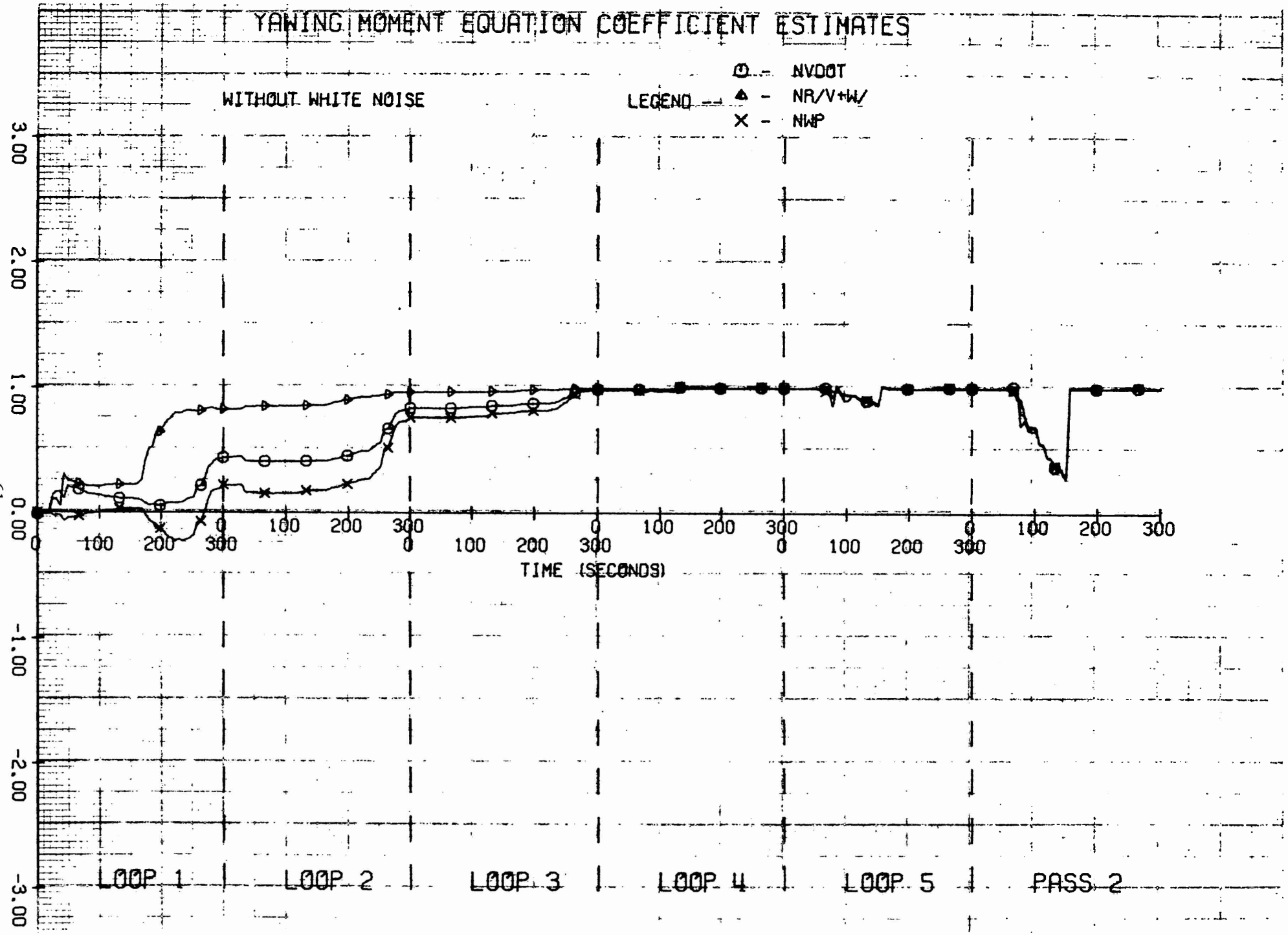
YAWING MOMENT EQUATION COEFFICIENT ESTIMATES
WITHOUT WHITE NOISE
LEGEND
NVDOT
NR/V+W/
NWP
3.00
2.00
1.00
0.00
-1.00
-2.00
-3.00
0
100
200
300
TIME (SECONDS)
LOOP 1
LOOP 2
LOOP 3
LOOP 4
LOOP 5
PASS 2

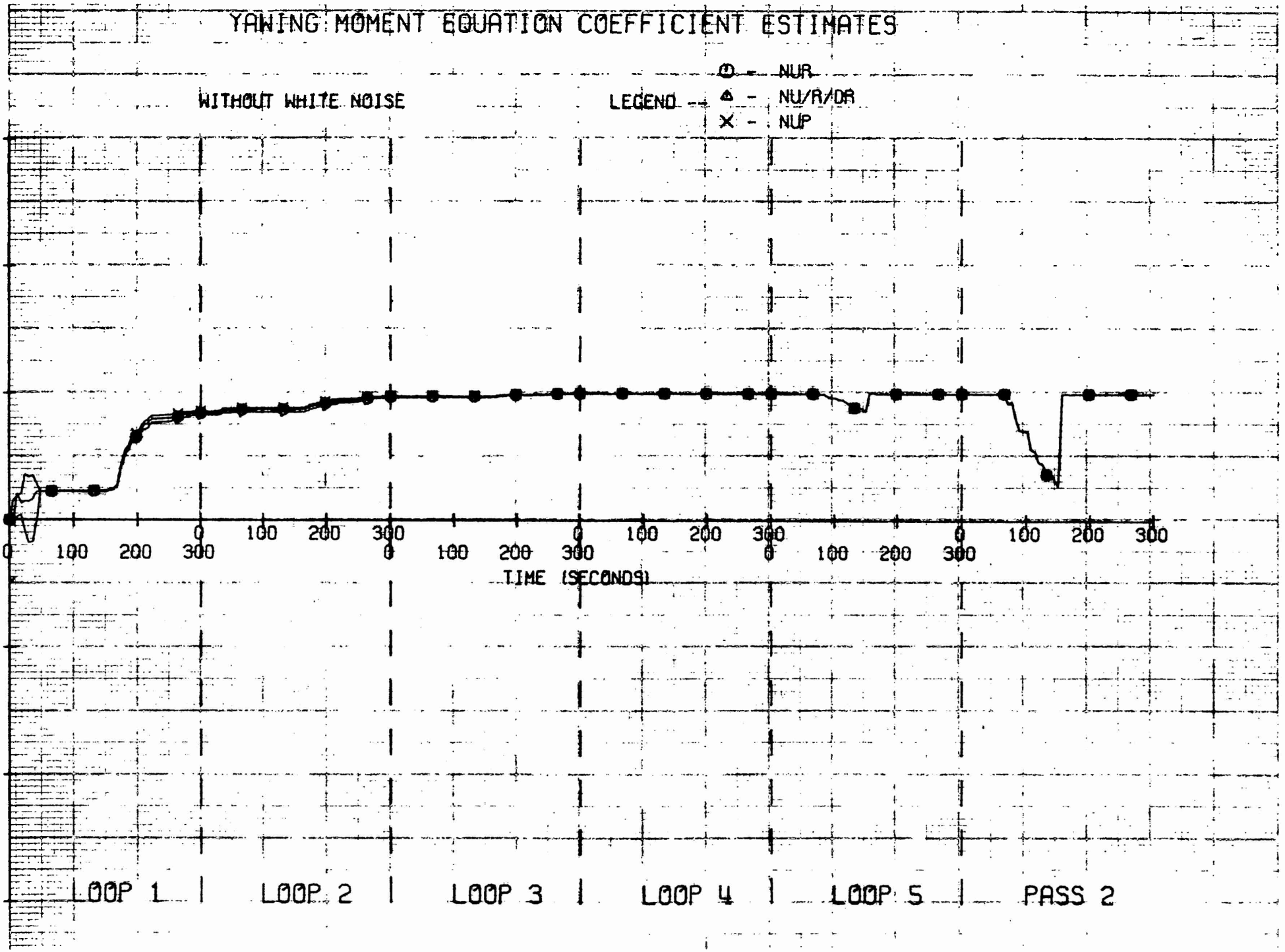
YAWING MOMENT EQUATION COEFFICIENT ESTIMATES
WITHOUT WHITE NOISE
LEGEND -- ⊙ - NUR
Δ - NU/R/DR
X - NUP
3.00
2.00
1.00
0.00
-1.00
-2.00
-3.00
0
100
200
300
TIME (SECONDS)
LOOP 1
LOOP 2
LOOP 3
LOOP 4
LOOP 5
PASS 2

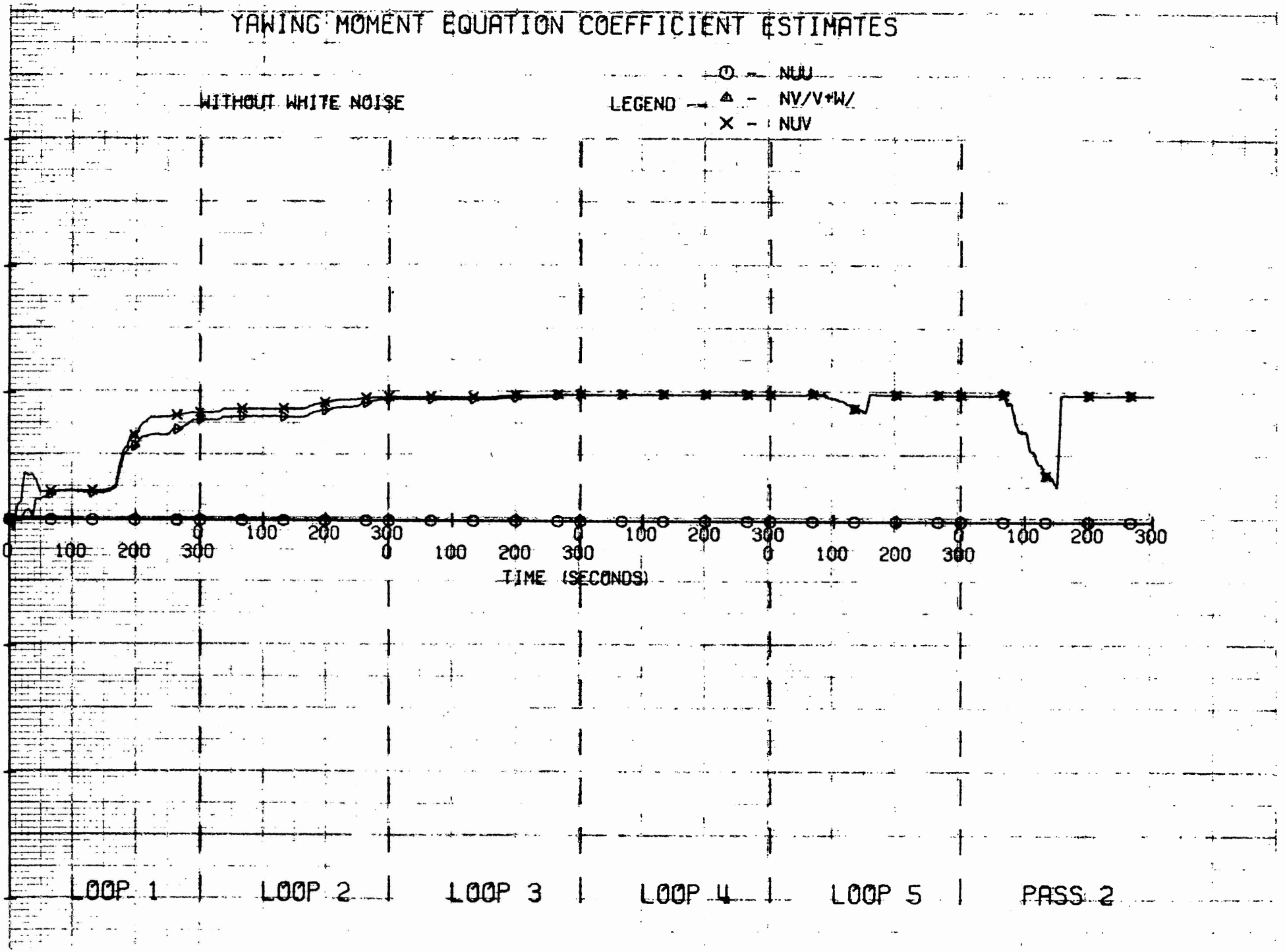
YAWING MOMENT EQUATION COEFFICIENT ESTIMATES
WITHOUT WHITE NOISE
LEGEND
NUU
NV/V+W/
NUV
3.00
2.00
1.00
0.00
-1.00
-2.00
-3.00
0
100
200
300
TIME (SECONDS)
LOOP 1
LOOP 2
LOOP 3
LOOP 4
LOOP 5
PASS 2

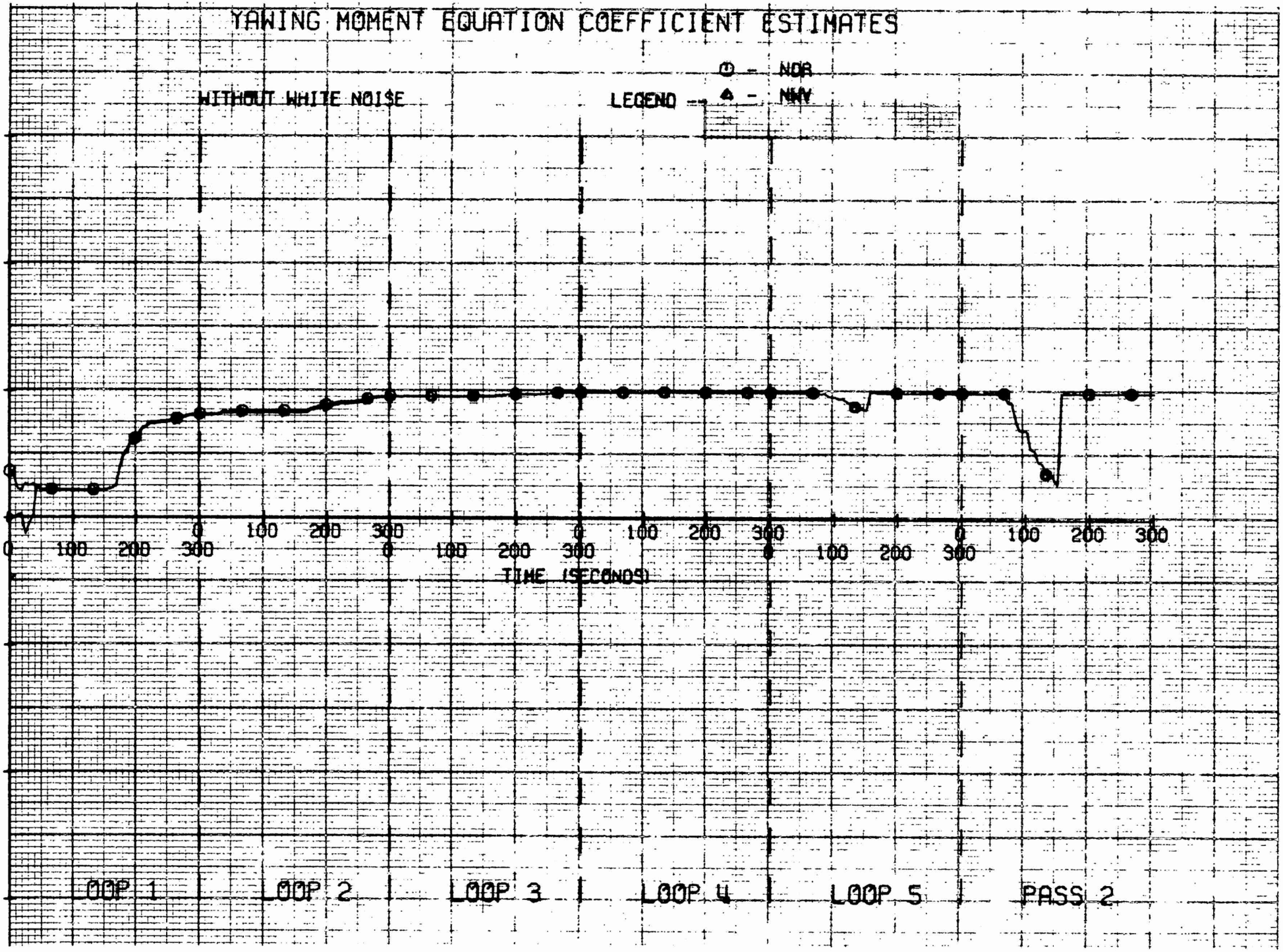
YAWING MOMENT EQUATION COEFFICIENT ESTIMATES
WITHOUT WHITE NOISE
LEGEND -- ○ - NDR
△ - NNV
3.00
2.00
1.00
0.00
-1.00
-2.00
-3.00
0
100
200
300
TIME (SECONDS)
LOOP 1
LOOP 2
LOOP 3
LOOP 4
LOOP 5
PASS 2

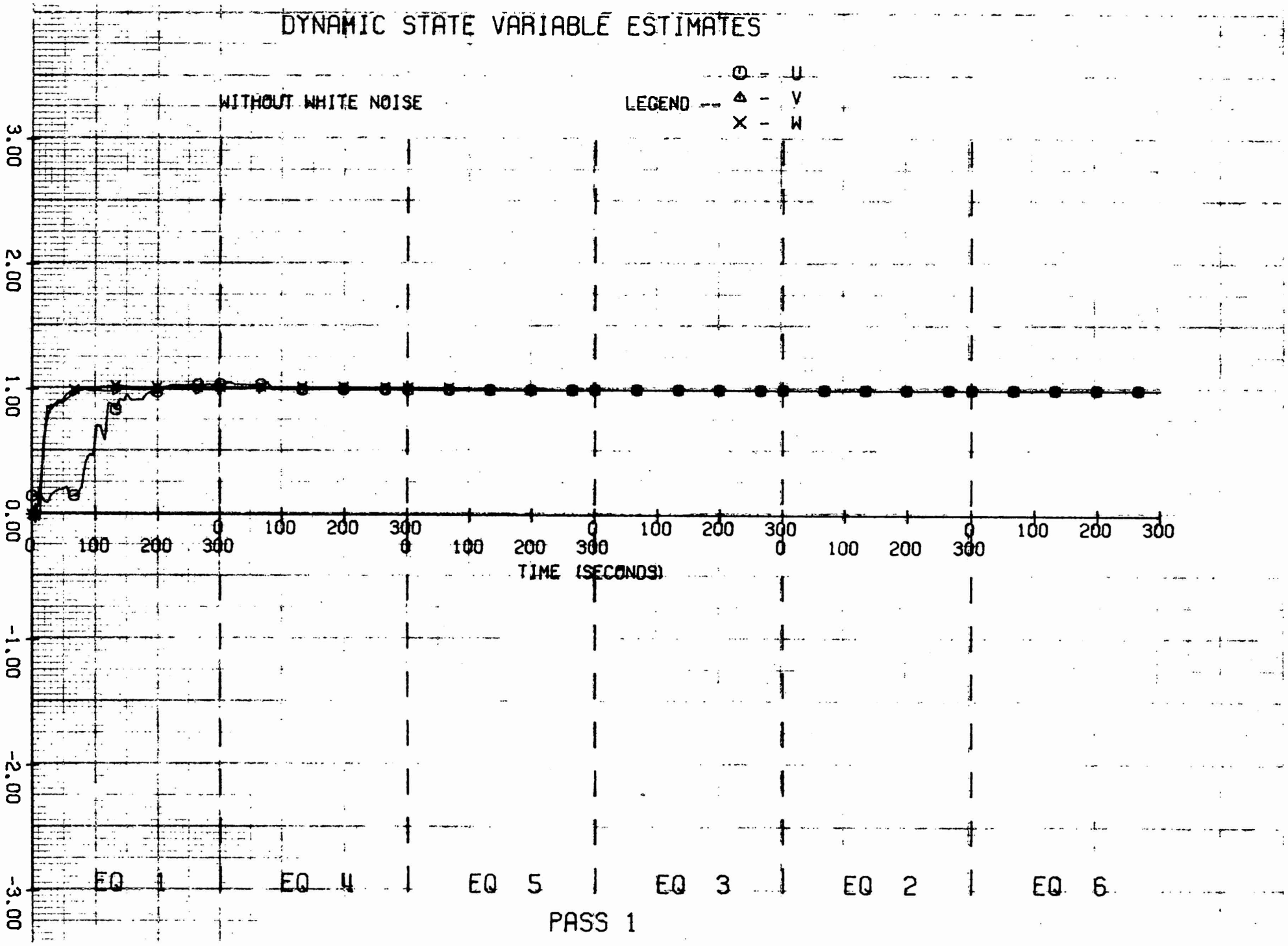
DYNAMIC STATE VARIABLE ESTIMATES
WITHOUT WHITE NOISE
LEGEND -- ○ - U
△ - V
× - W
3.00
2.00
1.00
0.00
-1.00
-2.00
-3.00
0
100
200
300
TIME (SECONDS)
EQ 1
EQ 4
EQ 5
EQ 3
EQ 2
EQ 6
PASS 1

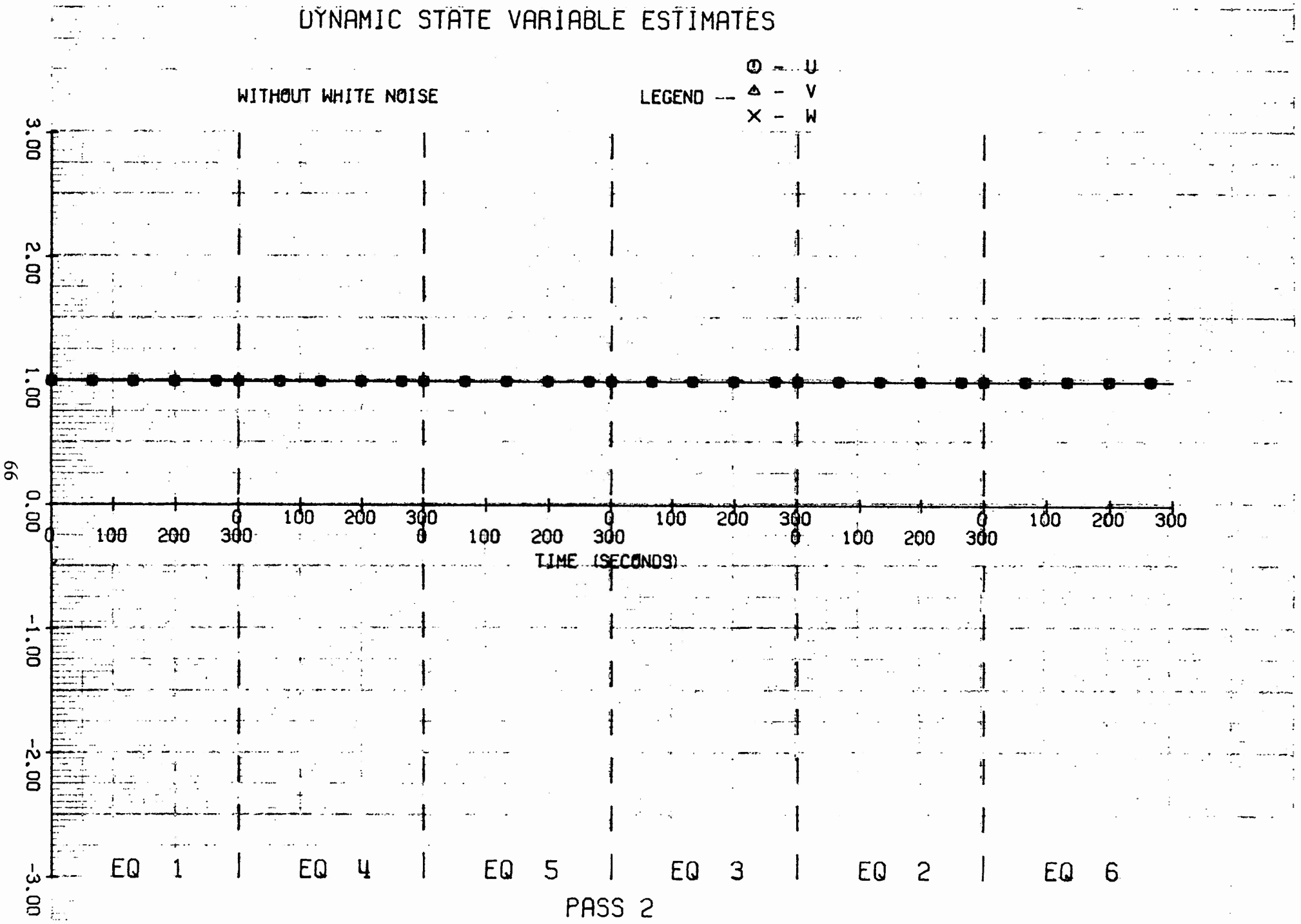
DYNAMIC STATE VARIABLE ESTIMATES
WITHOUT WHITE NOISE
LEGEND -- ⊙ - U
△ - V
× - W
3.00
2.00
1.00
0.00
-1.00
-2.00
-3.00
0
100
200
300
TIME (SECONDS)
EQ 1
EQ 4
EQ 5
EQ 3
EQ 2
EQ 6
PASS 2

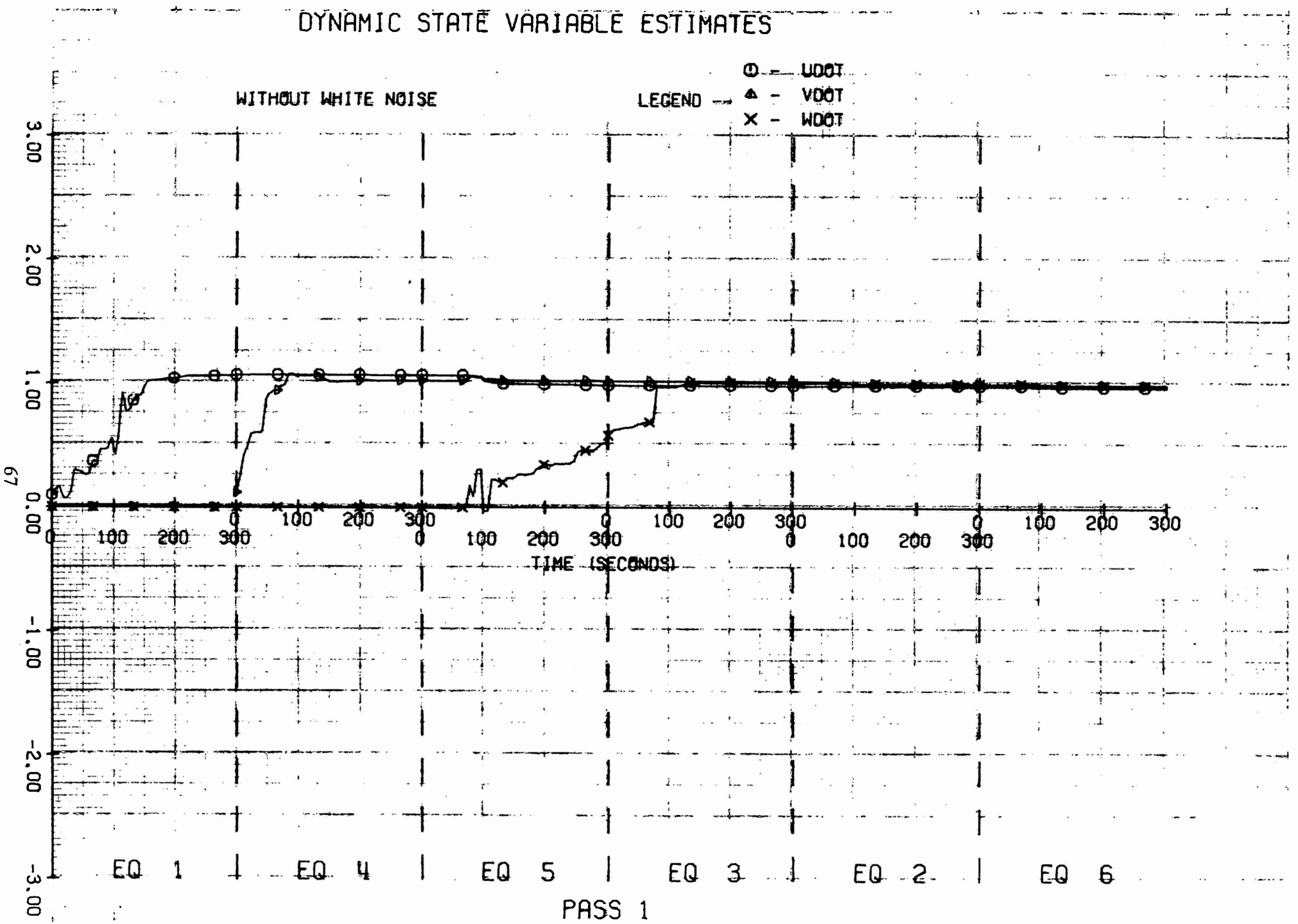
DYNAMIC STATE VARIABLE ESTIMATES
WITHOUT WHITE NOISE
LEGEND →
UDOT
VDOT
WDOT
3.00
2.00
1.00
0.00
-1.00
-2.00
-3.00
0
100
200
300
TIME (SECONDS)
EQ 1
EQ 4
EQ 5
EQ 3
EQ 2
EQ 6
PASS 1

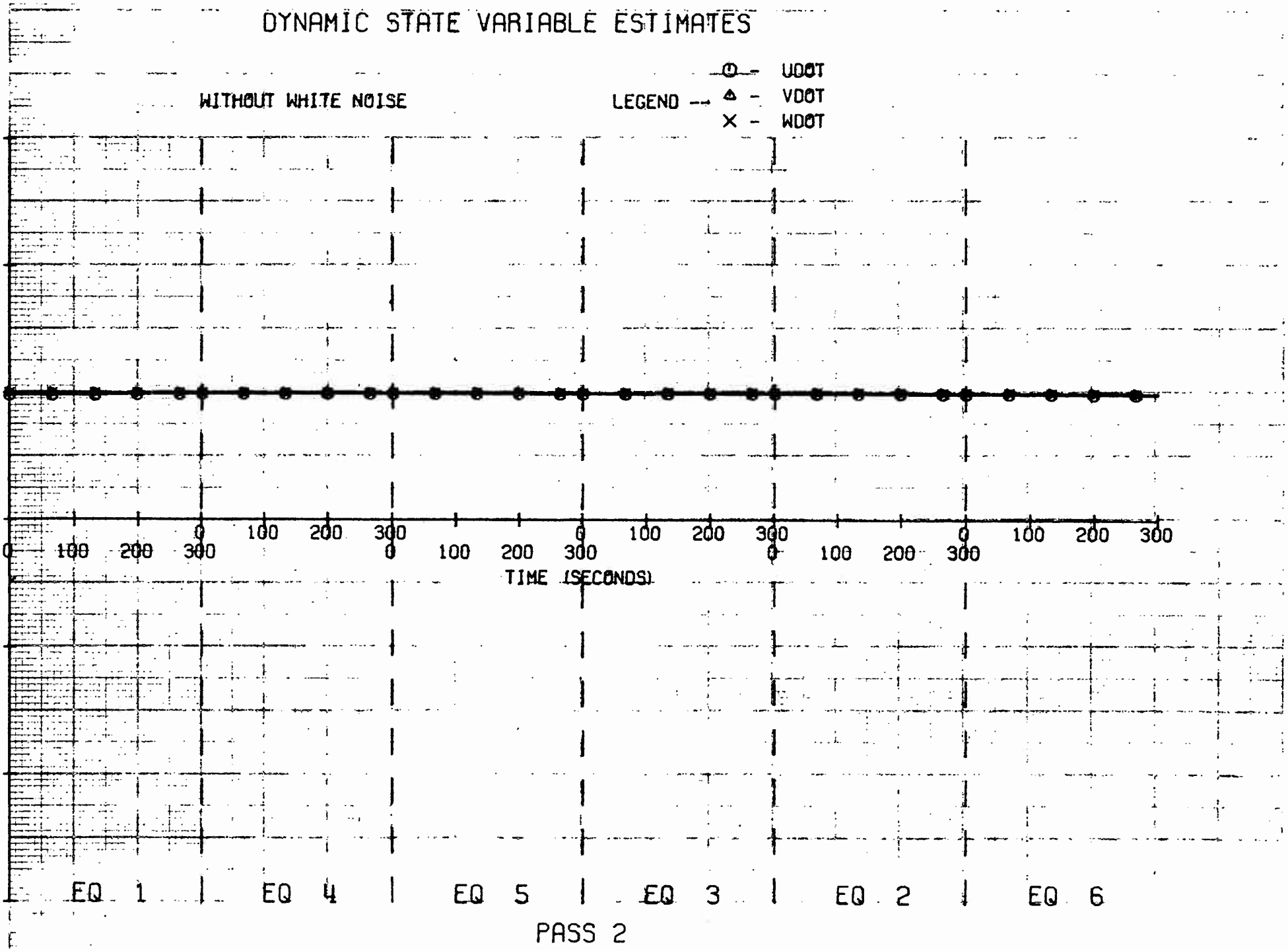
DYNAMIC STATE VARIABLE ESTIMATES
WITHOUT WHITE NOISE
LEGEND --
UDOT
VDOT
WDOT
3.00
2.00
1.00
0.00
-1.00
-2.00
-3.00
0
100
200
300
TIME (SECONDS)
EQ 1
EQ 4
EQ 5
EQ 3
EQ 2
EQ 6
PASS 2

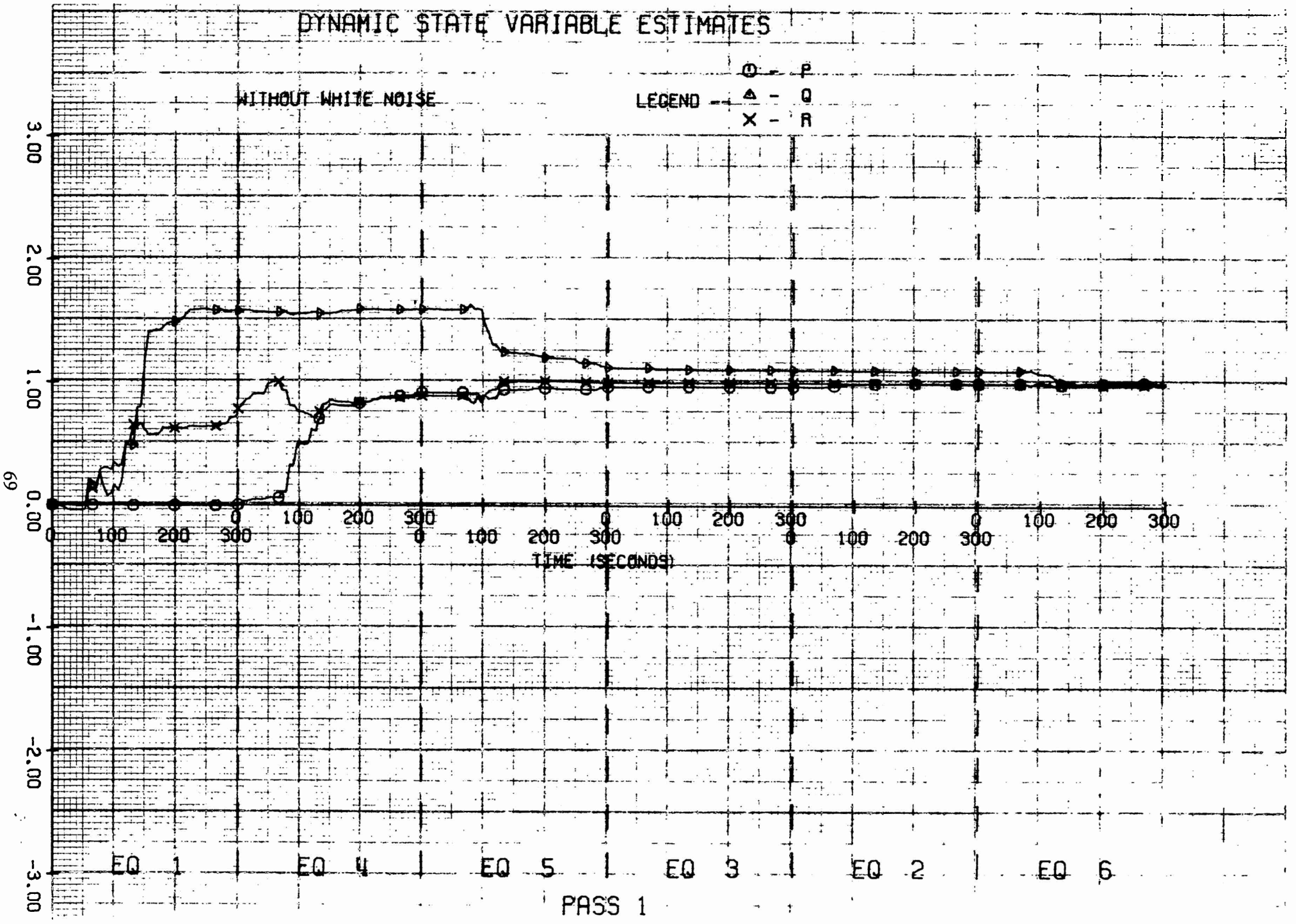
DYNAMIC STATE VARIABLE ESTIMATES
WITHOUT WHITE NOISE
LEGEND -- ○ - P
△ - Q
X - R
3.00
2.00
1.00
0.00
-1.00
-2.00
-3.00
0
100
200
300
TIME (SECONDS)
EQ 1
EQ 4
EQ 5
EQ 3
EQ 2
EQ 6
PASS 1

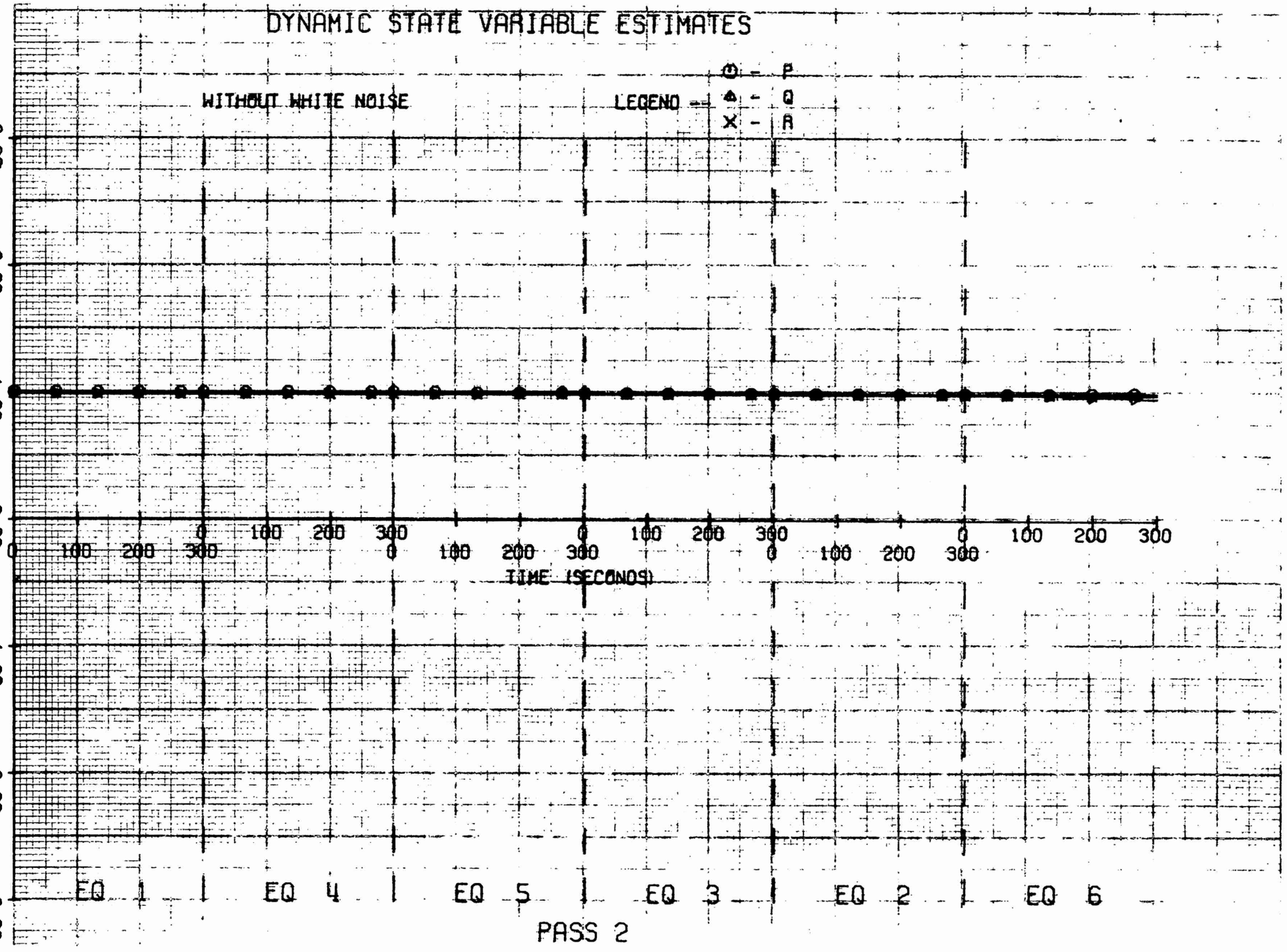
DYNAMIC STATE VARIABLE ESTIMATES
WITHOUT WHITE NOISE
LEGEND -- ⊙ - P
▲ - Q
X - R
3.00
2.00
1.00
0.00
-1.00
-2.00
-3.00
0 100 200 300 0 100 200 300 0 100 200 300 0 100 200 300
TIME (SECONDS)
EQ 1
EQ 4
EQ 5
EQ 3
EQ 2
EQ 6
PASS 2

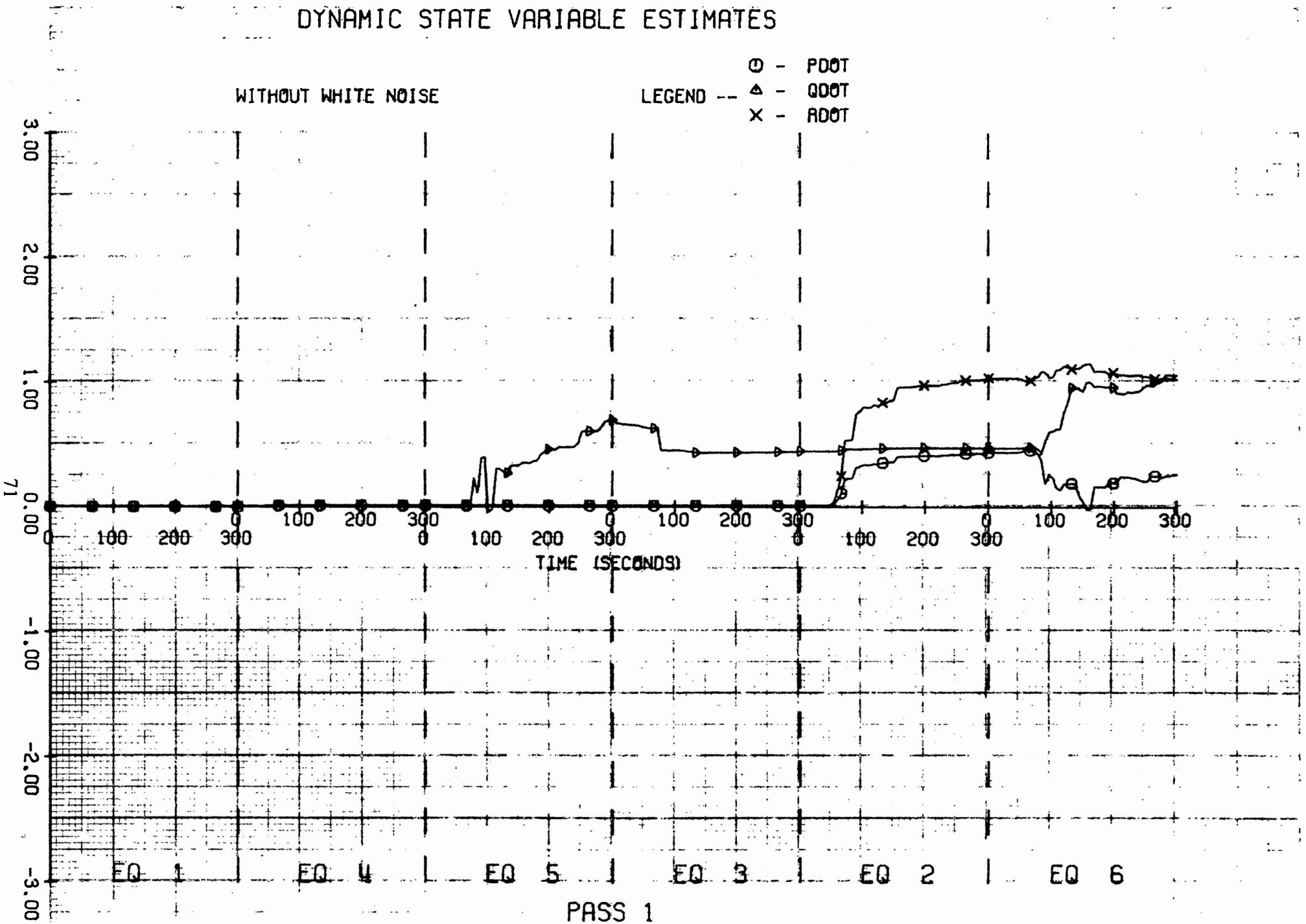
DYNAMIC STATE VARIABLE ESTIMATES
WITHOUT WHITE NOISE
LEGEND -- ⊙ - PDOT
△ - QDOT
× - RDOT
3.00
2.00
1.00
0.00
-1.00
-2.00
-3.00
0 100 200 300 0 100 200 300 0 100 200 300 0 100 200 300
TIME (SECONDS)
EQ 1
EQ 4
EQ 5
EQ 3
EQ 2
EQ 6
PASS 1

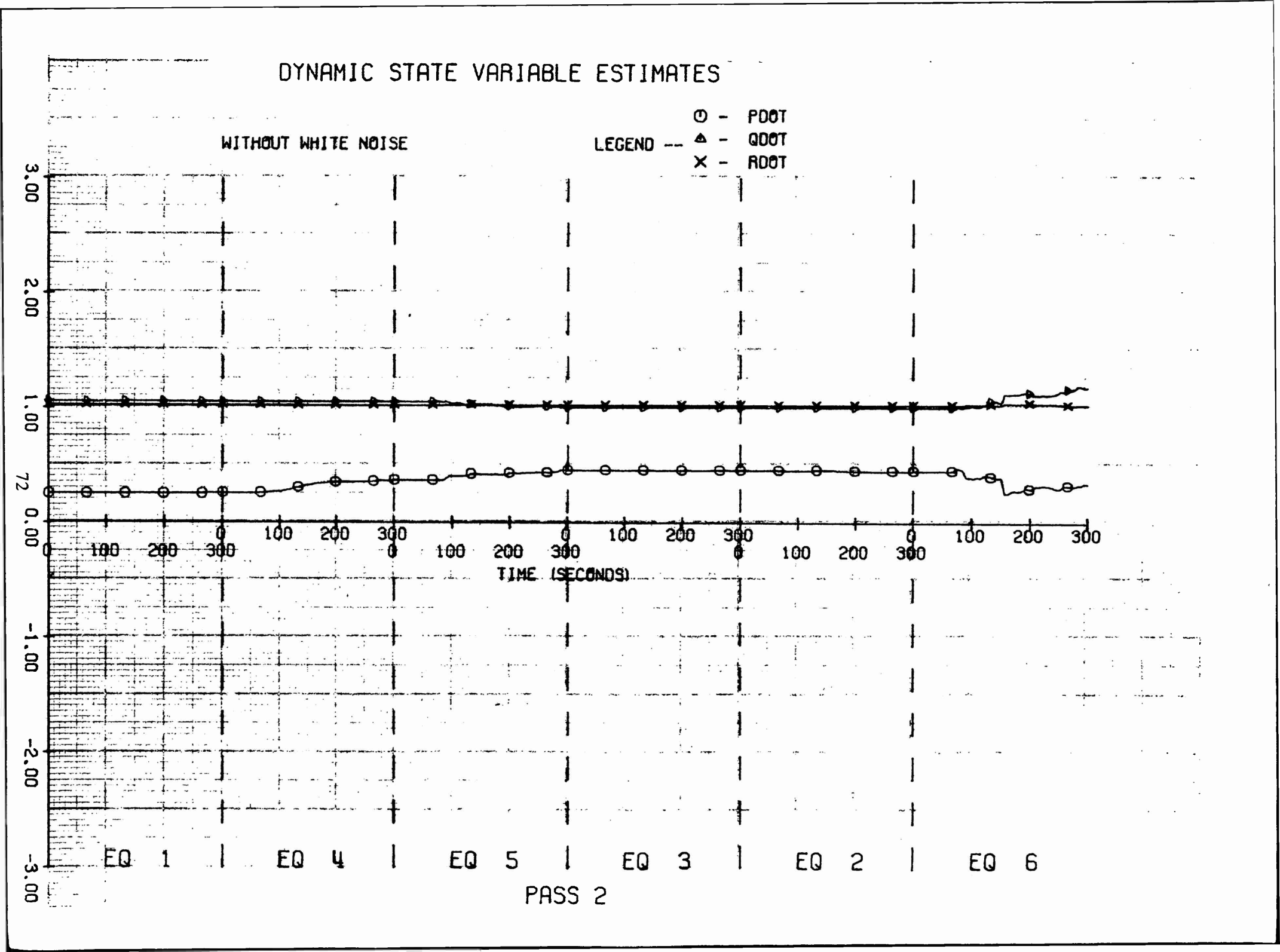
DYNAMIC STATE VARIABLE ESTIMATES
WITHOUT WHITE NOISE
LEGEND -- ⊙ - PDOT
△ - QDOT
× - RDOT
3.00
2.00
1.00
0.00
-1.00
-2.00
-3.00
0 100 200 300 0 100 200 300 0 100 200 300 0 100 200 300
TIME (SECONDS)
EQ 1
EQ 4
EQ 5
EQ 3
EQ 2
EQ 6
PASS 2

XII. PARAMETER ESTIMATE TRAJECTORIES WITH NOISE

This section presents trajectories showing the convergence of the normalized estimates of the various parameters, or coefficients, when the sensor data were corrupted by bias plus white noise.

The comments of Section XI on the sequencing of the equations and interpretation of the subscripts apply equally to this section. As in Section XI, the dynamic state variables are also shown in a normalized form.

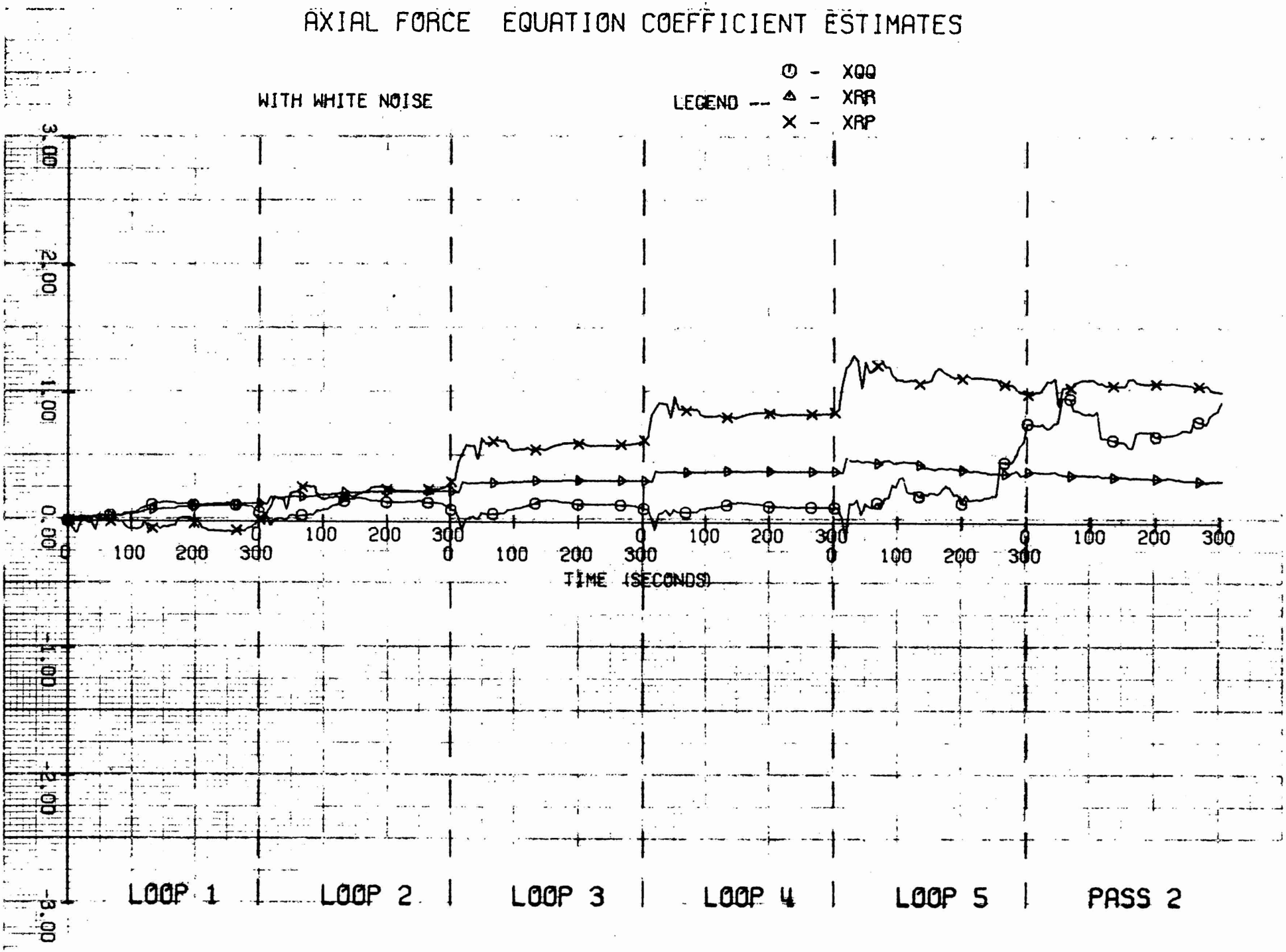
AXIAL FORCE EQUATION COEFFICIENT ESTIMATES
WITH WHITE NOISE
LEGEND -- ⓞ - XQQ
△ - XRR
× - XRP
3.00
2.00
1.00
0.00
-1.00
-2.00
-3.00
0
100
200
300
TIME (SECONDS)
LOOP 1
LOOP 2
LOOP 3
LOOP 4
LOOP 5
PASS 2

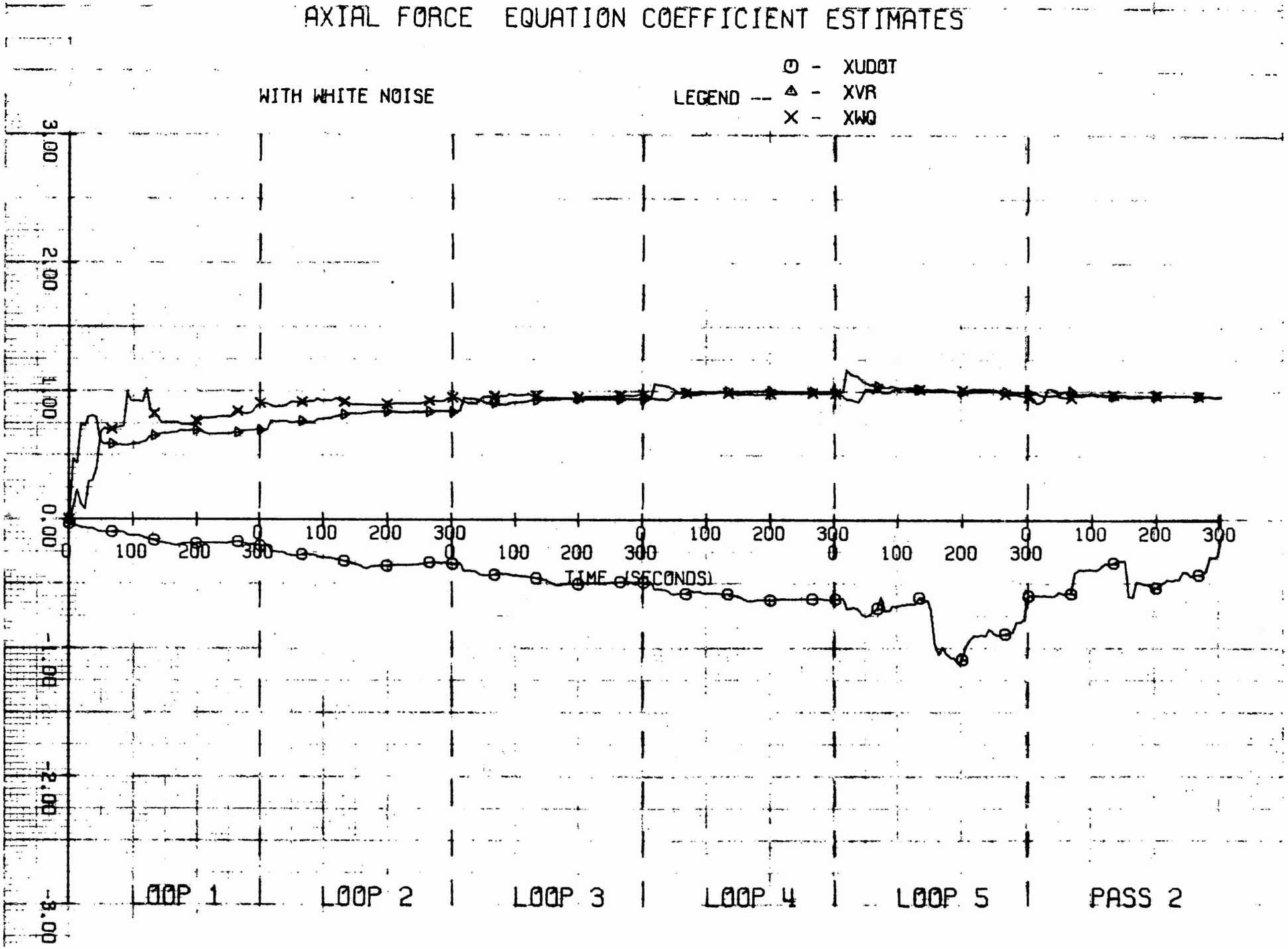
AXIAL FORCE EQUATION COEFFICIENT ESTIMATES
WITH WHITE NOISE
LEGEND -- ⊙ - XUDOT
△ - XVR
× - XWQ
3.00
2.00
1.00
0.00
-1.00
-2.00
-3.00
0
100
200
300
TIME (SECONDS)
LOOP 1
LOOP 2
LOOP 3
LOOP 4
LOOP 5
PASS 2

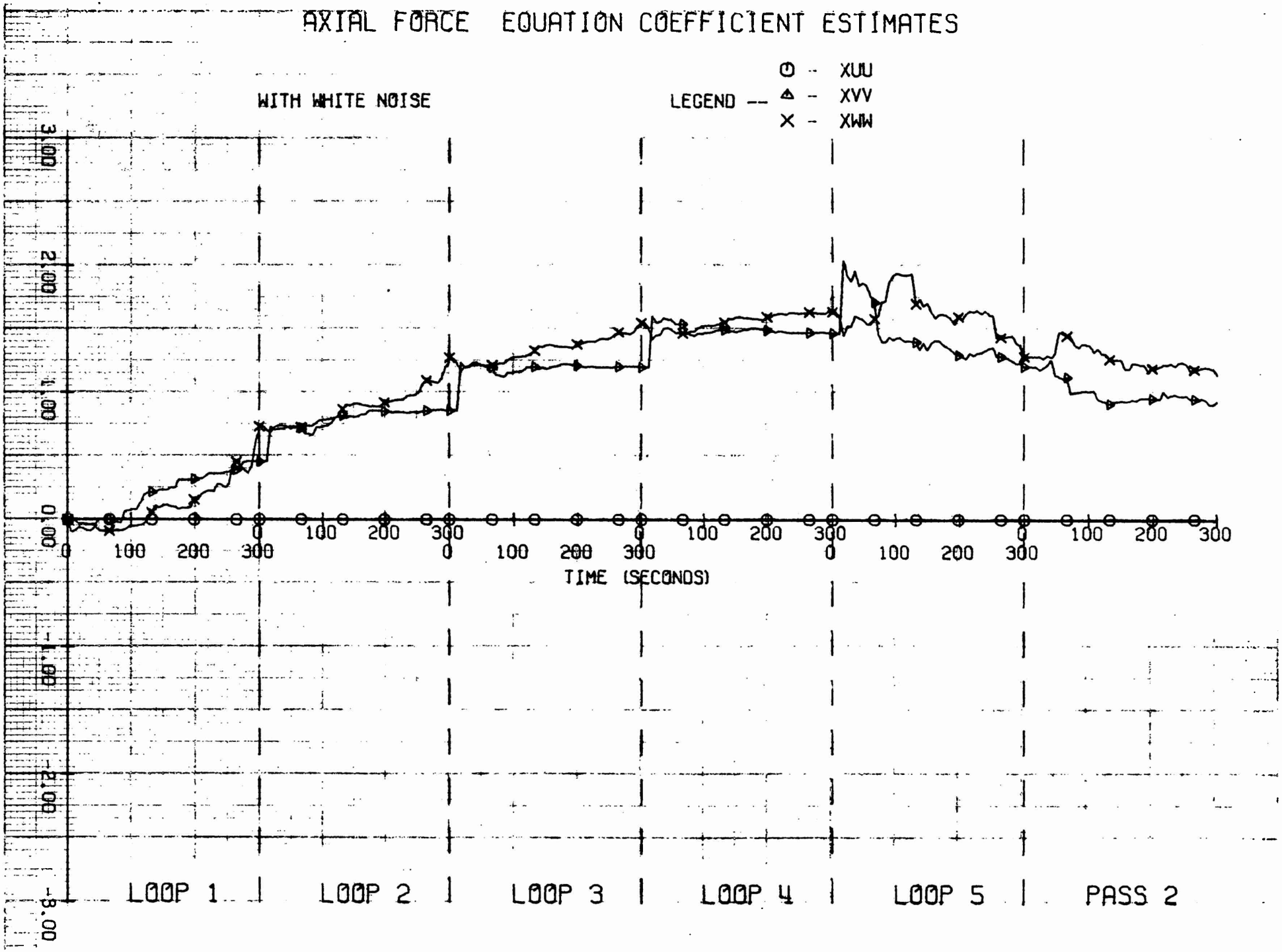
AXIAL FORCE EQUATION COEFFICIENT ESTIMATES
WITH WHITE NOISE
LEGEND -- XUU
XVV
XWW
3.00
2.00
1.00
.00
-1.00
-2.00
-3.00
0
100
200
300
TIME (SECONDS)
LOOP 1
LOOP 2
LOOP 3
LOOP 4
LOOP 5
PASS 2

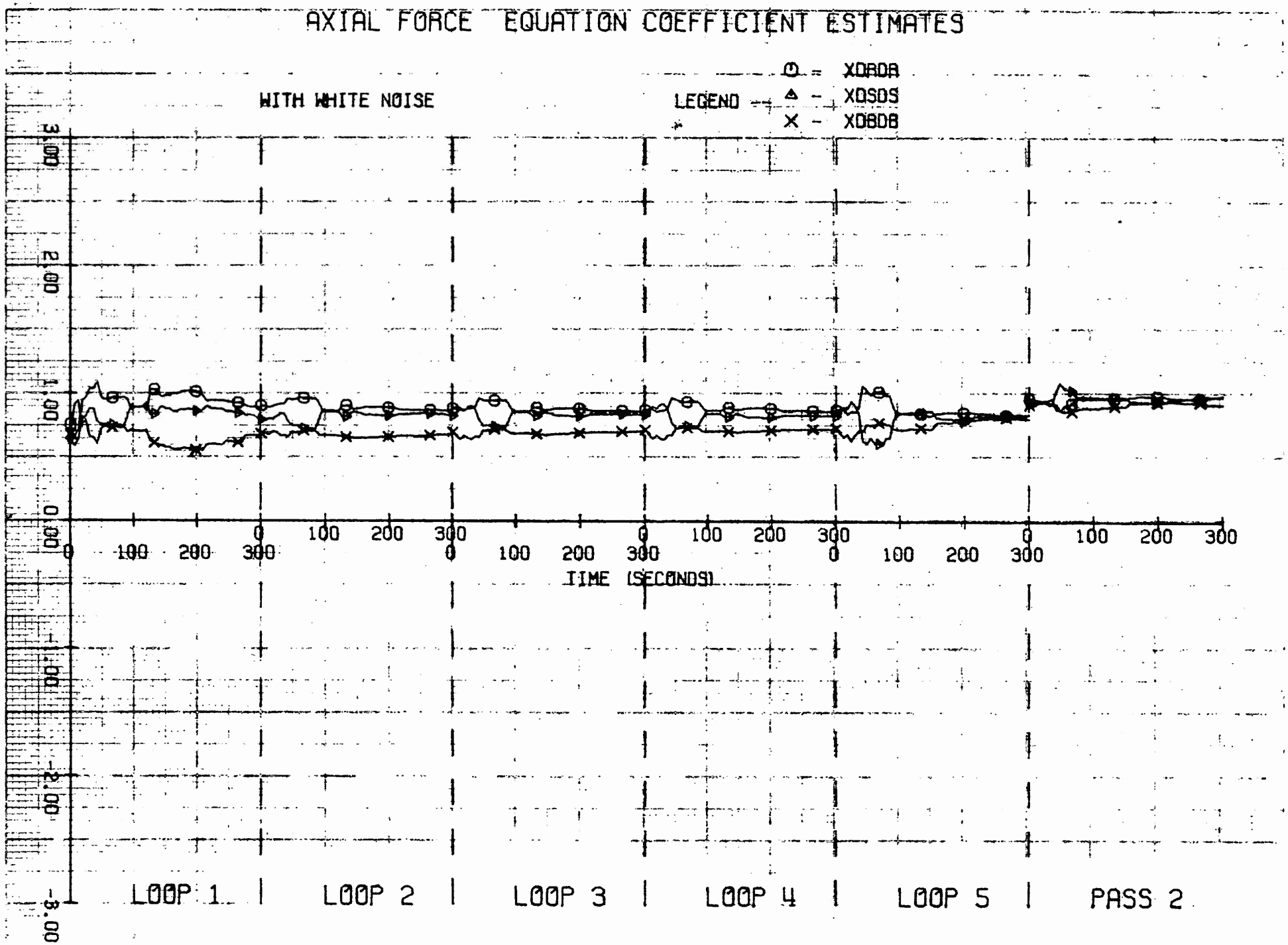
AXIAL FORCE EQUATION COEFFICIENT ESTIMATES
WITH WHITE NOISE
LEGEND
XDRDR
XDSDS
XDBDB
3.00
2.00
1.00
0.00
-1.00
-2.00
-3.00
0
100
200
300
TIME (SECONDS)
LOOP 1
LOOP 2
LOOP 3
LOOP 4
LOOP 5
PASS 2

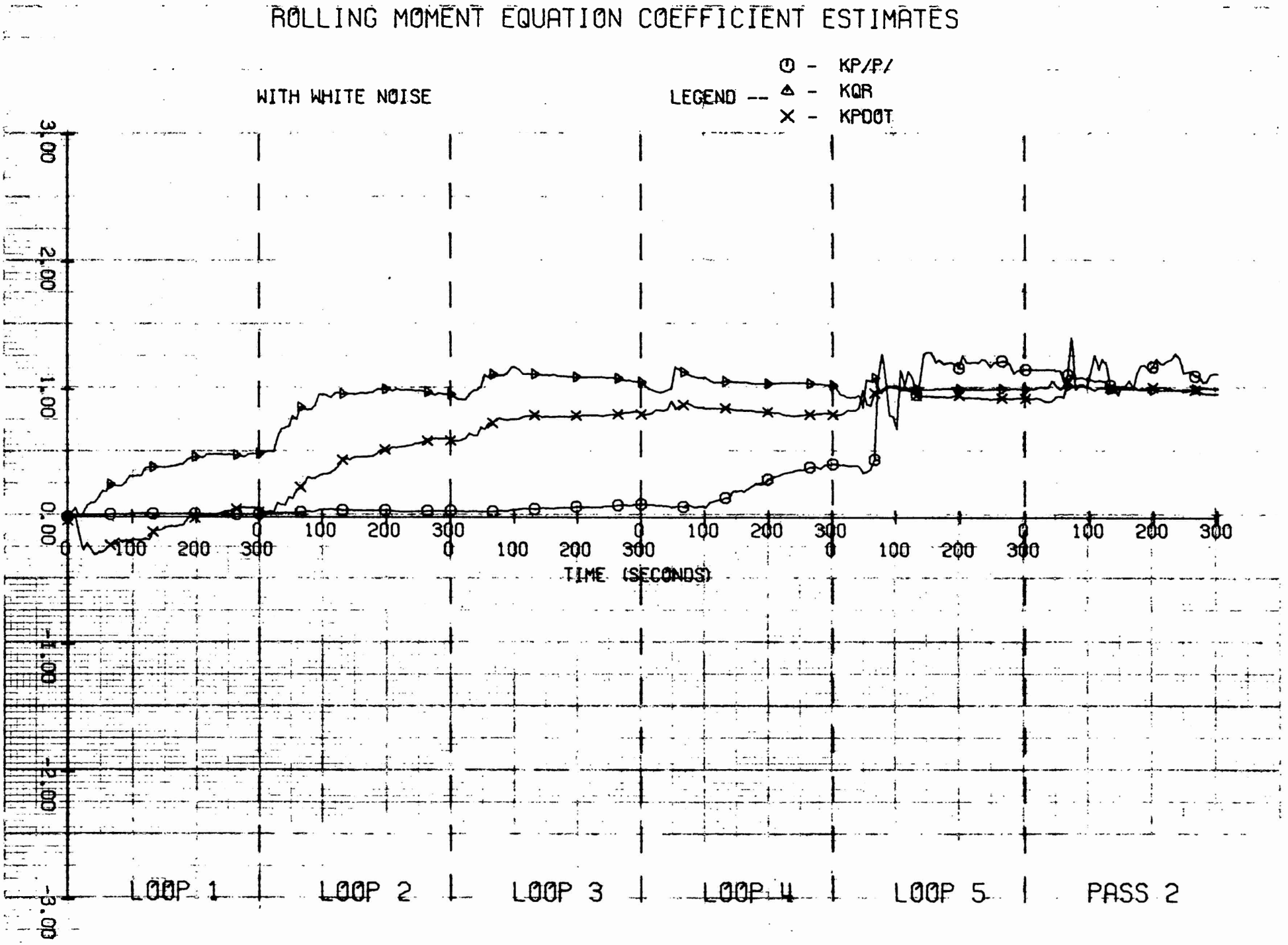
ROLLING MOMENT EQUATION COEFFICIENT ESTIMATES
WITH WHITE NOISE
LEGEND -- ⊙ - KP/P/
△ - KQR
× - KPDOT
3.00
2.00
1.00
0.00
-1.00
-2.00
-3.00
0
100
200
300
TIME (SECONDS)
LOOP 1
LOOP 2
LOOP 3
LOOP 4
LOOP 5
PASS 2

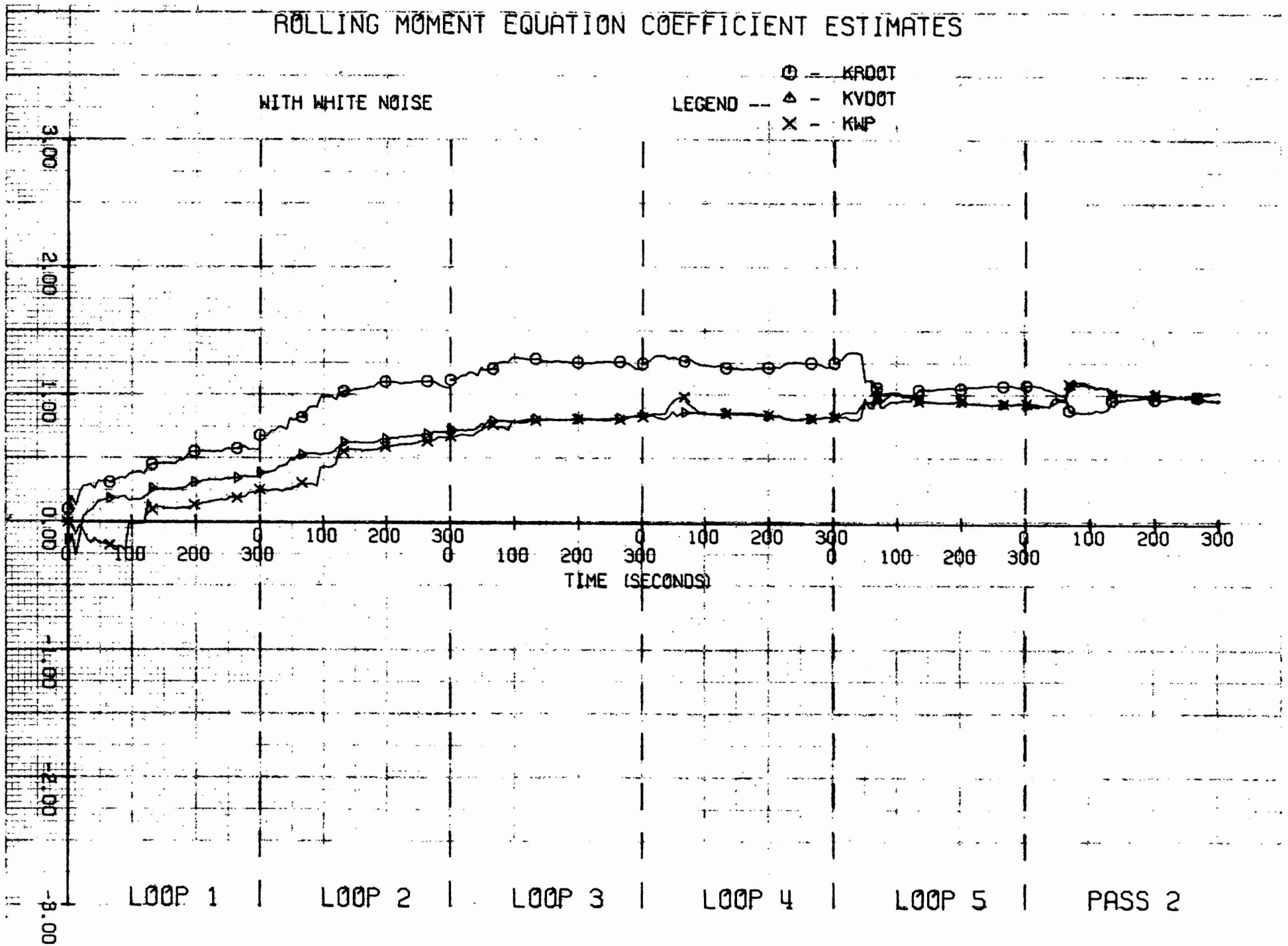
ROLLING MOMENT EQUATION COEFFICIENT ESTIMATES
WITH WHITE NOISE
LEGEND -- ⊙ - KRDOT
△ - KVDOT
× - KWP
3.00
2.00
1.00
0.00
-1.00
-2.00
-8.00
0
100
200
300
TIME (SECONDS)
LOOP 1
LOOP 2
LOOP 3
LOOP 4
LOOP 5
PASS 2

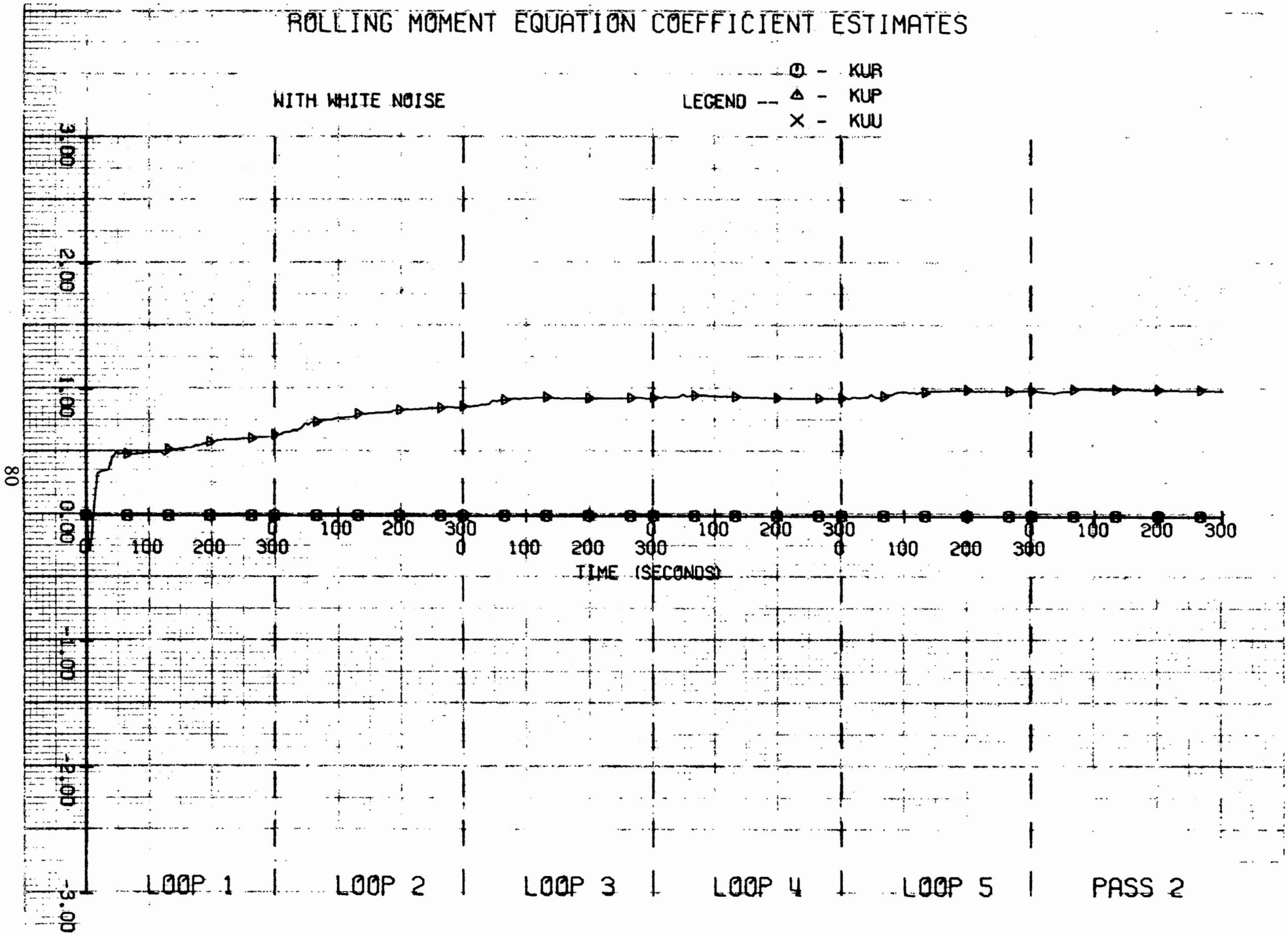
ROLLING MOMENT EQUATION COEFFICIENT ESTIMATES
WITH WHITE NOISE
LEGEND -- ① - KUR
△ - KUP
× - KUU
3.00
2.00
1.00
0.00
-1.00
-2.00
-3.00
0
100
200
300
TIME (SECONDS)
LOOP 1
LOOP 2
LOOP 3
LOOP 4
LOOP 5
PASS 2

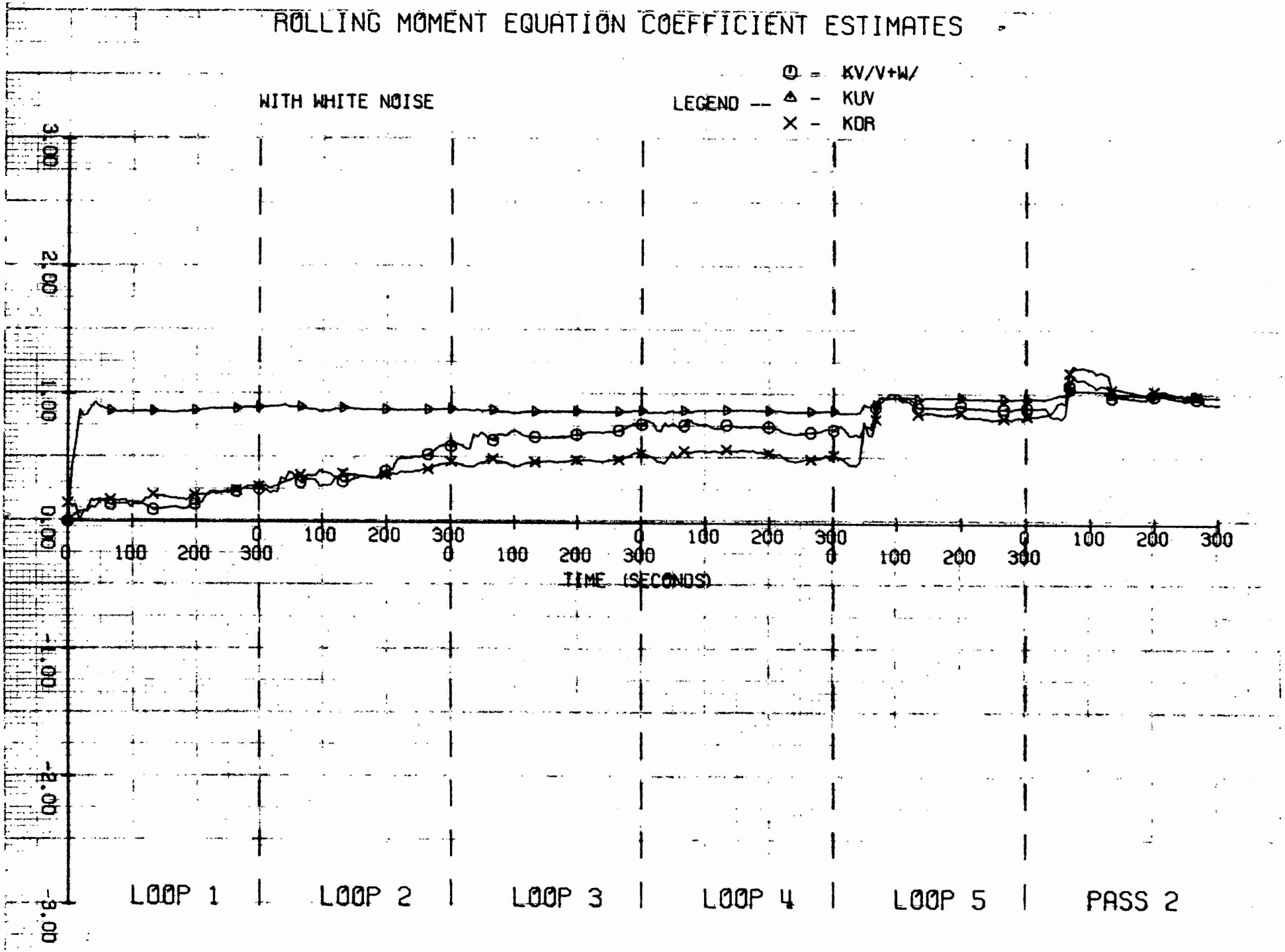
ROLLING MOMENT EQUATION COEFFICIENT ESTIMATES
WITH WHITE NOISE
LEGEND -- ⓘ = KV/V+W/
△ - KUV
× - KOR
3.00
2.00
1.00
0.00
-1.00
-2.00
-3.00
0
100
200
300
TIME (SECONDS)
LOOP 1
LOOP 2
LOOP 3
LOOP 4
LOOP 5
PASS 2

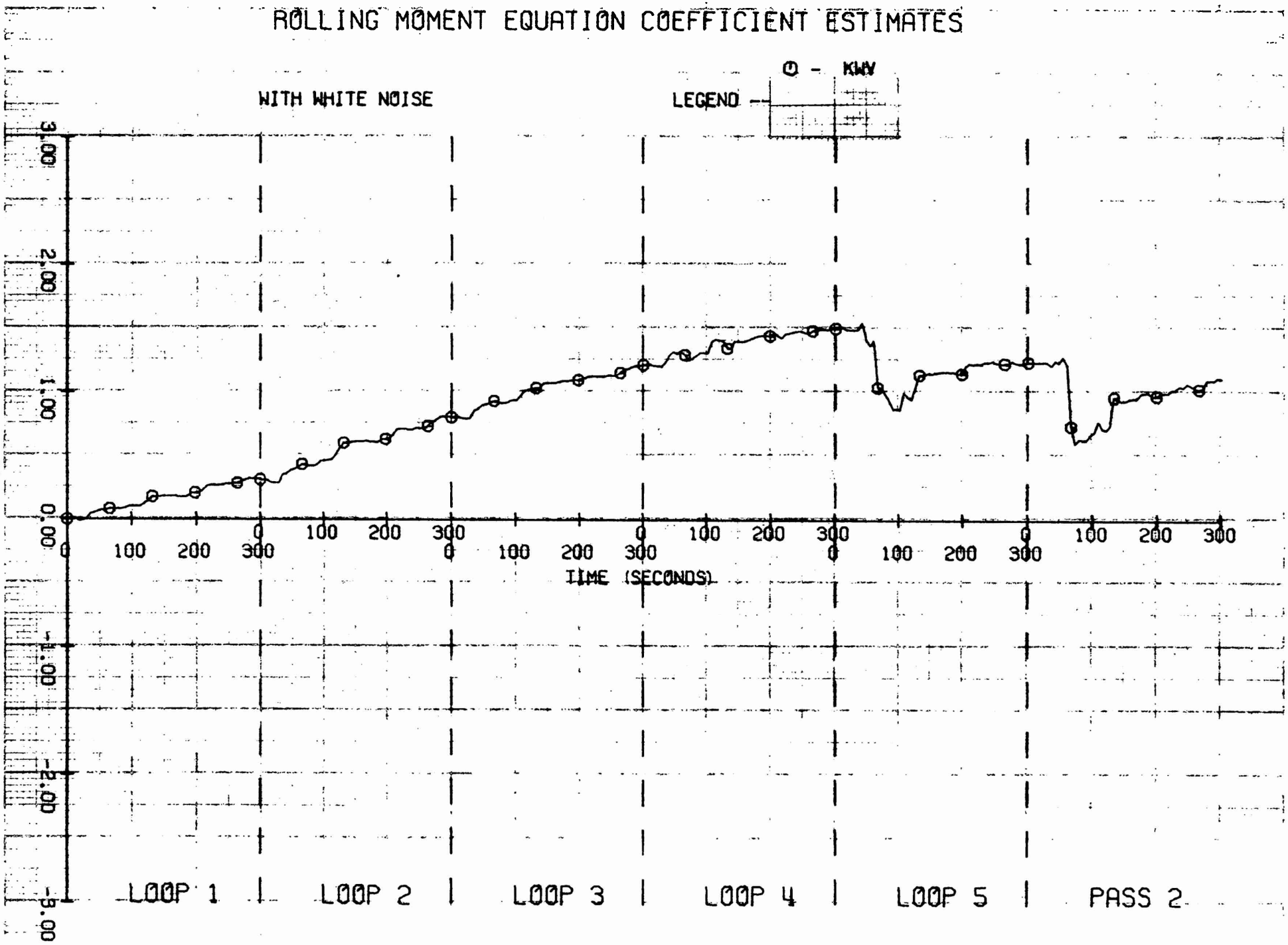
ROLLING MOMENT EQUATION COEFFICIENT ESTIMATES
WITH WHITE NOISE
LEGEND
KWV
3.00
2.00
1.00
0.00
-1.00
-2.00
-3.00
0
100
200
300
TIME (SECONDS)
LOOP 1
LOOP 2
LOOP 3
LOOP 4
LOOP 5
PASS 2

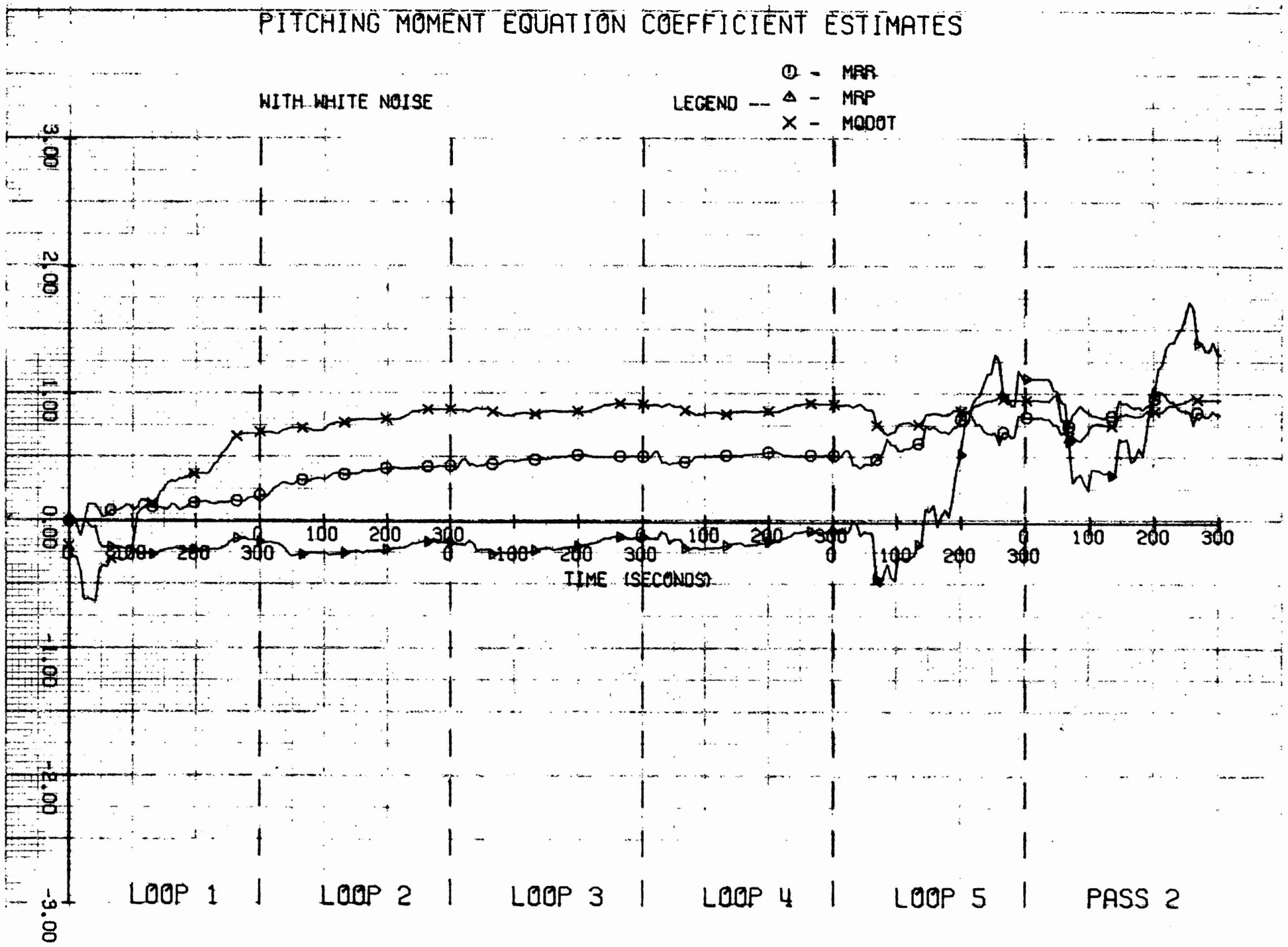
PITCHING MOMENT EQUATION COEFFICIENT ESTIMATES
WITH WHITE NOISE
LEGEND -- ○ - MRR
△ - MRP
× - MQDOT
3.00
2.00
1.00
0.00
-1.00
-2.00
-3.00
0
100
200
300
TIME (SECONDS)
LOOP 1
LOOP 2
LOOP 3
LOOP 4
LOOP 5
PASS 2

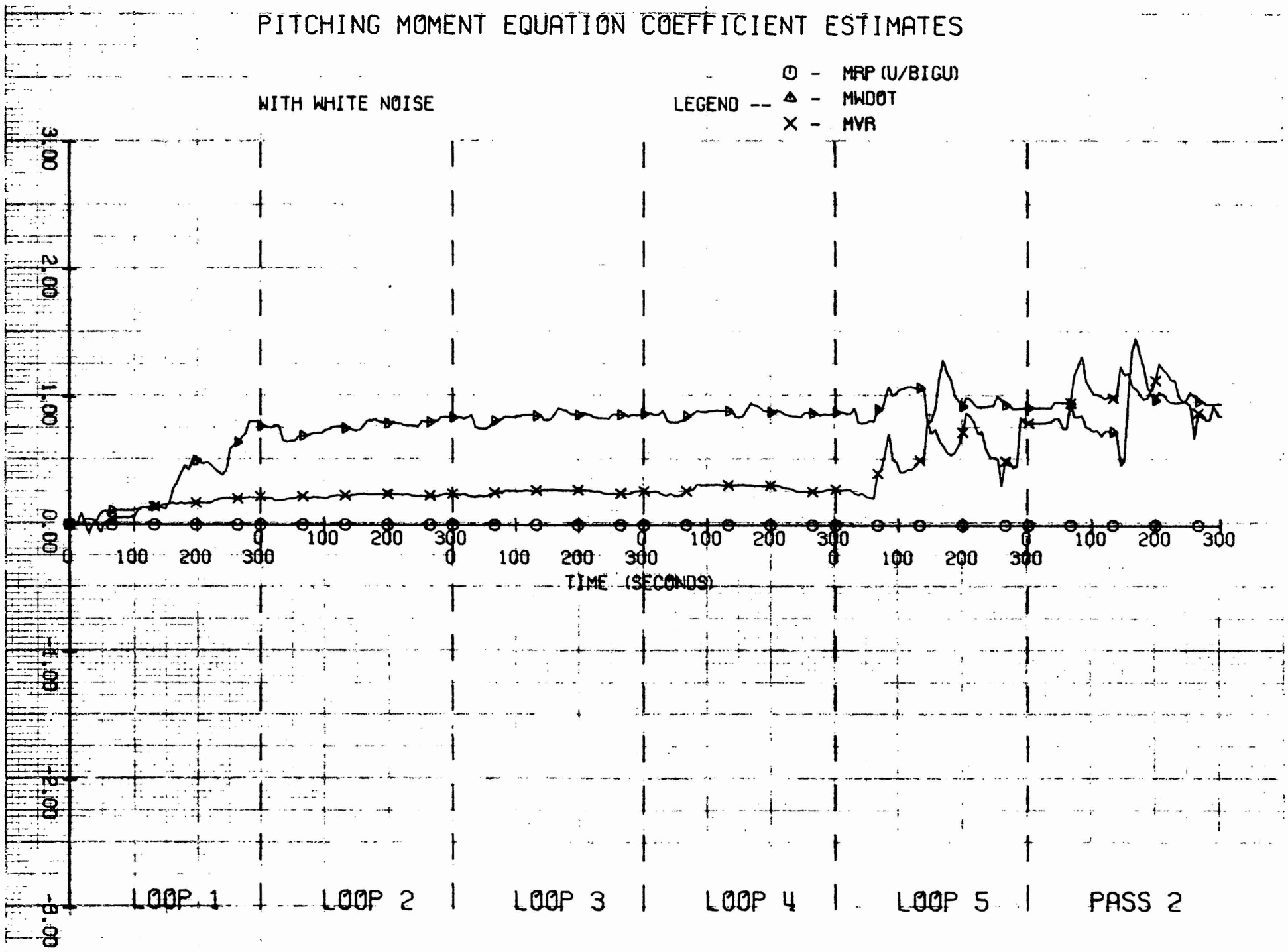
PITCHING MOMENT EQUATION COEFFICIENT ESTIMATES
WITH WHITE NOISE
LEGEND -- ○ - MRP (U/BIGU)
△ - MWDOT
× - MVR
3.00
2.00
1.00
0.00
-1.00
-2.00
-3.00
0 100 200 300 0 100 200 300 0 100 200 300 0 100 200 300 0 100 200 300
TIME (SECONDS)
LOOP 1
LOOP 2
LOOP 3
LOOP 4
LOOP 5
PASS 2

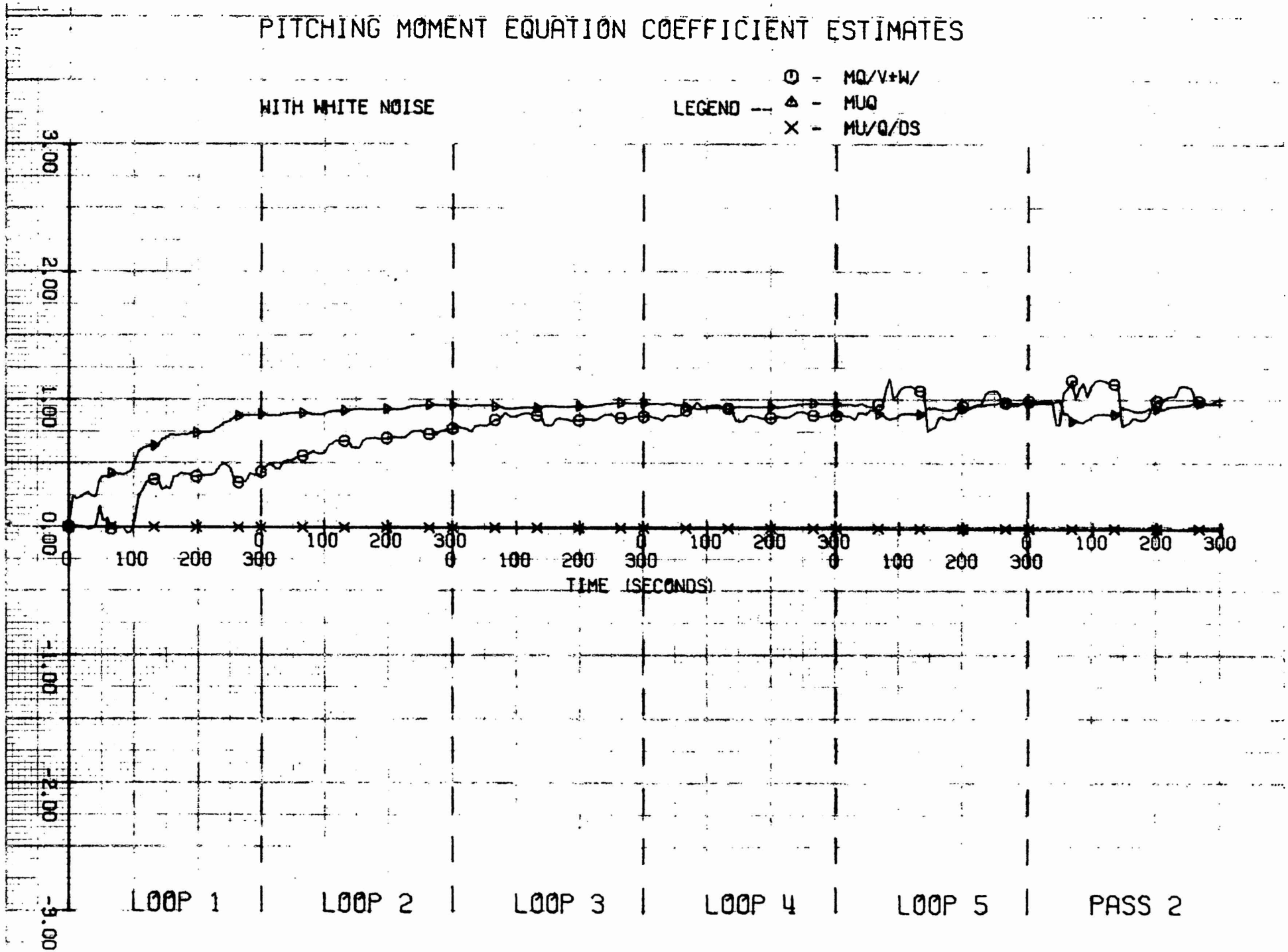
PITCHING MOMENT EQUATION COEFFICIENT ESTIMATES
WITH WHITE NOISE
LEGEND --
MQ/V+W/
MUQ
MU/Q/DS
3.00
2.00
1.00
0.00
-1.00
-2.00
-3.00
0
100
200
300
TIME (SECONDS)
LOOP 1
LOOP 2
LOOP 3
LOOP 4
LOOP 5
PASS 2

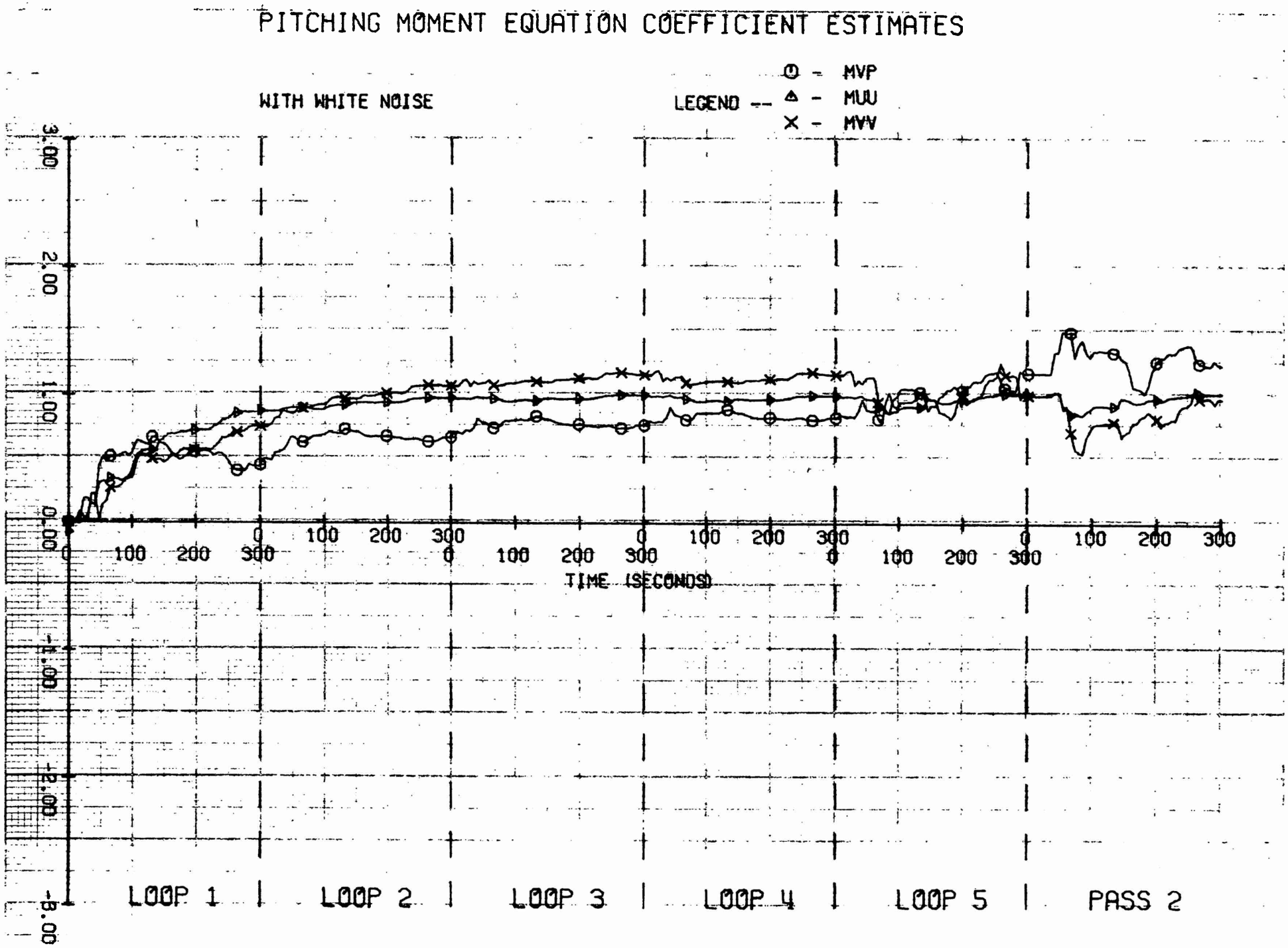
PITCHING MOMENT EQUATION COEFFICIENT ESTIMATES
WITH WHITE NOISE
LEGEND -- ⊙ - MVP
△ - MUU
× - MVV
3.00
2.00
1.00
0.00
-1.00
-2.00
-3.00
0 100 200 300 0 100 200 300 0 100 200 300 0 100 200 300 0 100 200 300
TIME (SECONDS)
LOOP 1
LOOP 2
LOOP 3
LOOP 4
LOOP 5
PASS 2

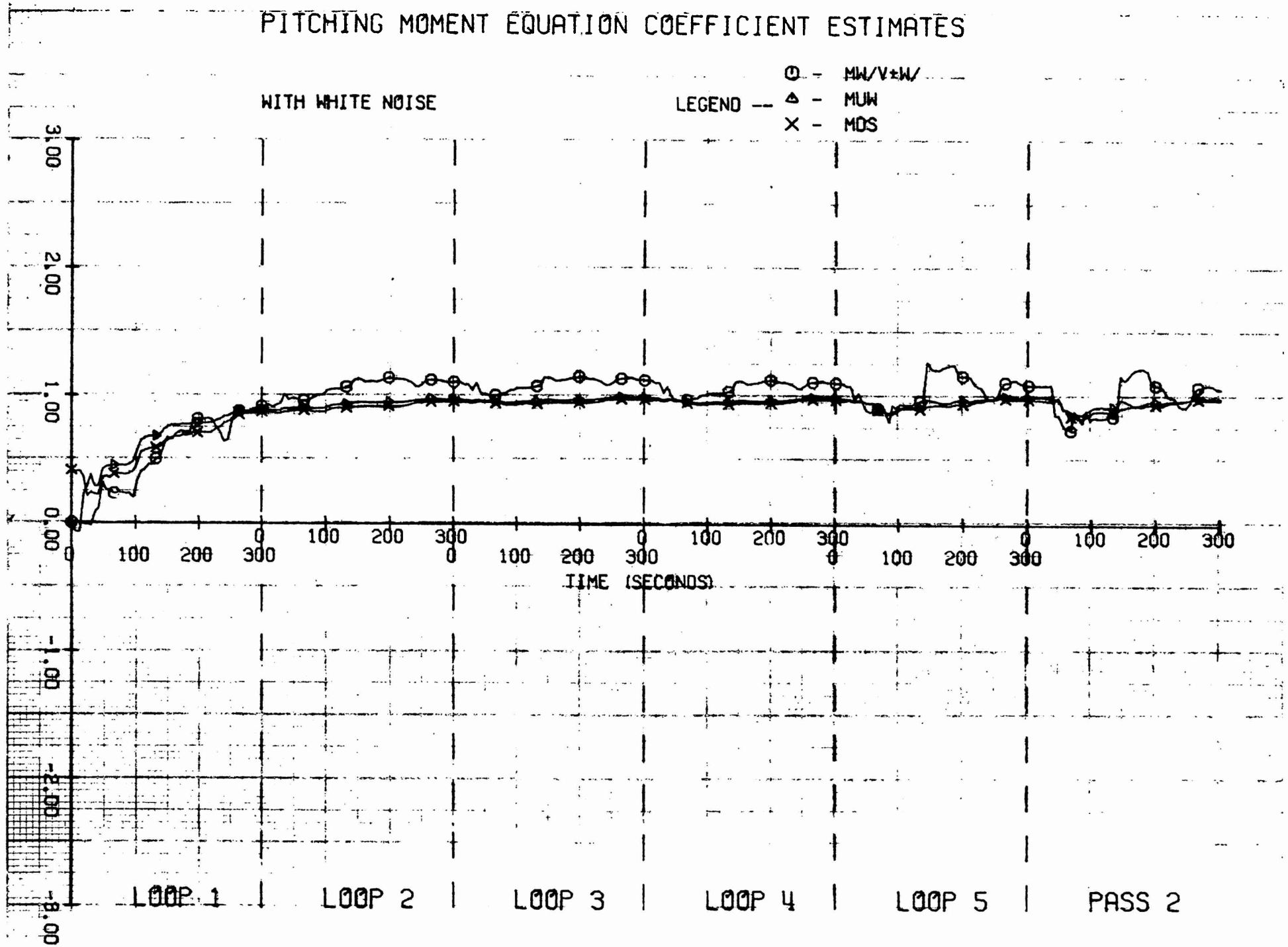
PITCHING MOMENT EQUATION COEFFICIENT ESTIMATES
WITH WHITE NOISE
LEGEND -- ① - MW/V±W/
△ - MUW
× - MDS
3.00
2.00
1.00
0.00
-1.00
-2.00
-3.00
0
100
200
300
TIME (SECONDS)
LOOP 1
LOOP 2
LOOP 3
LOOP 4
LOOP 5
PASS 2

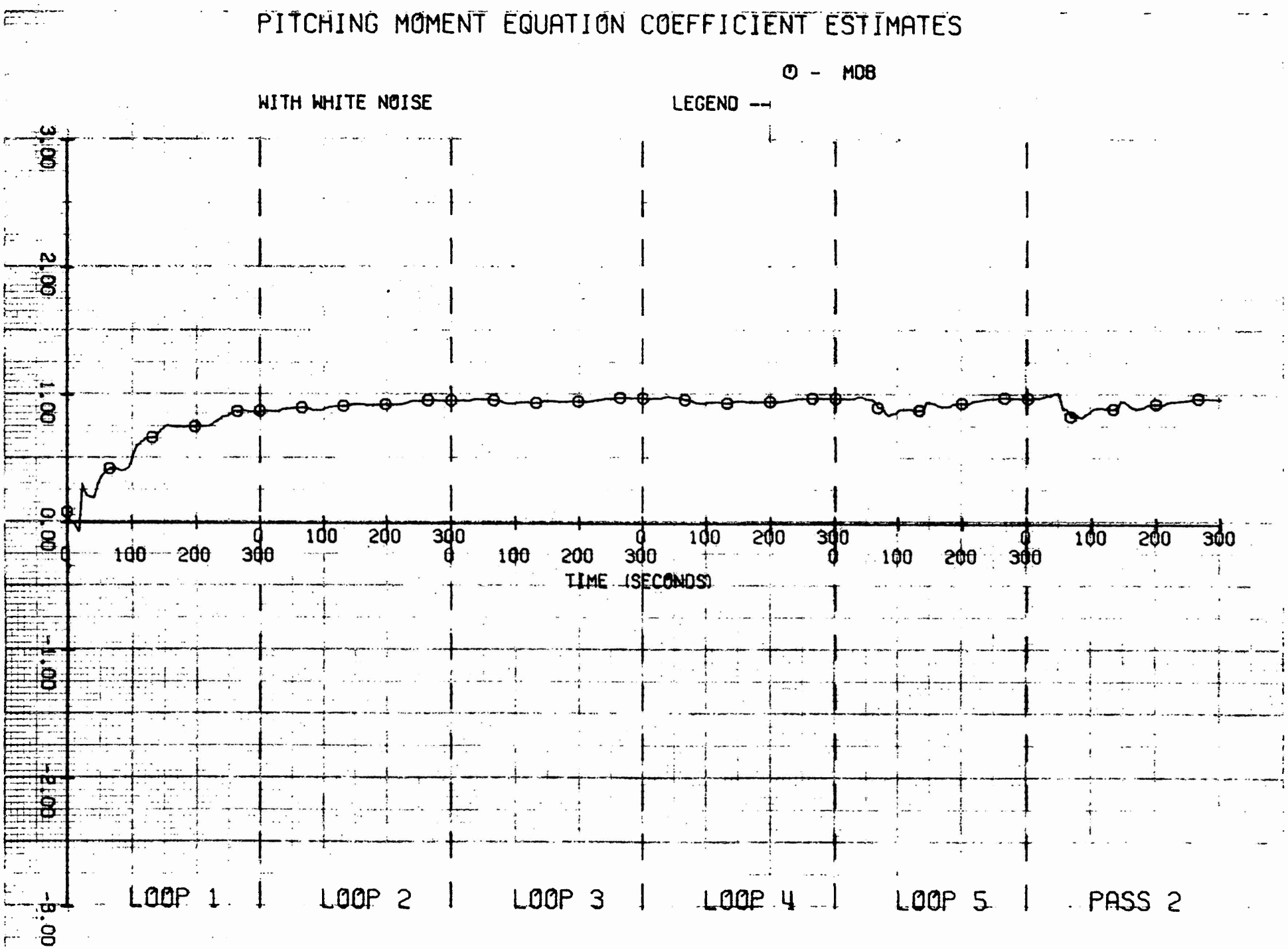
PITCHING MOMENT EQUATION COEFFICIENT ESTIMATES
WITH WHITE NOISE
LEGEND --
O - M08
3.00
2.00
1.00
0.00
-1.00
-2.00
-3.00
0
100
200
300
TIME (SECONDS)
LOOP 1
LOOP 2
LOOP 3
LOOP 4
LOOP 5
PASS 2

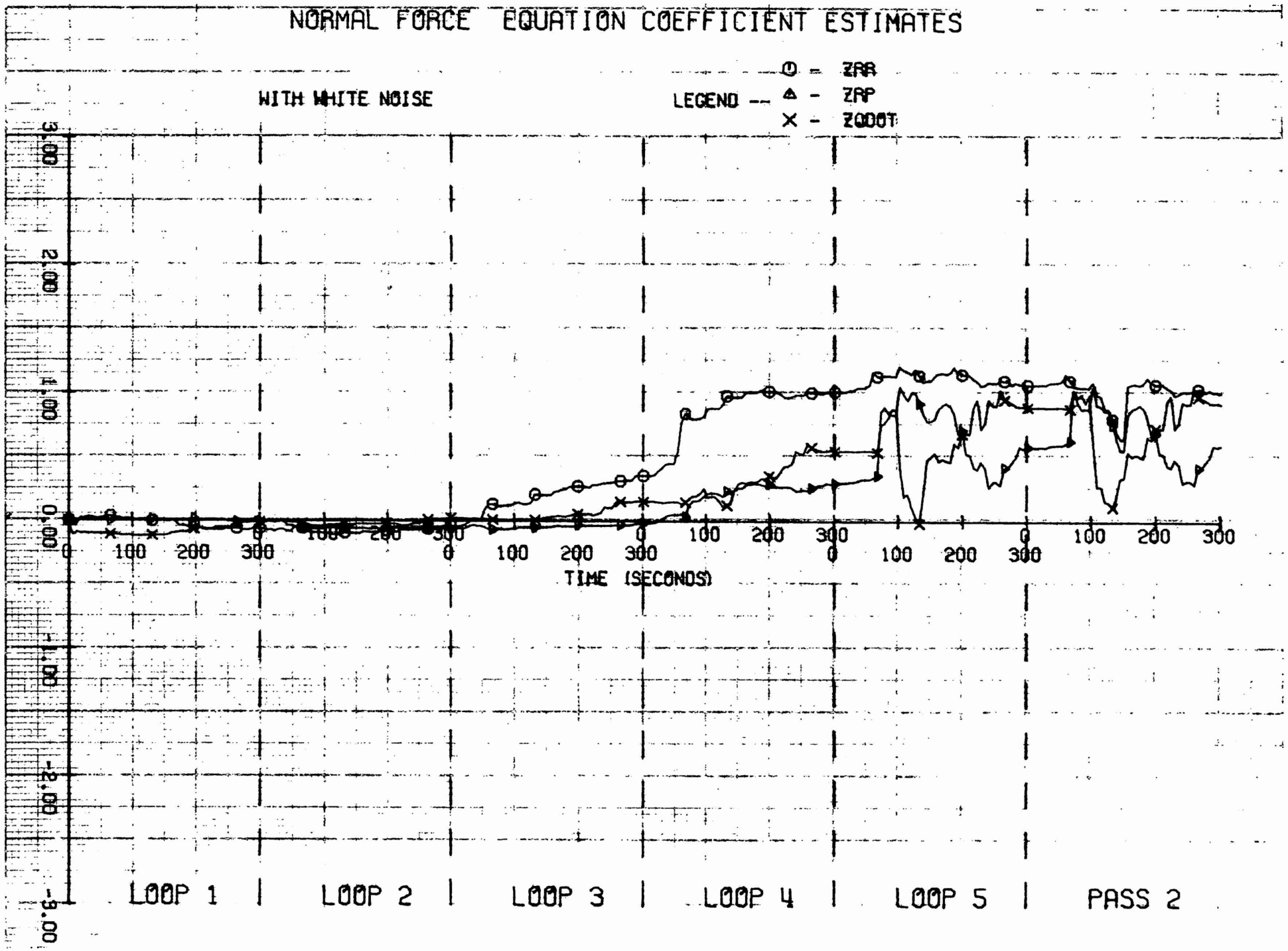
NORMAL FORCE EQUATION COEFFICIENT ESTIMATES
WITH WHITE NOISE
LEGEND -- ○ - ZAA
△ - ZAP
× - ZQQT
3.00
2.00
1.00
0.00
-1.00
-2.00
-3.00
0
100
200
300
TIME (SECONDS)
LOOP 1
LOOP 2
LOOP 3
LOOP 4
LOOP 5
PASS 2

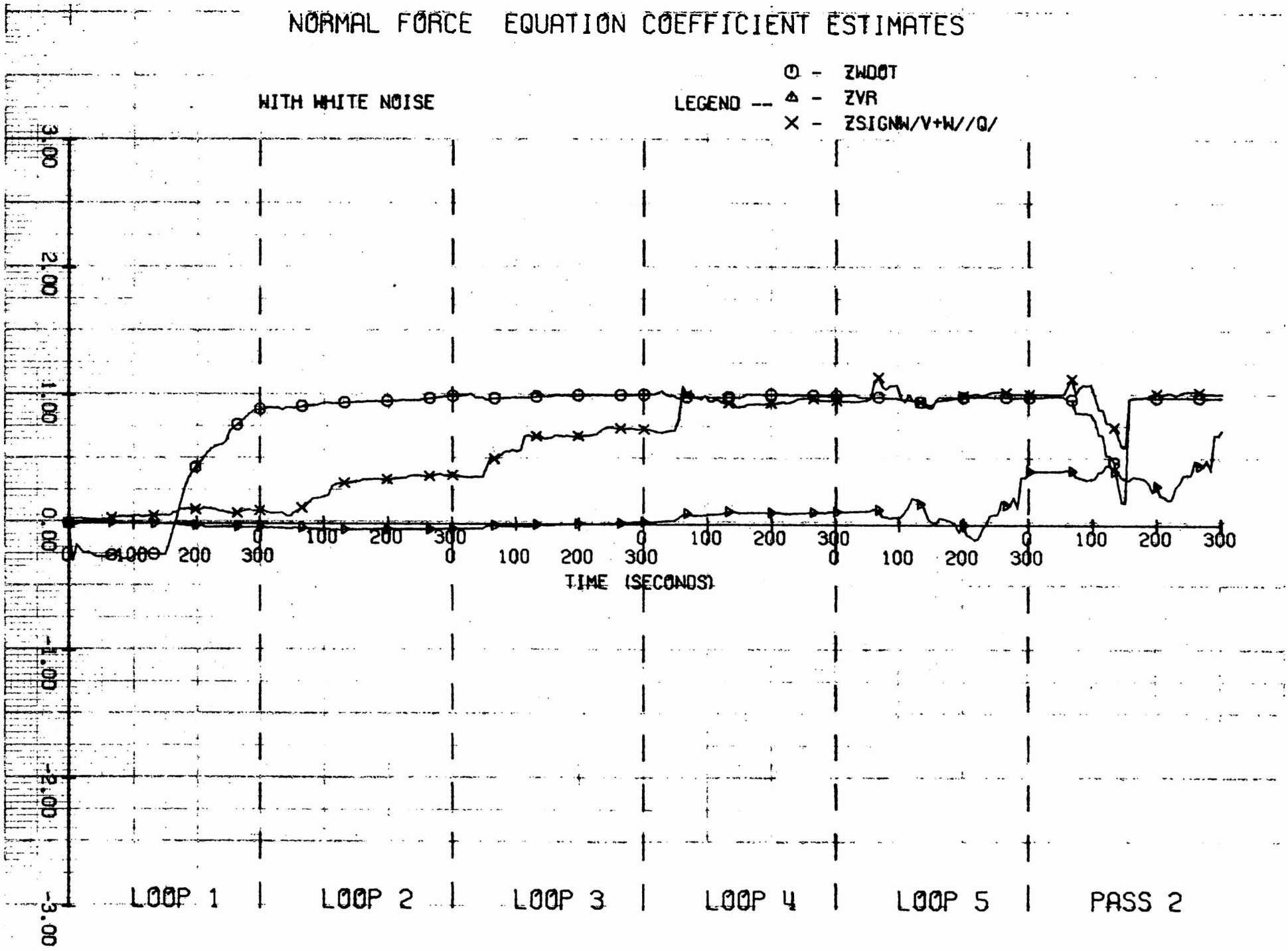
NORMAL FORCE EQUATION COEFFICIENT ESTIMATES
WITH WHITE NOISE
LEGEND --
⊙ - ZWDOT
△ - ZVR
× - ZSIGNW/V+W//Q/
3.00
2.00
1.00
0.00
-1.00
-2.00
-3.00
0
100
200
300
TIME (SECONDS)
LOOP 1
LOOP 2
LOOP 3
LOOP 4
LOOP 5
PASS 2

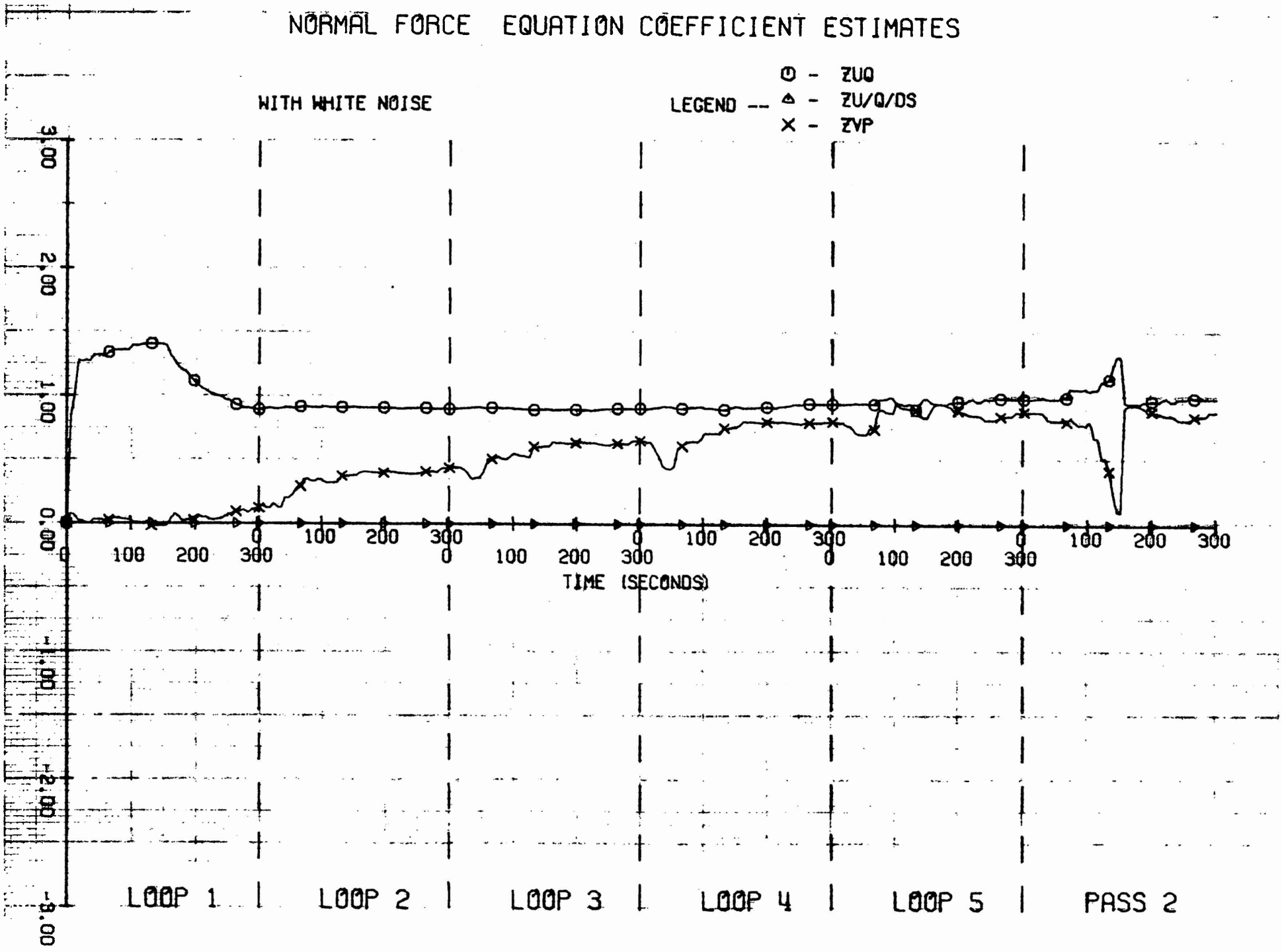
NORMAL FORCE EQUATION COEFFICIENT ESTIMATES
WITH WHITE NOISE
LEGEND -- ○ - ZUQ
△ - ZU/Q/DS
× - ZVP
3.00
2.00
1.00
0.00
-1.00
-2.00
-3.00
0
100
200
300
TIME (SECONDS)
LOOP 1
LOOP 2
LOOP 3
LOOP 4
LOOP 5
PASS 2

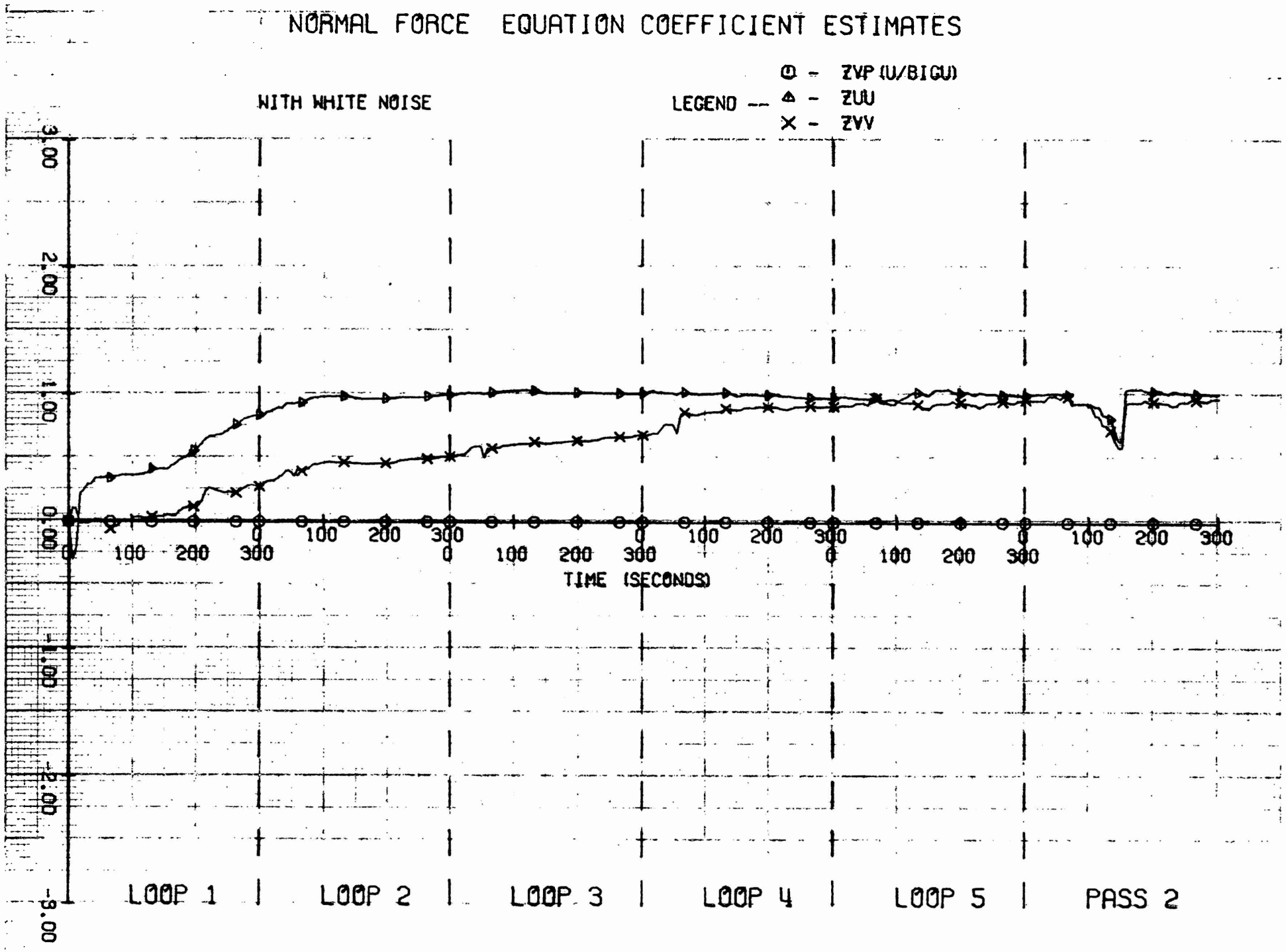
NORMAL FORCE EQUATION COEFFICIENT ESTIMATES
WITH WHITE NOISE
LEGEND --- ⊙ - ZVP (U/BIGU)
△ - ZUU
× - ZVV
3.00
2.00
1.00
0.00
-1.00
-2.00
-3.00
0
100
200
300
TIME (SECONDS)
LOOP 1
LOOP 2
LOOP 3
LOOP 4
LOOP 5
PASS 2

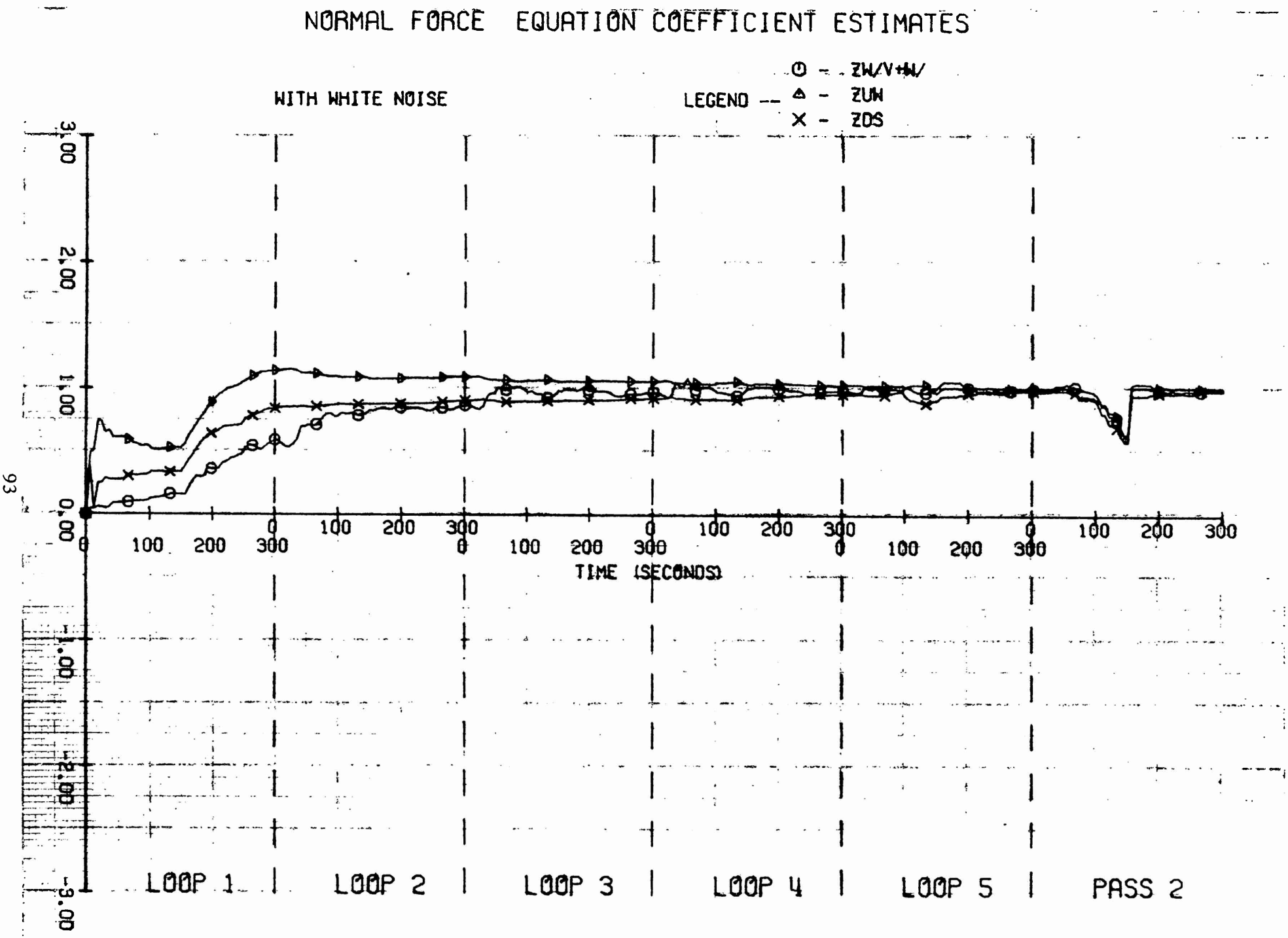
NORMAL FORCE EQUATION COEFFICIENT ESTIMATES
WITH WHITE NOISE
LEGEND -- ○ - ZW/V+W/
△ - ZUW
× - ZDS
3.00
2.00
1.00
0.00
-1.00
-2.00
-3.00
0
100
200
300
TIME (SECONDS)
LOOP 1
LOOP 2
LOOP 3
LOOP 4
LOOP 5
PASS 2

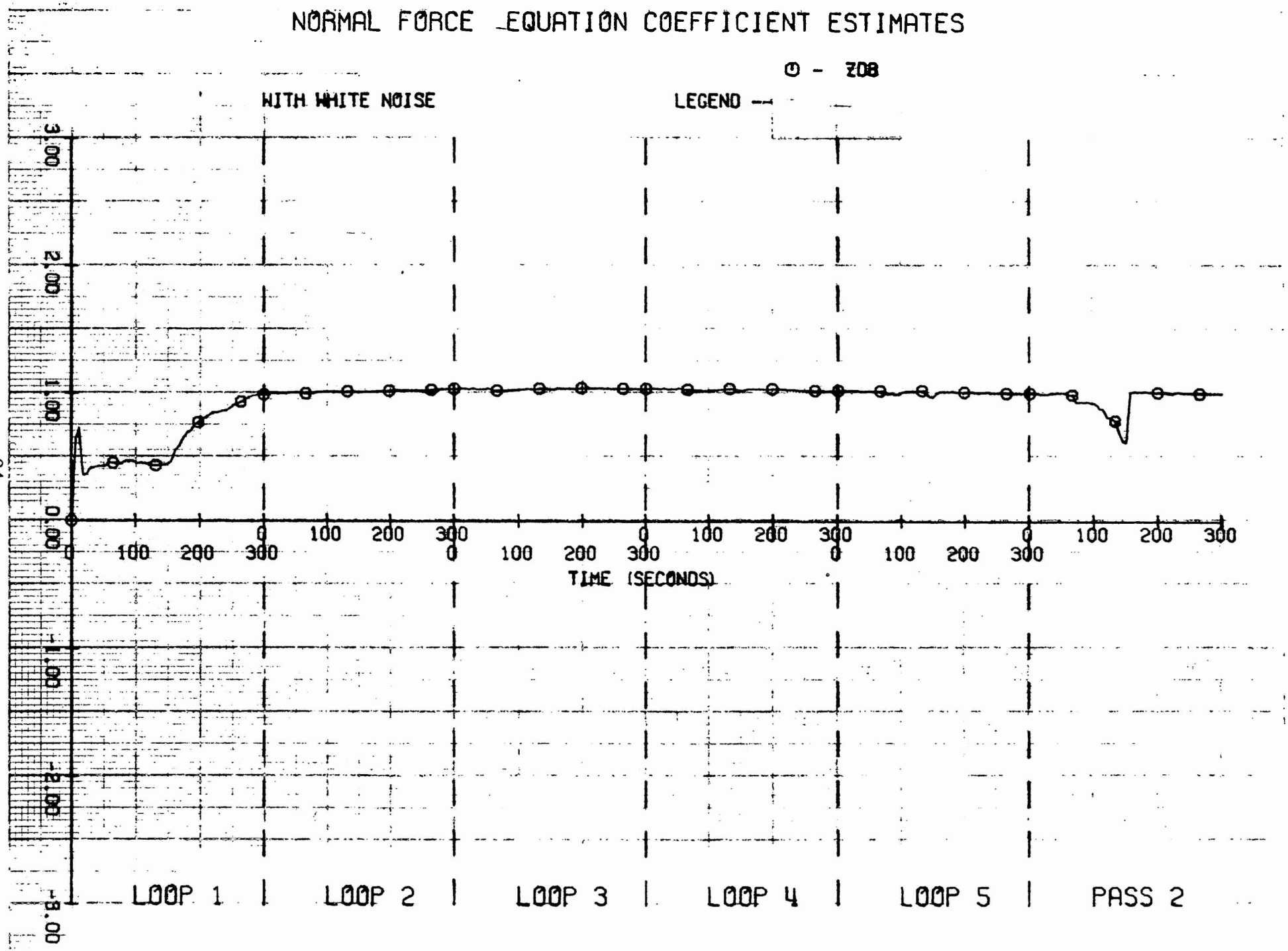
NORMAL FORCE EQUATION COEFFICIENT ESTIMATES
WITH WHITE NOISE
LEGEND --
O - Z08
3.00
2.00
1.00
0.00
-1.00
-2.00
-8.00
0
100
200
300
TIME (SECONDS)
LOOP 1
LOOP 2
LOOP 3
LOOP 4
LOOP 5
PASS 2

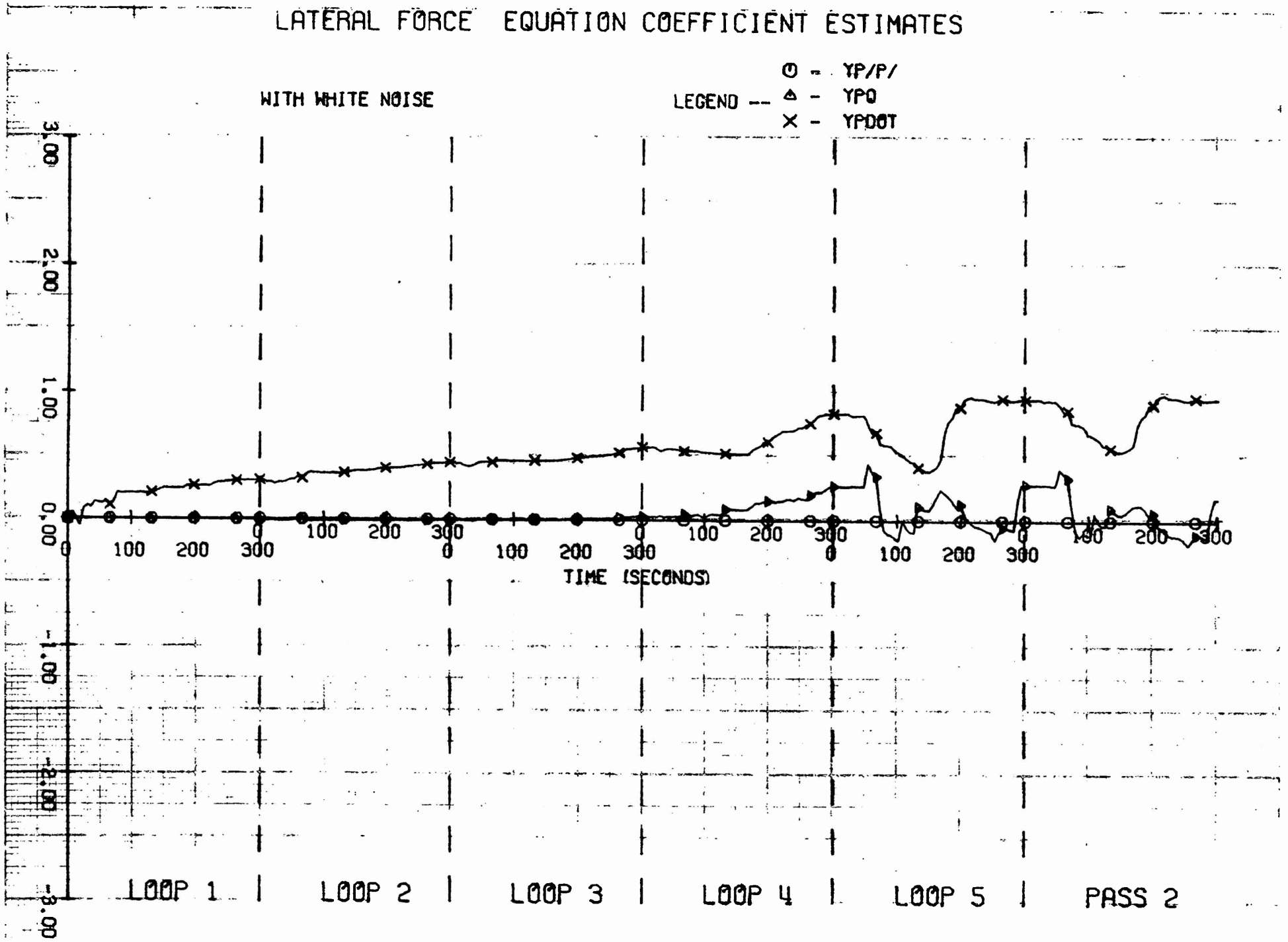
LATERAL FORCE EQUATION COEFFICIENT ESTIMATES
WITH WHITE NOISE
LEGEND -- ⊙ - YP/P/
△ - YPQ
× - YPDOT
3.00
2.00
1.00
0.00
-1.00
-2.00
-3.00
0
100
200
300
TIME (SECONDS)
LOOP 1
LOOP 2
LOOP 3
LOOP 4
LOOP 5
PASS 2

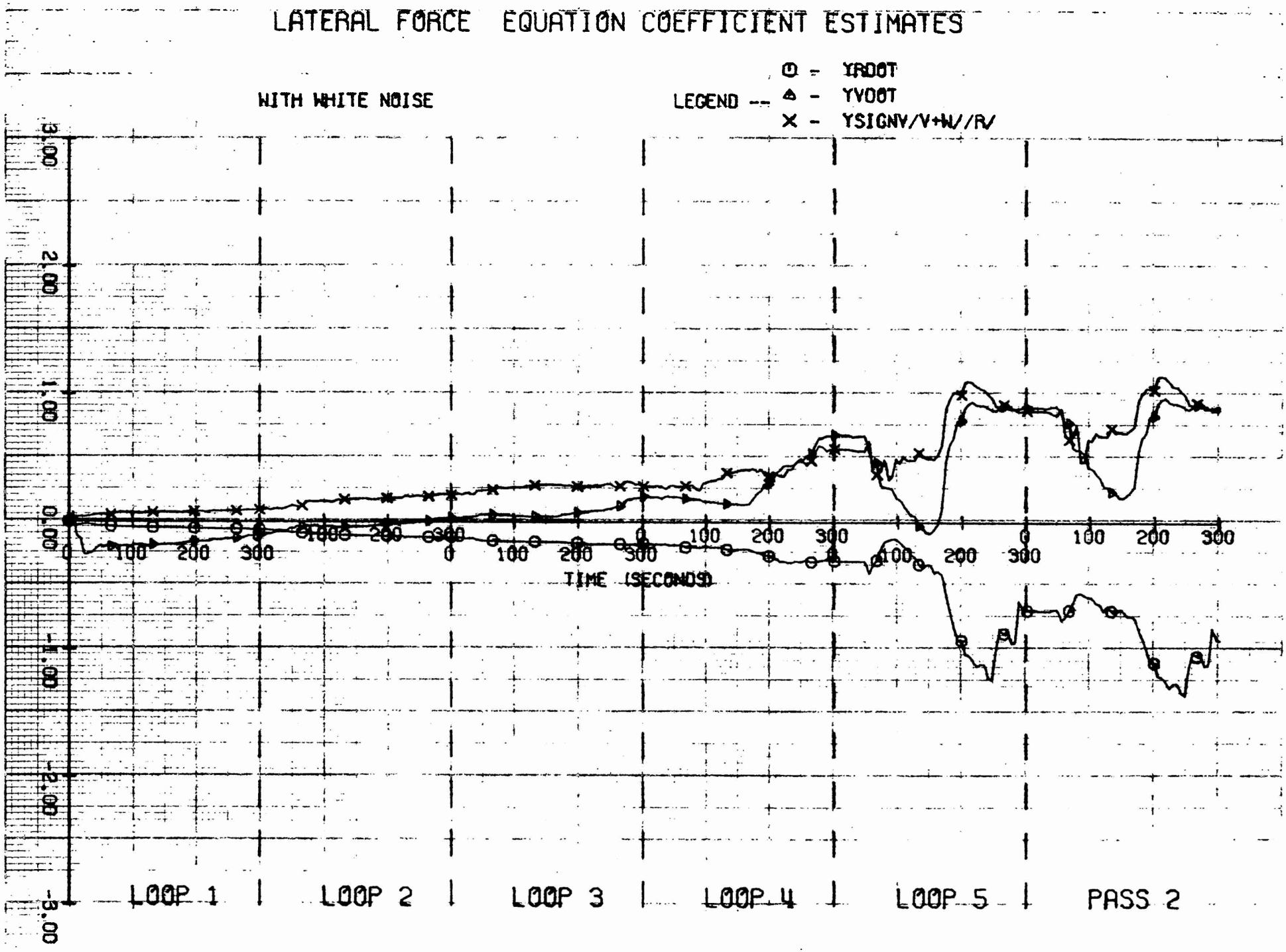
LATERAL FORCE EQUATION COEFFICIENT ESTIMATES
WITH WHITE NOISE
LEGEND -- ⊙ - YROOT
△ - YVOOT
× - YSIGNV/V+W//R/
3.00
2.00
1.00
0.00
-1.00
-2.00
-3.00
0
100
200
300
TIME (SECONDS)
LOOP 1
LOOP 2
LOOP 3
LOOP 4
LOOP 5
PASS 2

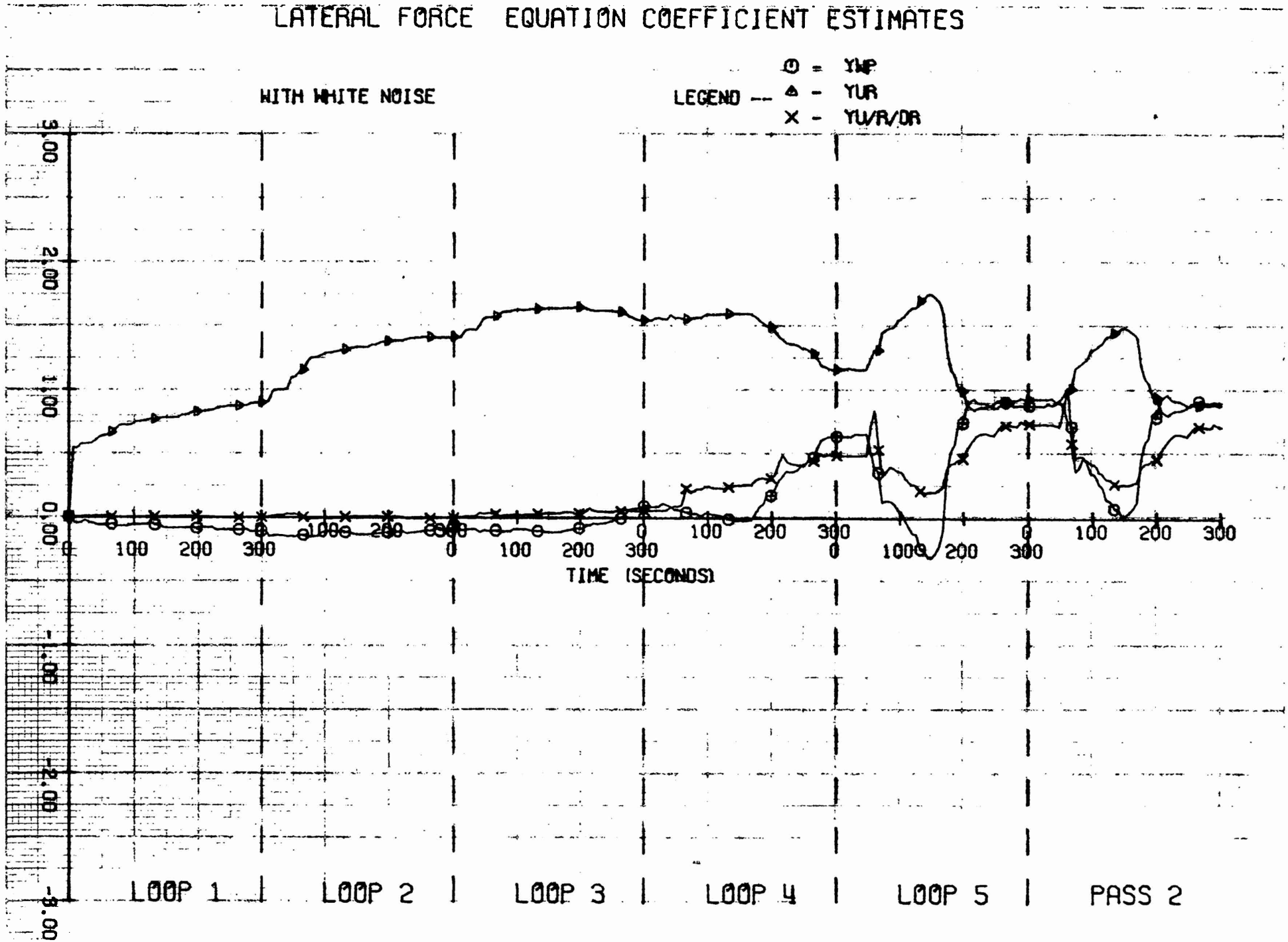
LATERAL FORCE EQUATION COEFFICIENT ESTIMATES
WITH WHITE NOISE
LEGEND -- ⊙ = YWP
△ - YUR
× - YU/R/DR
3.00
2.00
1.00
0.00
-1.00
-2.00
-3.00
0
100
200
300
TIME (SECONDS)
LOOP 1
LOOP 2
LOOP 3
LOOP 4
LOOP 5
PASS 2

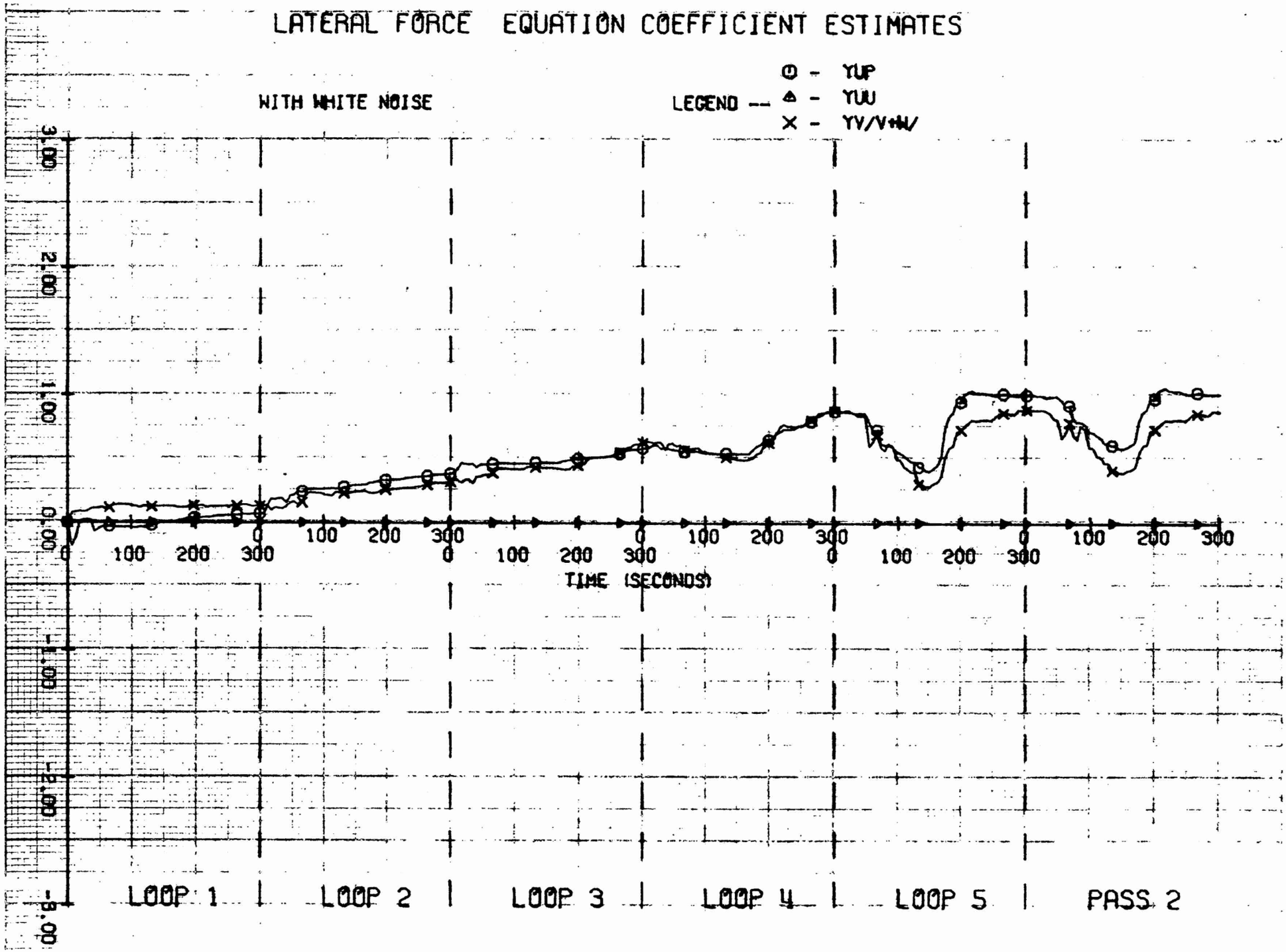
LATERAL FORCE EQUATION COEFFICIENT ESTIMATES
WITH WHITE NOISE
LEGEND --
⊙ - YUP
△ - YUU
× - YV/V+W/
3.00
2.00
1.00
0.00
-1.00
-2.00
-3.00
0
100
200
300
TIME (SECONDS)
LOOP 1
LOOP 2
LOOP 3
LOOP 4
LOOP 5
PASS 2

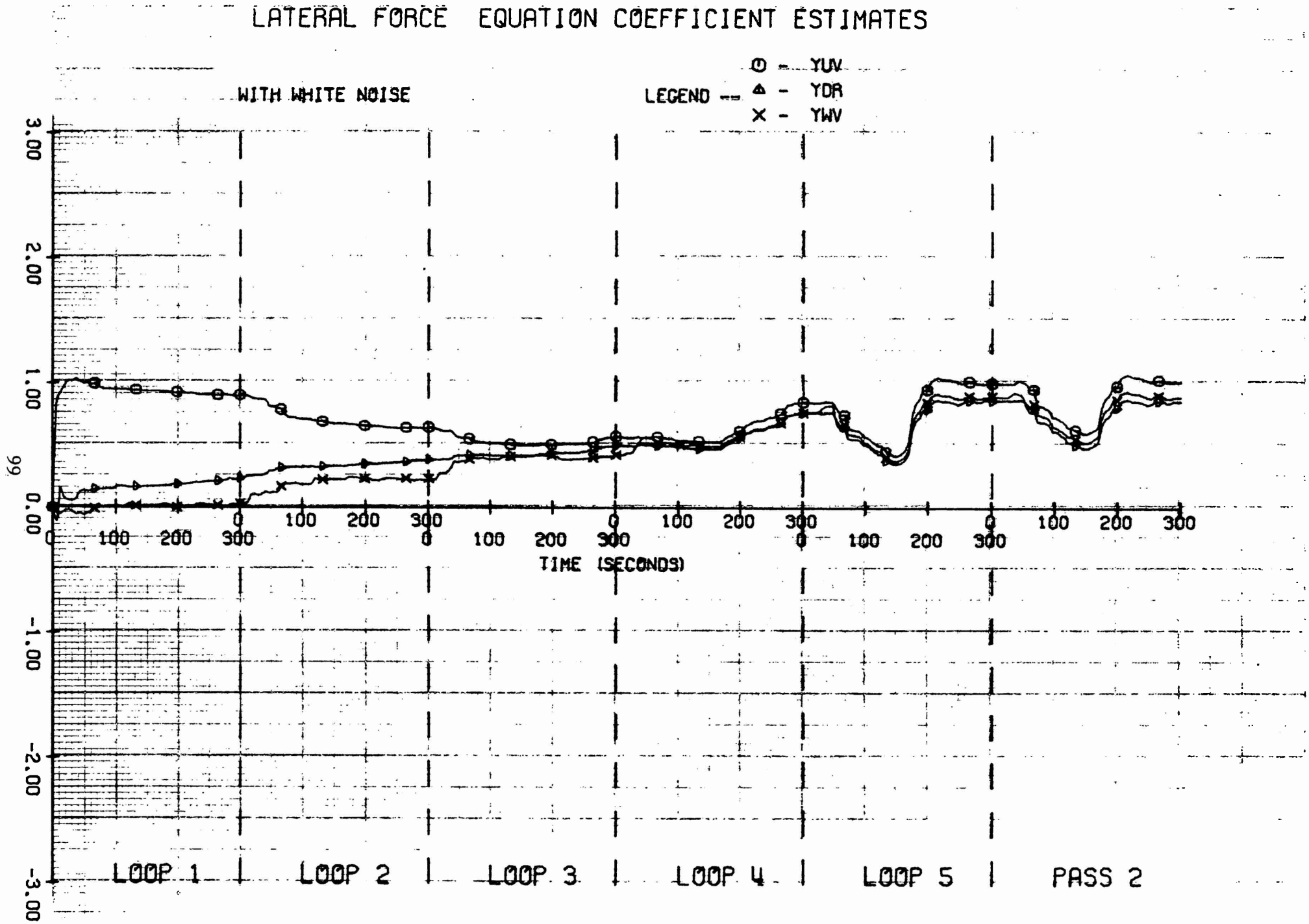
LATERAL FORCE EQUATION COEFFICIENT ESTIMATES
WITH WHITE NOISE
LEGEND -- ⊙ - YUV
△ - YDR
× - YWV
3.00
2.00
1.00
0.00
-1.00
-2.00
-3.00
0
100
200
300
TIME (SECONDS)
LOOP 1
LOOP 2
LOOP 3
LOOP 4
LOOP 5
PASS 2

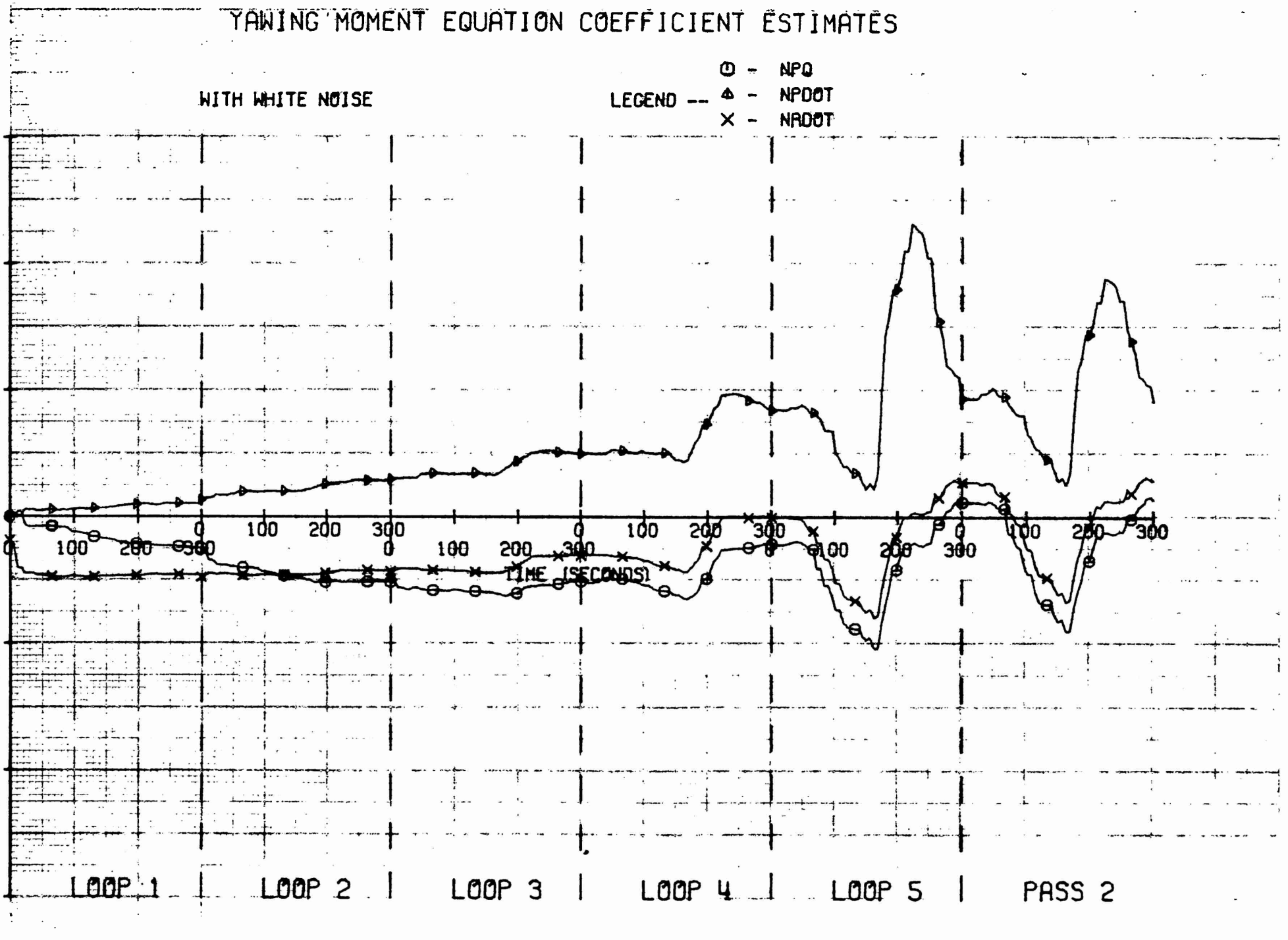
YAWING MOMENT EQUATION COEFFICIENT ESTIMATES
WITH WHITE NOISE
LEGEND -- ⊙ - NPQ
▲ - NPDOT
× - NRDOT
3.00
2.00
1.00
0.00
-1.00
-2.00
-3.00
0
100
200
300
TIME (SECONDS)
LOOP 1
LOOP 2
LOOP 3
LOOP 4
LOOP 5
PASS 2

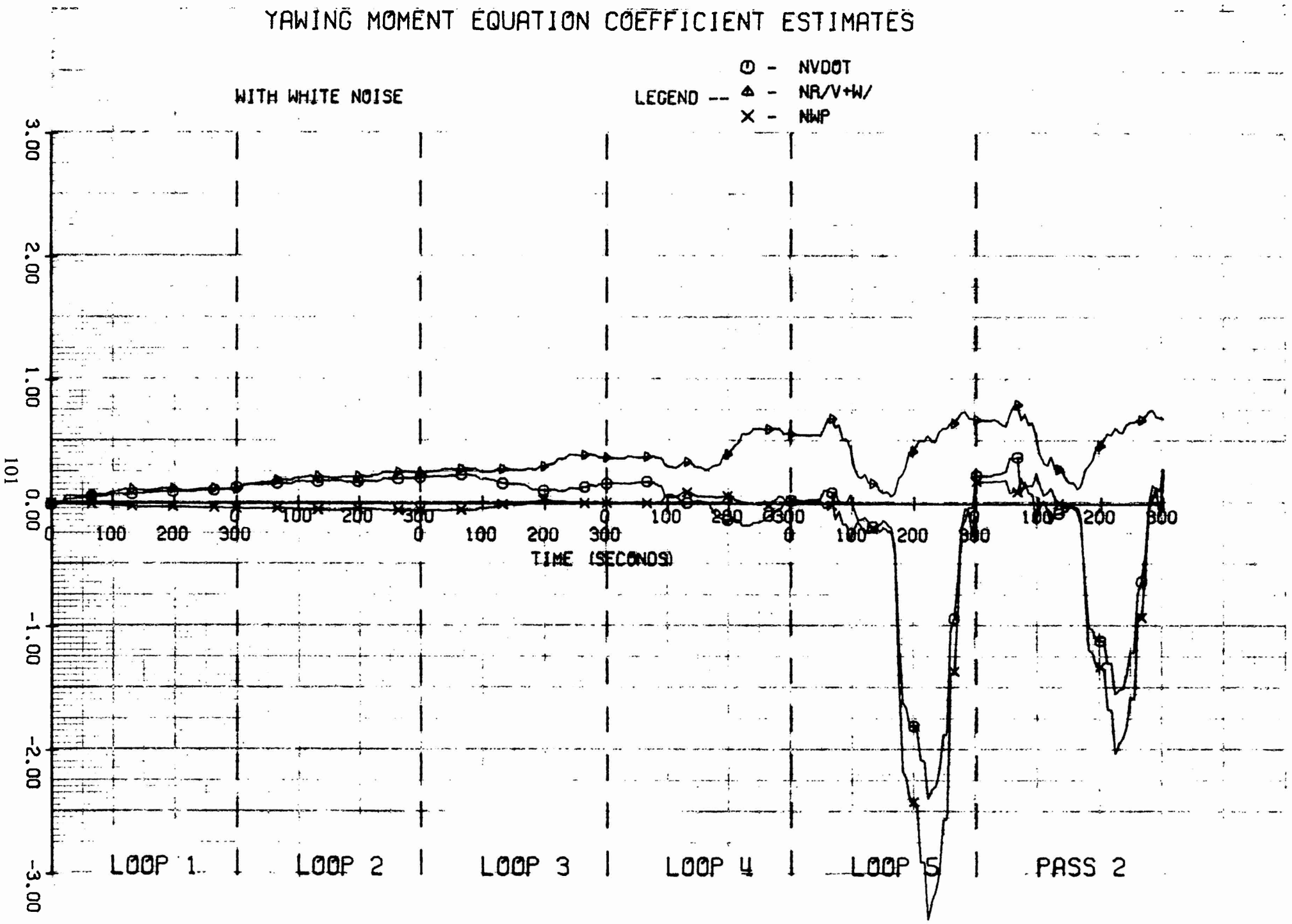
YAWING MOMENT EQUATION COEFFICIENT ESTIMATES
WITH WHITE NOISE
LEGEND -- ⊙ - NVDOT
△ - NR/V+W/
× - NWP
3.00
2.00
1.00
0.00
-1.00
-2.00
-3.00
0
100
200
300
TIME (SECONDS)
LOOP 1
LOOP 2
LOOP 3
LOOP 4
LOOP 5
PASS 2

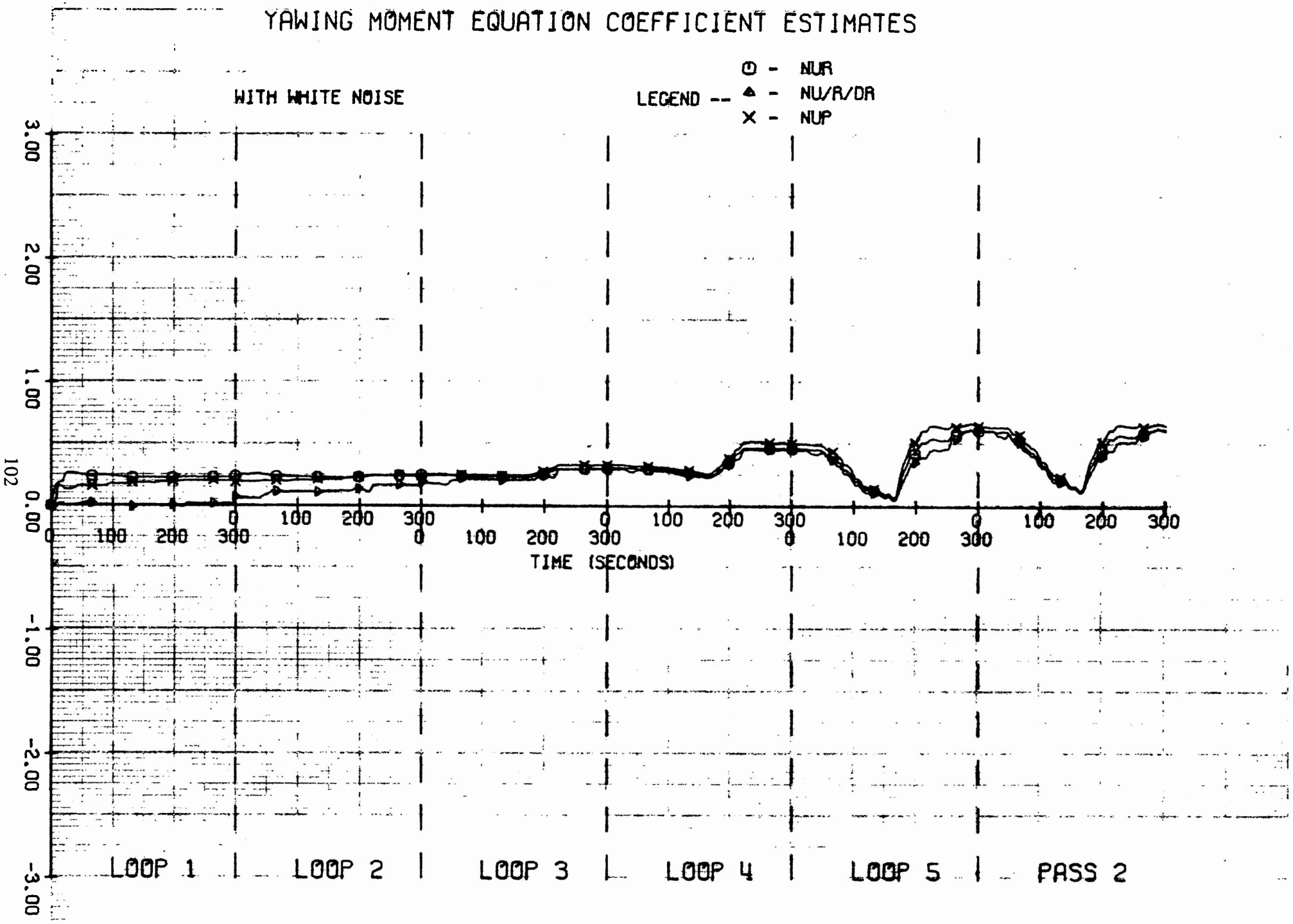
YAWING MOMENT EQUATION COEFFICIENT ESTIMATES
WITH WHITE NOISE
LEGEND -- ⊙ - NUR
▲ - NU/R/DR
× - NUP
3.00
2.00
1.00
0.00
-1.00
-2.00
-3.00
0 100 200 300 0 100 200 300 0 100 200 300 0 100 200 300
TIME (SECONDS)
LOOP 1
LOOP 2
LOOP 3
LOOP 4
LOOP 5
PASS 2

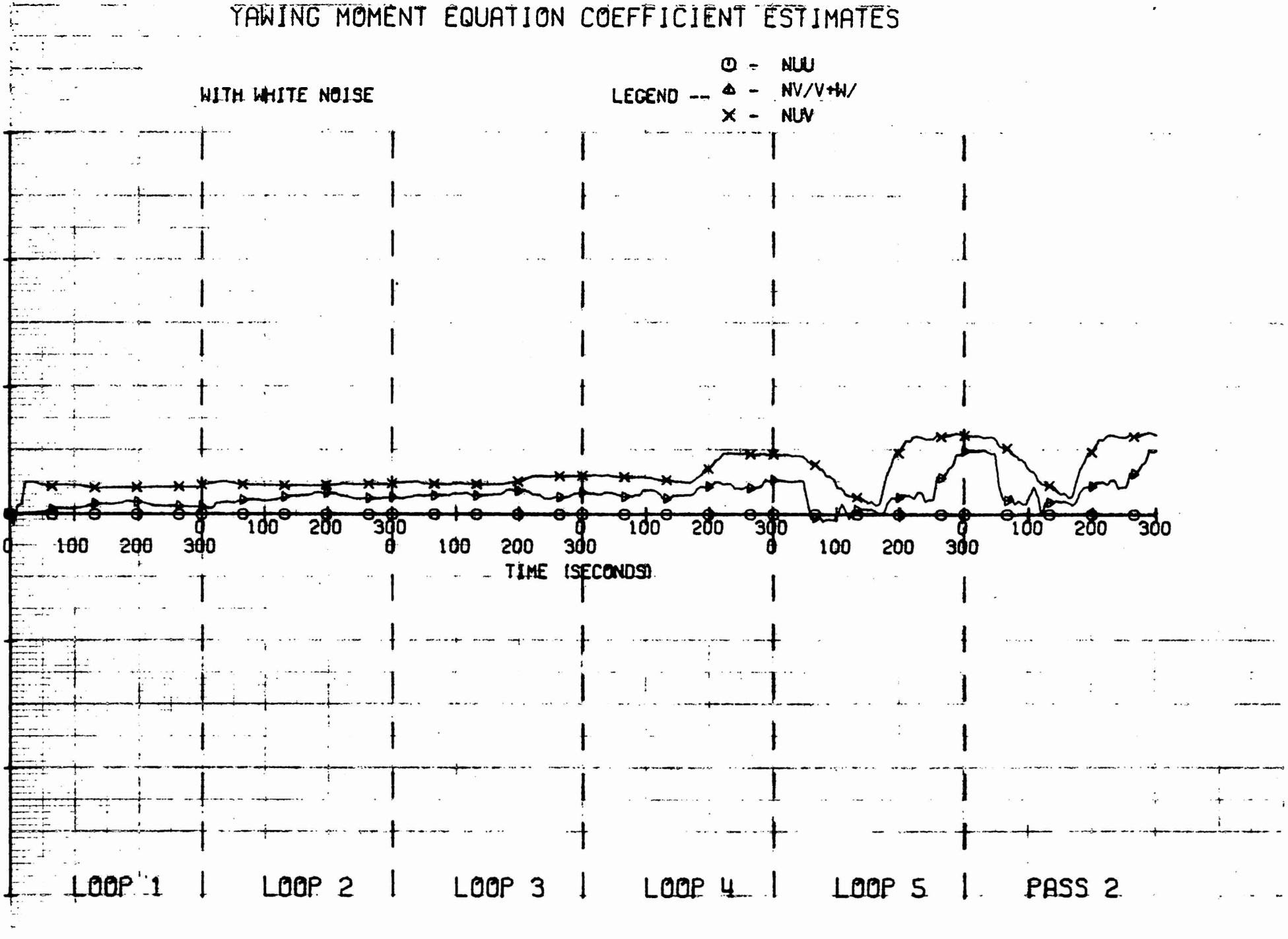
YAWING MOMENT EQUATION COEFFICIENT ESTIMATES
WITH WHITE NOISE
LEGEND -- ⊙ - NUU
△ - NV/V+W/
× - NUV
3.00
2.00
1.00
0.00
-1.00
-2.00
-3.00
0
100
200
300
TIME (SECONDS)
LOOP 1
LOOP 2
LOOP 3
LOOP 4
LOOP 5
PASS 2

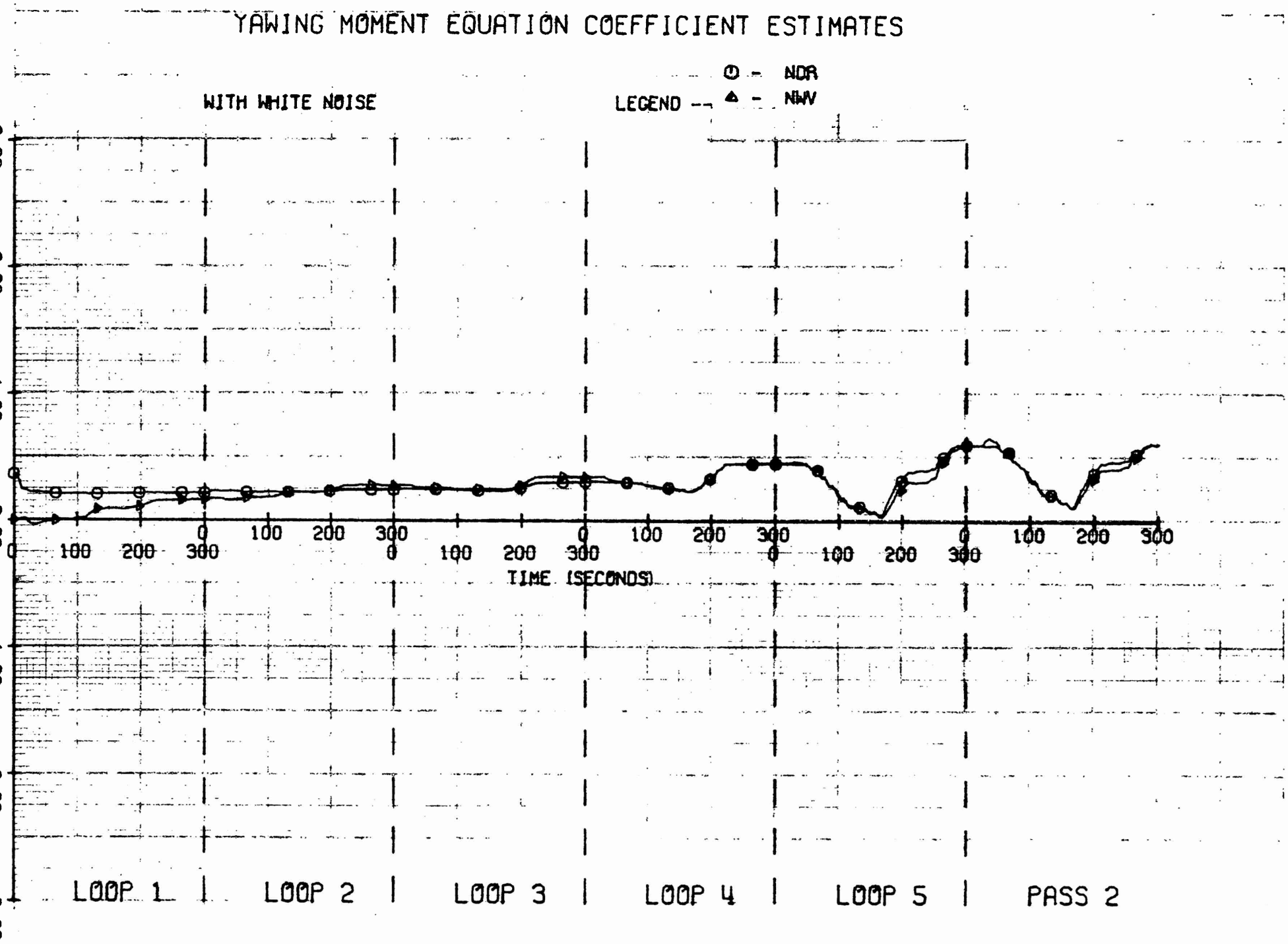
YAWING MOMENT EQUATION COEFFICIENT ESTIMATES
WITH WHITE NOISE
LEGEND -- ① - NDR
▲ - NWV
3.00
2.00
1.00
0.00
-1.00
-2.00
-3.00
0
100
200
300
TIME (SECONDS)
LOOP 1
LOOP 2
LOOP 3
LOOP 4
LOOP 5
PASS 2

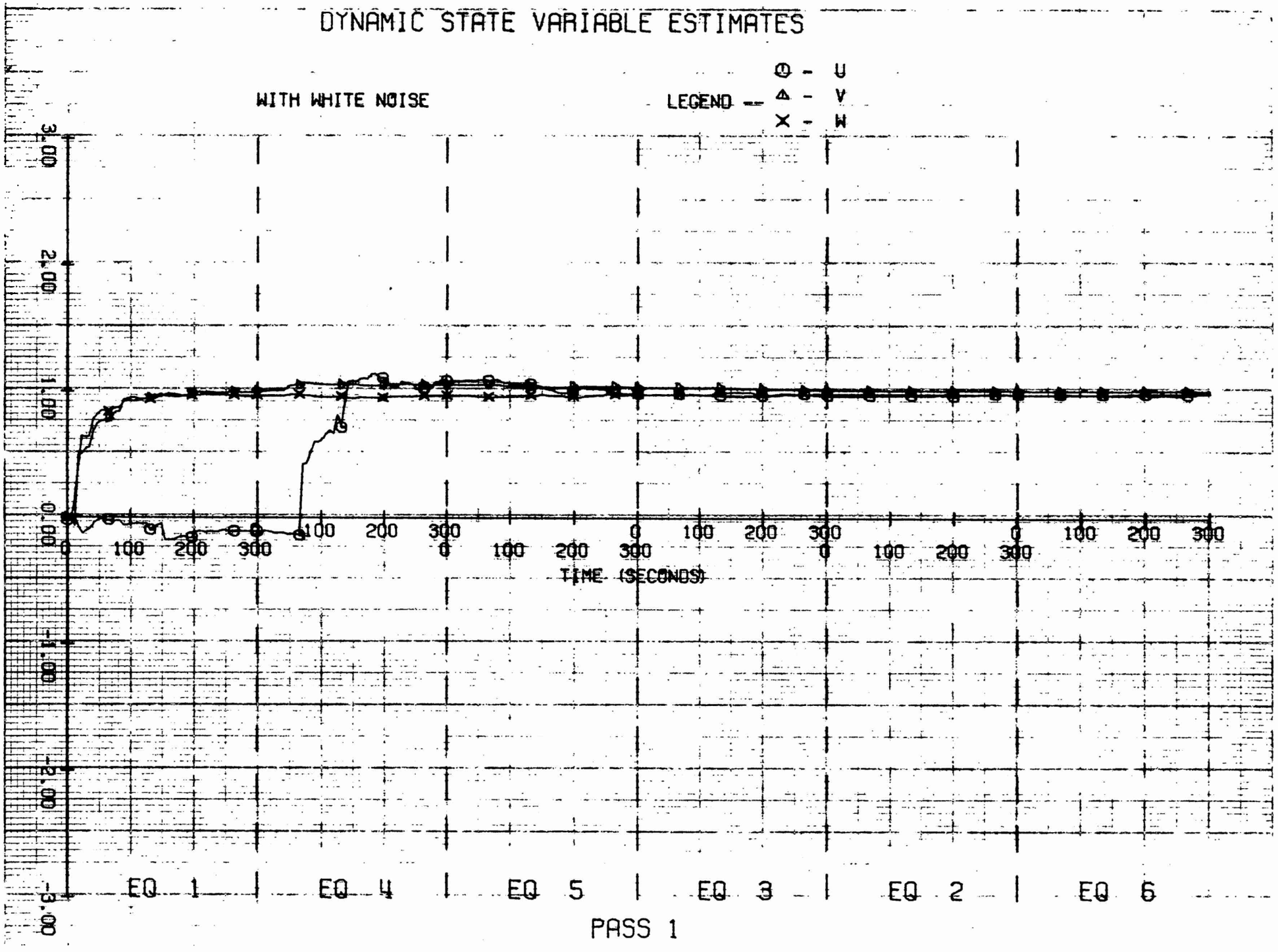
DYNAMIC STATE VARIABLE ESTIMATES
WITH WHITE NOISE
LEGEND -- ○ - U
△ - V
× - W
3.00
2.00
1.00
0.00
-1.00
-2.00
-3.00
0
100
200
300
TIME (SECONDS)
EQ 1
EQ 4
EQ 5
EQ 3
EQ 2
EQ 6
PASS 1

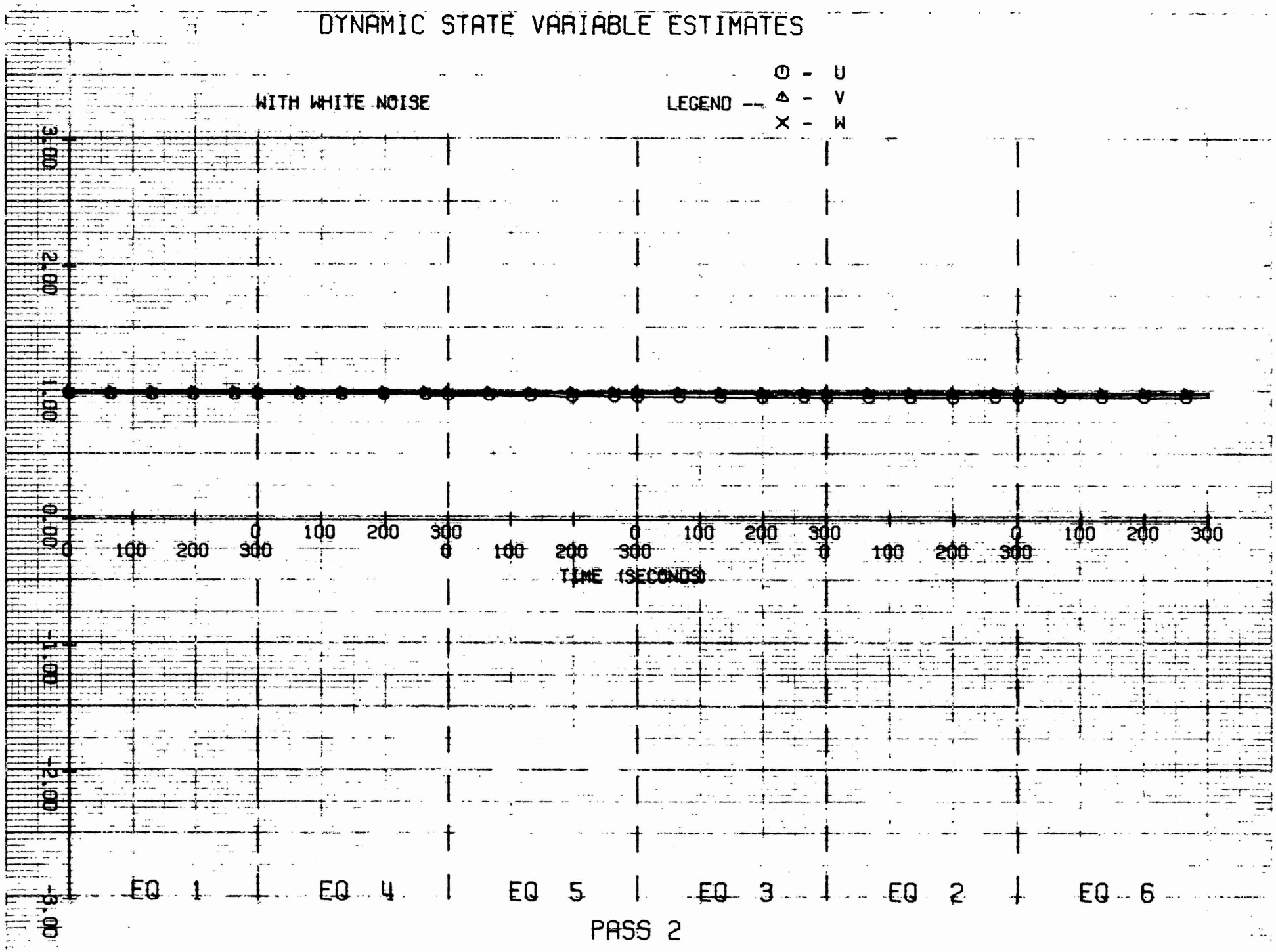
DYNAMIC STATE VARIABLE ESTIMATES
WITH WHITE NOISE
LEGEND -- ⊙ - U
△ - V
× - W
3.00
2.00
1.00
0.00
-1.00
-2.00
-3.00
0 100 200 300 0 100 200 300 0 100 200 300 0 100 200 300
TIME (SECONDS)
EQ 1
EQ 4
EQ 5
EQ 3
EQ 2
EQ 6
PASS 2

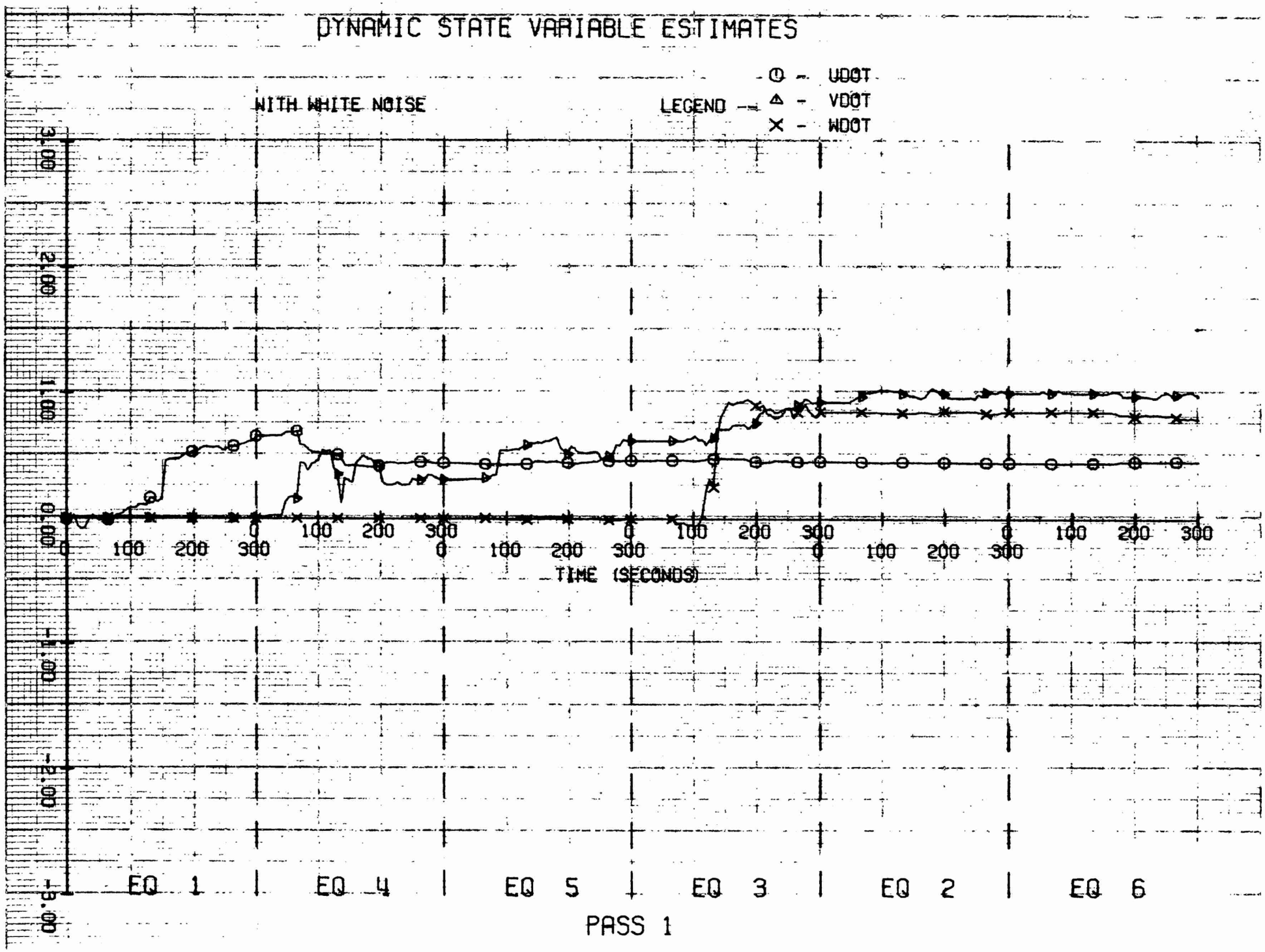
DYNAMIC STATE VARIABLE ESTIMATES
WITH WHITE NOISE
LEGEND
UDOT
VDOT
WDOT
3.00
2.00
1.00
0.0
-1.00
-2.00
-3.00
0
100
200
300
TIME (SECONDS)
EQ 1
EQ 4
EQ 5
EQ 3
EQ 2
EQ 6
PASS 1

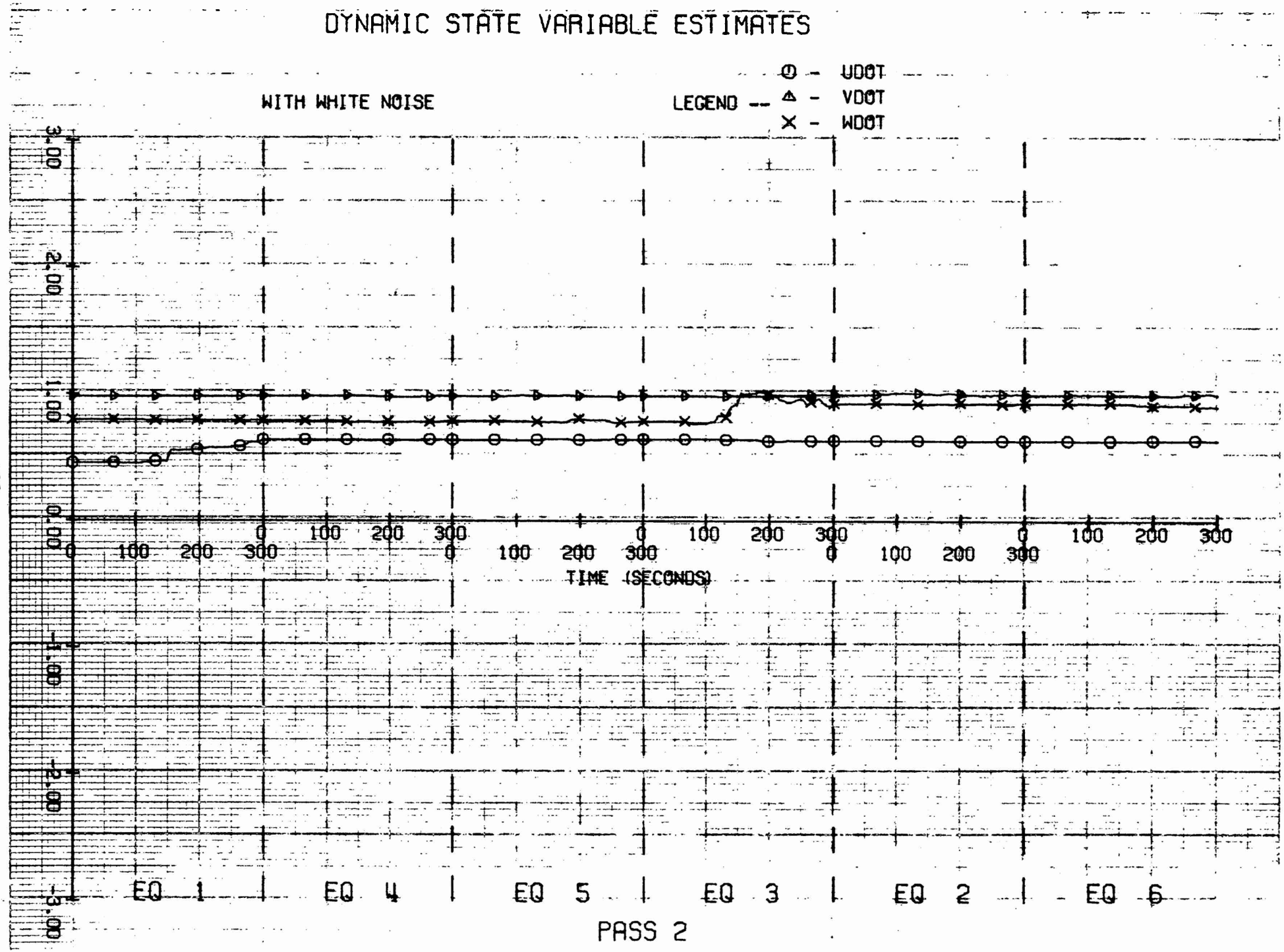
DYNAMIC STATE VARIABLE ESTIMATES
WITH WHITE NOISE
LEGEND -- ○ - UDOT
△ - VDOT
× - WDOT
3.00
2.00
1.00
0.00
-1.00
-2.00
-3.00
0 100 200 300 0 100 200 300 0 100 200 300 0 100 200 300
TIME (SECONDS)
EQ 1
EQ 4
EQ 5
EQ 3
EQ 2
EQ 6
PASS 2

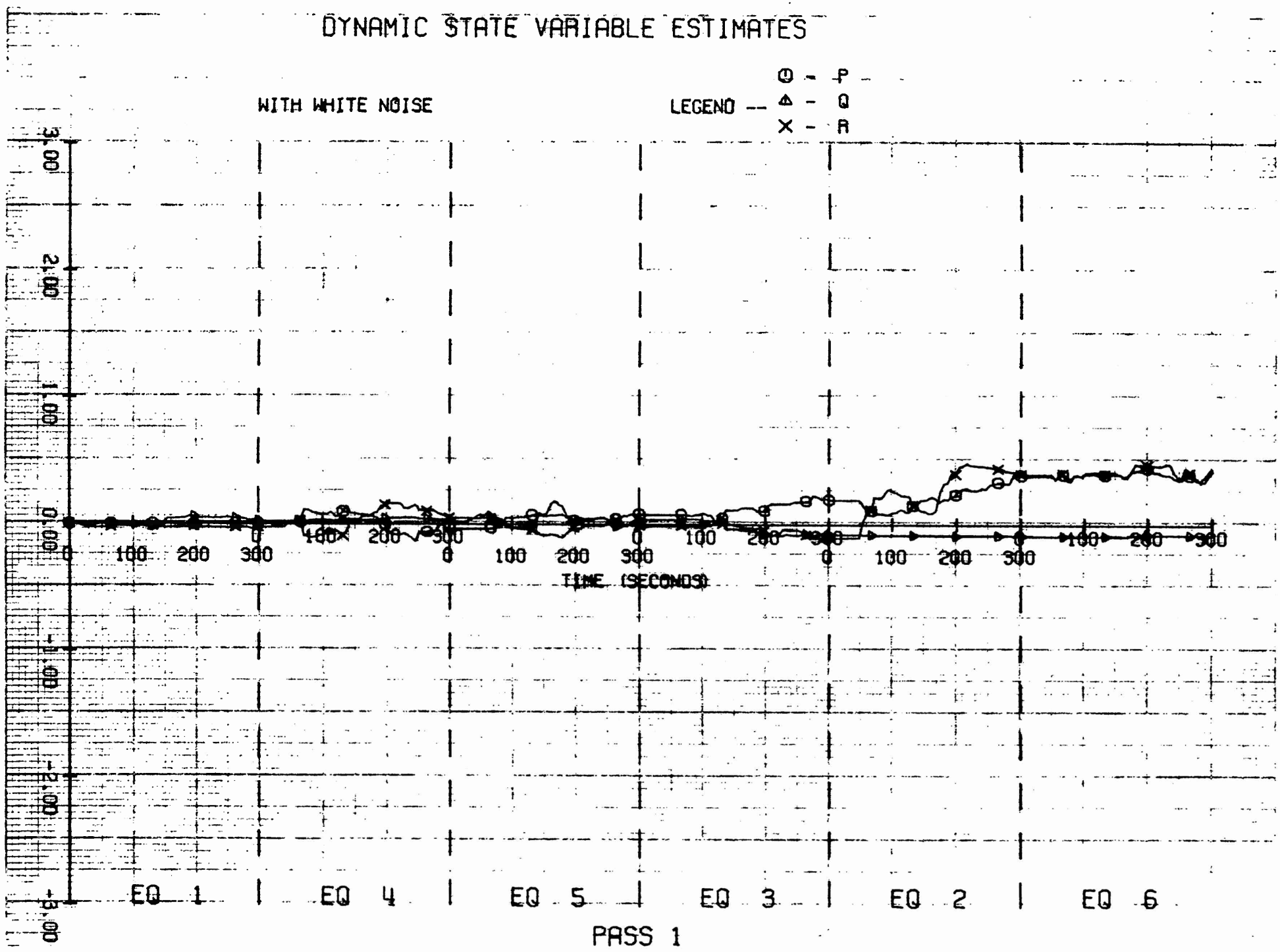
DYNAMIC STATE VARIABLE ESTIMATES
WITH WHITE NOISE
LEGEND -- ⊙ - P
△ - Q
× - R
3.00
2.00
1.00
0.00
-1.00
-2.00
-3.00
0
100
200
300
TIME (SECONDS)
EQ 1
EQ 4
EQ 5
EQ 3
EQ 2
EQ 6
PASS 1

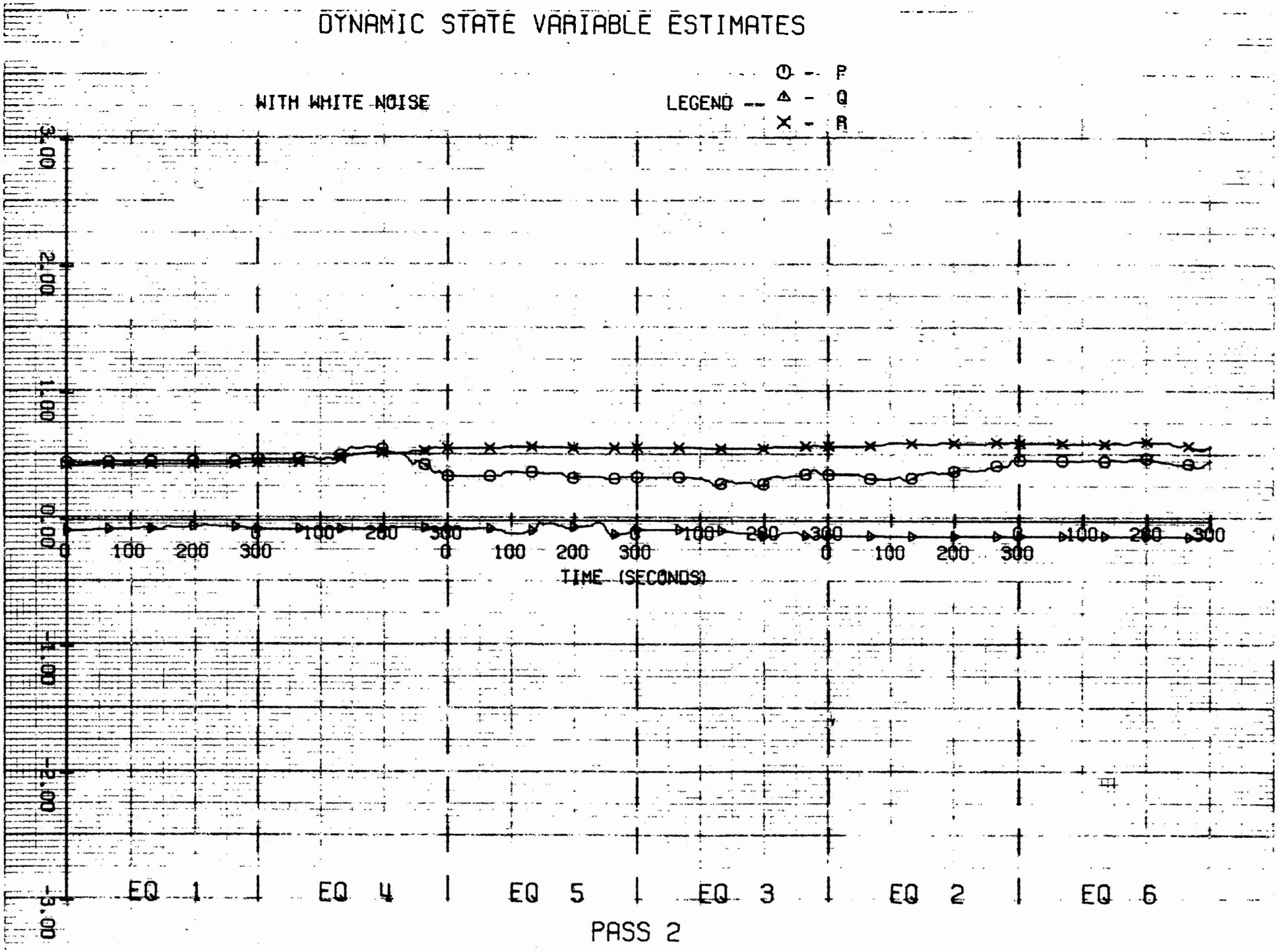
DYNAMIC STATE VARIABLE ESTIMATES
WITH WHITE NOISE
LEGEND -- ⊙ - P
△ - Q
× - R
3.00
2.00
1.00
0.00
-1.00
-2.00
-3.00
0
100
200
300
TIME (SECONDS)
EQ 1
EQ 4
EQ 5
EQ 3
EQ 2
EQ 6
PASS 2

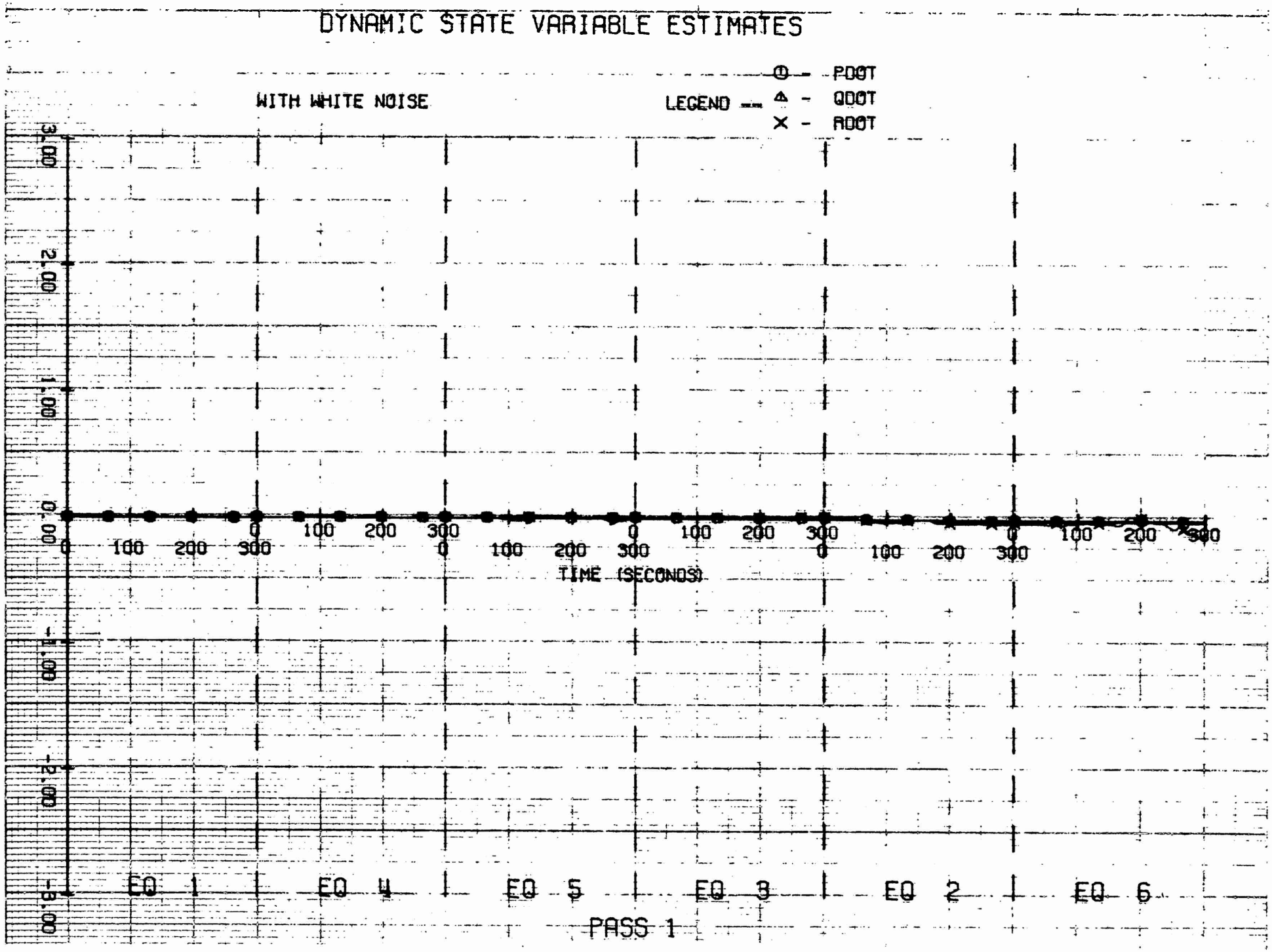
DYNAMIC STATE VARIABLE ESTIMATES
WITH WHITE NOISE
LEGEND
PDOT
QDOT
RDOT
3.00
2.00
1.00
0.00
-1.00
-2.00
-3.00
0
100
200
300
TIME (SECONDS)
EQ 1
EQ 4
EQ 5
EQ 3
EQ 2
EQ 6
PASS 1

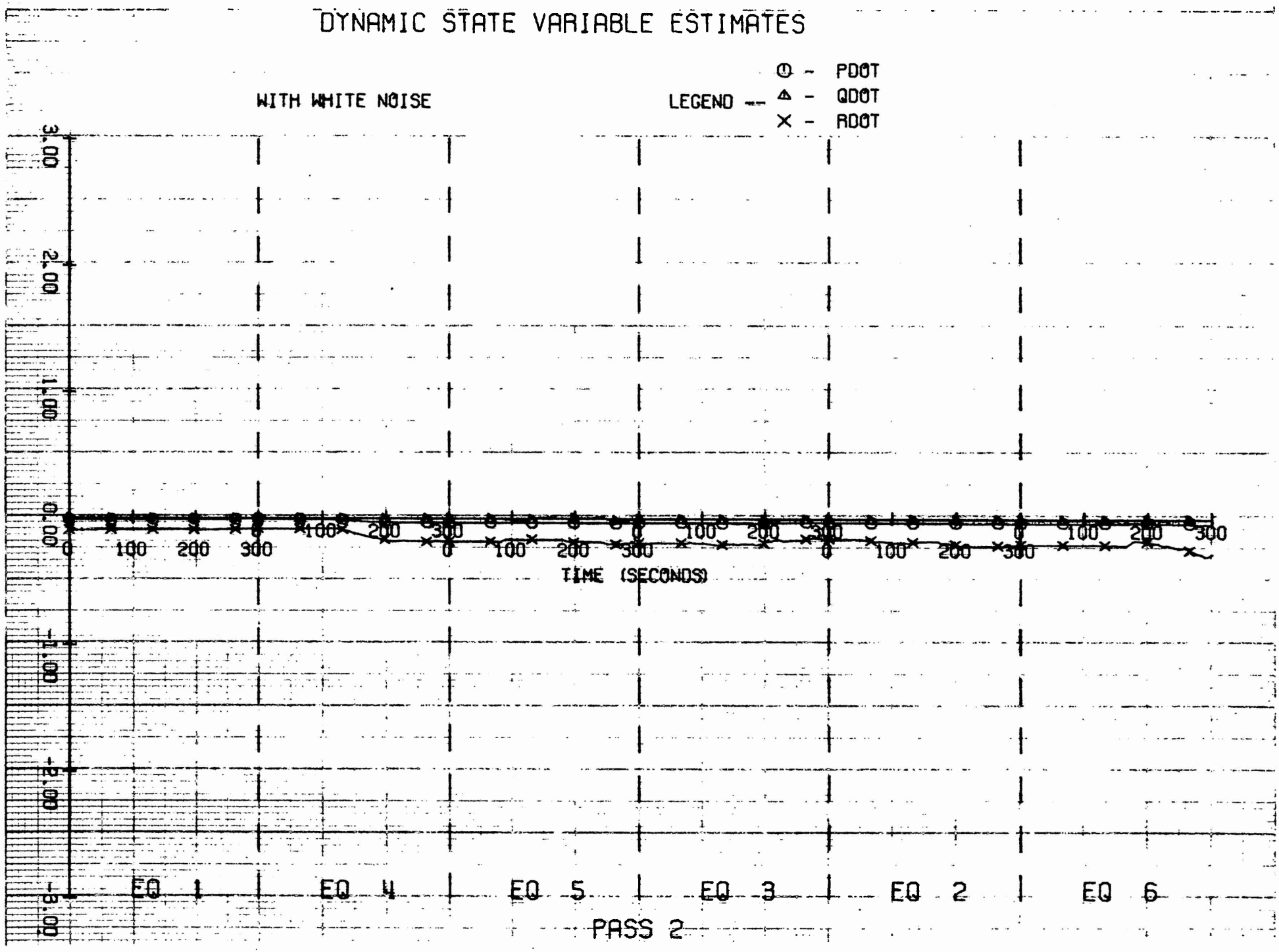
DYNAMIC STATE VARIABLE ESTIMATES
WITH WHITE NOISE
LEGEND
PDOT
QDOT
RDOT
3.00
2.00
1.00
0.00
-1.00
-2.00
-3.00
0
100
200
300
TIME (SECONDS)
EQ 1
EQ 4
EQ 5
EQ 3
EQ 2
EQ 6
PASS 2

XIII. REFERENCES

1. Gertler, M., and Hagen, G.R., "Standard Equations of Motion for Submarine Simulation," NSRDC Report No. 2510, 1967.

2. Kalman, R.E., "A New Approach to Linear Filtering and Prediction Problems," Trans. ASME, Series D, *Journal of Basic Engineering,* Vol. 82, 1960, pp. 35-45.

3. Voigt, S.J., McCain, J.H., "A Computer Program for Simulating Submarine Motion with Six Degrees of Motion," Applied Mathematics Lab., AML-12-68.

4. Young, P.C., "Identification Problems Associated with the Equation Error Approach to Process Parameter Estimation," Proc., Asilomar Conference of Circuits and Systems, Oct. 1968.

5. Mehra, R.K., "Maximum Likelihood Identification of Aircraft Parameter," *JACC,* 1970.

6. Denery, D.G., "Identification of a Nonlinear System Using A Combined Algorithm," *JACC,* 1970.

APPENDIX A
DISCUSSION OF THE COMPUTATIONAL METHOD

Before proceeding it is necessary to point out that the symbols used in this section are for the purpose of discussion, and are not to be confused with the use of similar symbols in the body of the report.

The general algorithm presented in Section VI is difficult to explain in terms of a simple system – since it was specifically developed to handle complex systems that are structured with a large number of variables (exceeding 100). However, a conceptual basis that will facilitate understanding of the general algorithm can be obtained via a simple example.

Let z be a scalar variable whose time derivative is governed by the following equation,

$$\dot{z} = g_1 (z, u_c) + c_1 g_2 (z, u_c) + c_2 g_3 (z, u_c)$$

where u_c is a control variable and c_1, c_2 are unknown coefficients; $g_i (z, u_c)$, i = 1, 2, 3 denotes a general function that is dependent upon z and u_c. It is assumed that z and $\dot{z}$ are directly instrumented or constructed from measurements that are a function of them. It is necessary to recognize that z and $\dot{z}$ are not perfectly known.

In the following the central idea is that the error characteristics of the estimates for z and $\dot{z}$ be specified. Let $\hat{z}$, $\hat{\dot{z}}$ denote the estimated values of z and $\dot{z}$; then the errors in z and $\dot{z}$ are denoted by

$$\tilde{z} = \hat{z} - z$$
$$\tilde{\dot{z}} = \hat{\dot{z}} - \dot{z};$$

the nature of $\tilde{z}$ and $\tilde{\dot{z}}$ is usually given in terms of their time derivatives. To avoid confusion, let $x_1 = \tilde{z}$ and $x_2 = \tilde{\dot{z}}$. If the trivial case where x_1 and x_2 are constant is assumed, then

$$\dot{x}_1 = 0$$
$$\dot{x}_2 = 0.$$

Note that in this situation $\dot{\tilde{z}} \neq \tilde{\dot{z}}$ if for example z and $\dot{z}$ are measured separately by different instruments. These considerations also apply to the parameters c_1 and c_2. From an a priori understanding of the physical situation represented by the differential equation for $\dot{z}$, the nature of the uncertainty in c_1 and c_2 can also be ascertained.

If a priori values for c_1 and c_2 can not be guessed, the choice of zero becomes appropriate. As above, the estimated values for c_1 and c_2 are denoted by $\hat{c}_1$ and $\hat{c}_2$. If it is known that c_1 and c_2 are constant, then the errors in the estimates are characterized as follows:

$$\dot{\tilde{c}}_1 = 0,$$
$$\dot{\tilde{c}}_2 = 0.$$

Let $\tilde{c}_1 = x_3$ and $\tilde{c}_2 = x_4$, then the error dynamics for x_i, i = 1, 2, 3, 4 can be summarized in vector form

$$\dot{x} = \begin{pmatrix} \dot{x}_1 \\ \dot{x}_2 \\ \dot{x}_3 \\ \dot{x}_4 \end{pmatrix} = 0.$$

In the following x will be referred to as the state vector. A more general linear stochastic model for $\dot{x}$ may of course be possible,

$$\dot{x} = Fx + u_w$$

where F is a matrix and u_w is a white noise vector. This is the familiar form for error dynamics in which Kalman filtering is applied. For the example above F and u_w are a zero matrix, and zero vector respectively.

Let the differential equation for $\dot{z}$ be written in terms of the estimated quantities,

$$\hat{\dot{z}} = g_1(\hat{z}, \hat{u}_c) + \hat{c}_1 g_2(\hat{z}, \hat{u}_c) + \hat{c}_2 g_3(\hat{z}, \hat{u}_c).$$

Note that $\hat{}$ appears over u_c since it also is an imperfectly measured quantity. For the following it will be assumed that $\hat{u}_c$ will have only a white noise component of error. It is readily recognized that if the estimated quantities are not perfect then the equation above will not be satisfied. An error signal can now be defined,

$$\tilde{y} = \hat{\dot{z}} - g_1 - \hat{c}_1 g_2 - \hat{c}_2 g_3.$$

For ease of presentation the following definition has been introduced

$$g_i = g_i(\hat{z}, \hat{u}_c).$$

This equation represents exactly how the actual error signal would be computed. The problem now is to express $\tilde{y}$ in terms of the basic error vector x. A linear approximation is of course desired so that the Kalman filter algorithm can be employed to computed gains that multiply $\tilde{y}$ and obtain a correction for the estimated state vector x. Since $\hat{z} = z + \tilde{z}$, $\tilde{y}$ can be expanded about the true variables,

$$\tilde{y} = \dot{z} - g_1(z, u_c) - c_1 g_2(z, u_c) - c_2 g_3(z, u_c)$$
$$+ \dot{\tilde{z}} - \frac{\partial g_1}{\partial z}\tilde{z} - \frac{\partial g_1}{\partial u_c}\tilde{u}_c - \tilde{c}_1 g_2 - c_1 \frac{\partial g_2}{\partial z}\tilde{z} - c_1 \frac{\partial g_2}{\partial u_c}\tilde{u}_c$$
$$- \tilde{c}_2 g_3 - c_2 \frac{\partial g_3}{\partial z}\tilde{z} - c_2 \frac{\partial g_3}{\partial u_c}\tilde{u}_c + \text{higher order terms.}$$

By hypothesis the first four terms above add up to zero; after collecting terms $\tilde{y}$ can be put into the following form,

$$\tilde{y} = Mx + v + \text{higher order terms}$$

where M is a single row matrix whose elements are given by

$$m_1 = -\frac{\partial g_1}{\partial z} - c_1 \frac{\partial g_2}{\partial z} - c_2 \frac{\partial g_3}{\partial z}$$

$$m_2 = 1$$

$$m_3 = -g_2$$

$$m_4 = -g_3$$

$$v = -\left[\frac{\partial g_1}{\partial u_c} - c_1 \frac{\partial g_2}{\partial u_c} - c_2 \frac{\partial g_3}{\partial u_c}\right] \tilde{u}_o .$$

Since the evaluation of g_i and the associated partial derivatives can only be done with estimated quantities an additional, higher order, error is introduced into the linear expansion for $\tilde{y}$. Use of the Kalman filter algorithm implicitly ignores these higher order terms. However, the effect of these terms can be accounted for by computing the Kalman gains with a larger level of measurement noise.

Since the partial derivatives and M elements (m_i) are functions of the states which are to be estimated, multiple computation of the linearized Kalman filter will be required. The phrase "computation of the Kalman filter" implies the computation of the error covariance matrix, optimal gains and estimation of the states for the time interval that data are available. Throughout the remainder of this report this computational sequence will be designated as a sweep or loop. Typically $\hat{c}_1$ and $\hat{c}_2$ would be initialized at zero, so that the first time the filter is iterated (looped) m_i and the computation of the noise variance, $E\{v^2\}$, would be incorrect. It is stipulated that a loop will be made with one set of values for the c_i's. This is an important feature of the algorithm; generally it seems natural that as soon as improved estimates of c_i are obtained the more accurate computation of m_i should be made. This notion is incorrect because if different values of c_i are used in the computation of m_i, for any sweep, a high degree of false observability is inserted into M and correspondingly into the error covariance matrix. The covariance matrix becomes unreliable and divergence is likely to occur. The solution taken here is to loop the Kalman filter with different levels of measurement noise – starting at some high level and decreasing it, possibly in some linear or quadratic manner. The $\hat{c}_i$ are of course held constant for the sweep. The corrections for $\hat{c}_i$ obtained from the loop are stored into a separate array and used to update the $\hat{c}_i$ array at the completion of the current sweep.

This technique can be readily extended to the multidimensional-nonlinear parameter estimation problem. The procedure is the same as that followed here; only in this case M will be a matrix with the number of rows equal to the number of differential equations for the dynamical system.

The method presented here is similar to the traditional extended Kalman filter applications to estimation of nonlinear systems, in the sense that the error covariance of the dynamic variables (as distinguished from system parameters) is part of the identification procedure. The notion

introduced here is that the nature and accuracy of the actual measurements made on the system uniquely establish the error covariance matrix for the dynamic variables. Thus, a velocity meter and accelerometer, for all practical purposes, alone establish the accuracy (biases and covariance) of velocity and acceleration, and little or nothing is gained by incorporating the linearized differential equation for the error behavior of the nonlinear system, as is done in standard extended Kalman filtering. It is essentially hypothesized that introduction of the equations of motion as measurements on the error space will be adequate to obtain a stable unbiased estimation algorithm.

There might be a tendency to call this method "Extended Recursive Least Squares Estimation"; it is felt that the term "Least Squares" is misleading since traditionally a direct matrix inversion (nonsingular) is associated with these "Least Squares" methods. The Kalman filter is an orthogonal projection of the measurements into the state (error-parameter) space which, taking all error characteristics into account, yields unbiased estimates, and a reliable covariance matrix which indicates what parameters are poorly estimated and to what extent they are independent. It should also be mentioned that if an algorithm is unbiased, it minimizes a large number of error criteria (of which least-square is only one).

It is well known that the traditional "Least Squares Method", which ignores white noise and bias errors, gives poor results (4, 5, 6). The work of Kalman (2) has elevated the level of thought towards stochastic filtering, and it is not appropriate to refer to any applications of his ideas in terms of ad hoc principles such as least square or maximum likelihood.

BELL AEROSPACE
REPORT NO. 9500-920237

DISTRIBUTION LIST FOR REPORTS PREPARED UNDER THE GENERAL HYDROMECHANICS RESEARCH PROGRAM

40 Commander
Naval Ship Research and
Development Center
Bethesda, Maryland 20034
Attn: Code 1505
Code 5614

1 Officer-in-Charge
Annapolis Laboratory
Naval Ship Research and
Development Center
Annapolis, Maryland 21402
Attn: Code 5642(Library)

5 Commander
Naval Ship Systems Command
Washington, D. C. 20360
Attn: SHIPS 2052
SHIPS 03412B
SHIPS 0372

12 Director
Defense Documentation Center
5010 Duke Street
Alexandria, Virginia 22314

1 Office of Naval Research
800 N. Quincy Street
Arlington, Virginia 22217
Attn: Mr. R. D. Cooper (Code 438)

1 Office of Naval Research
Branch Office
492 Summer Street
Boston, Mass 02210

1 Office of Naval Research
Branch Office (493)
536 S. Clark Street
Chicago, Illinois 60605

1 Chief Scientist
Office of Naval Research
Branch Office
1030 E. Green Street
Pasadena, CA 91106

1 Office of Naval Research
Resident Representative
207 West 24th Street
New York, New York 10011

1 Office of Naval Research
Resident Representative
50 Fell Street
San Francisco, CA 94102

2 Director
Naval Research Laboratory
Washington, D. C. 20390
Attn: Code 2027
Code 2629(ONRL)

1 Commander
Naval Facilities Engineering
Command(Code 032C)
Washington, D. C. 20390

1 Library of Congress
Science & Technology Division
Washington, D. C. 20540

1 Commander
Naval Ordnance Systems
Command (ORD 035)
Washington, D. C. 20360

1 Commander
Naval Electronics Laboratory
Center (Library)
San Diego, CA 92152

8 Commander
Naval Ship Engineering Center
Center Building
Prince Georges Center
Hyattsville, Maryland 20782
Attn: SEC 6034B
SEC 6110
SEC 6114H
SEC 6120
SEC 6136
SEC 6144G
SEC 6140B
SEC 6148

1 Naval Ship Engineering Center
Norfolk Division
Small Craft Engr Dept
Norfolk, Virginia 23511
Attn: D. Blount (6660.03)

1 Library (Code 1640)
Naval Oceanographic Office
Washington, D. C. 20390

1 Technical Library
Naval Proving Ground
Dehlgren, Virginia 22448

1 Commander (ADL)
Naval Air Development Center
Warminster, Penna 18974

1 Naval Underwater Weapons Research
& Engineering Station (Library)
Newport, R.I. 02840

1 Commanding Officer (L31)
Naval Civil Engineering Laboratory
Port Hueneme, CA 93043

1 Commander
Naval Undersea Research
and Development Center
San Diego, CA 92132
Attn: Dr. A. Fabula (6005)

2 Officer-in-Charge
Naval Undersea Research
and Development Center
Pasadena, CA 91107
Attn: Dr. J. Hoyt (2501)
Library (13111)

1 Director
Naval Research Laboratory
Underwater Sound Reference Division
P.O. Box 8337
Orlando, Florida 32806

1 Library
Naval Underwater Systems Center
Newport, R. I. 02840

1 Research Center Library
Waterways Experiment Station
Corp of Engineers
P.O. Box 631
Vicksburg, Mississippi 39180

2 National Bureau of Standards
Washington, D. C. 20234
Attn: P. Klebanoff (FM 105)
Fluid Mechanics
Hydraulic Section

1 AFOSR/NAM
1400 Wilson Blvd
Arlington, Virginia 22209

1 AFFOL/FYS (J. Olsen)
Wright Patterson AFB
Dayton, Ohio 45433

1 Dept. of Transportation
Library TAD-491.1
400 - 7th Street S.W.
Washington, D. C. 20590

1 Boston Naval Shipyard
Planning Dept Bldg 39
Technical Library, Code 202.2
Boston, Mass 02129

1 Charleston Naval Shipyard
Technical Library
Naval Base
Charleston, S. C. 29408

1 Norfolk Naval Shipyard
Technical Library
Portsmouth, Virginia 23709

1 Philadelphia Naval Shipyard
Philadelphia, Penna 19112
Attn: Code 240

1 Portsmouth Naval Shipyard
Technical Library
Portsmouth, N. H. 03801

1 Puget Sound Naval Shipyard
Engineering Library
Bremerton, Wash 98314

1 Long Beach Naval Shipyard
Technical Library (246L)
Long Beach, CA 90801

1 Hunters Point Naval Shipyard
Technical Library (Code 202.3)
San Francisco, CA 94135

1 Pearl Harbor Naval Shipyard
Code 202.32
Box 400, FPO
San Francisco, CA 96610

1 Mare Island Naval Shipyard
Shipyard Technical Library
Code 202.3
Vallejo, CA 94592

1 Assistant Chief Design Engineer
for Naval Architecture (Code 250)
Mare Island Naval Shipyard
Vallejo, CA 94592

3 U. S. Naval Academy
Annapolis, Maryland 21402
Attn: Technical Library
Dr. Bruce Johnson
Prof. P. Van Mater, Jr.

3 Naval Postgraduate School
Monterey, CA 93940
Attn: Library, Code 2124
Dr. T. Sarpkaya
Prof. J. Miller

1 Capt. L. S. McCready, USMS
Director, National Maritime
Research Center
U. S. Merchant Marine Academy
Kings Point, L.I., N.Y. 11204

1 U. S. Merchant Marine Academy
Kings Point, L.I., N.Y. 11204
Attn: Academy Library

1 Library
The Pennsylvania State University
Ordnance Research Laboratory
P. O. Box 30
State College, Penna 16801

1 Bolt, Beranek & Newman
1501 Wilson Blvd
Arlington, Virginia 22209
Attn: Dr. F. Jackson

1 Bolt, Beranek & Newman
50 Moulton Street
Cambridge, Mass 02138
Attn: Library

1 Bethlehem Steel Corporation
Center Technical Division
Sparrows Point Yard
Sparrows Point, Maryland 21219

1 Bethlehem Steel Corporation
25 Broadway
New York, New York 10004
Attn: Library (Shipbuilding)

1 Cambridge Acoustical Associates, Inc.
1033 Mass Avenue
Cambridge, Mass 02138
Attn: Dr. M. Junger

1 Cornell Aeronautical Laboratory
Aerodynamic Research Dept.
P.O. Box 235
Buffalo, N.Y. 14221
Attn: Dr. A. Ritter

1 Eastern Research Group
P.O. Box 222
Church Street Station
New York, New York 10008

1 Esso International
Design Division, Tanker Dept.
15 West 51st Street
New York, New York 10019

1 Mr. V. Boatwright, Jr.
R & D Manager
Electric Boat Division
General Dynamics Corporation
Groton, Conn 06340

1 Gibbs & Cox, Inc.
21 West Street
New York, New York 10006
Attn: Technical Info. Control

2 Hydronautics, Inc.
Pindell School Road
Howard County
Laurel, Maryland 20810
Attn: Library
Mr. M. Gertler

2 McDonnell Douglas Aircraft Co.
3855 Lakewood Blvd
Long Beach, CA 90801
Attn: J. Hess
A.M.O. Smith

1 Lockheed Missiles & Space Co.
P.O. Box 504
Sunnyvale, CA 94088
Attn: Mr. R. L. Waid, Dept 57-74
Bldg. 150, Facility 1

1 Newport News Shipbuilding &
Dry Dock Company
4101 Washington Avenue
Newport News, Virginia 23607
Attn: Technical Library Dept.

1 North American Aviation, Inc.
Space & Information Systems Div.
12214 Lakewood Blvd
Downey, CA 90241
Attn: Mr. Ben Ujihara (SL-20)

1 Nielsen Engineering & Research, Inc.
850 Maude Avenue
Mountain View, CA 94040
Attn: Mr. S. B. Spangler

1 Oceanics, Inc.
Technical Industrial Park
Plainview, L.I., N.Y. 11803

1 Society of Naval Architects
and Marine Engineers
74 Trinity Place
New York, New York 10006
Attn: Technical Library

1 Sun Shipbuilding & Dry Dock Co.
Chester, Penna 19000
Attn: Chief Naval Architect

1 Sperry Systems Management Division
Sperry Rand Corporation
Great Neck, N. Y. 11020
Attn: Technical Library

1 Stanford Research Institute
Menlo Park, CA 94025
Attn: Library G-021

2 Southwest Research Institute
P. O. Drawer 28510
San Antonio, Texas 78284
Attn: Applied Mechanics Review
Dr. H. Abramson

1 Tracor, Inc.
6500 Tracor Lane
Austin, Texas 78721

1 Mr. Robert Taggart
3930 Walnut Street
Fairfax, Virginia 22030

1 Ocean Engr Department
Woods Hole Oceanographic Inst.
Woods Hole, Mass 02543

1 Worcester Polytechnic Inst.
Alden Research Laboratories
Worcester, Mass 01609
Attn: Technical Library

1 Applied Physics Laboratory
University of Washington
1013 N. E. 40th Street
Seattle, Washington 98105
Attn: Technical Library

1 University of Bridgeport
Bridgeport, Conn 06602
Attn: Dr. E. Uram

1 Cornell University
Graduate School of Aerospace Engr
Ithaca, New York 14850
Attn: Prof. W. R. Sears

4 University of California
Naval Architecture Department
College of Engineering
Berkeley, CA 94720
Attn: Library
Prof. W. Webster
Prof. J. Paulling
Prof. J. Wehausen

3 California Institute of Technology
Pasadena, CA 91109
Attn: Aeronautics Library
Dr. T. Y. Wu
Dr. A. J. Acosta

1 Docs/Repts/Trans Section
Scripps Institution of
Oceanography Library
University of California, San Diego
P.O. Box 2367
La Jolla, CA 92037

1 Catholic University of America
Washington, D. C. 20017
Attn: Dr. S. Heller, Dept of
Civil & Mech Engr

1 Colorado State University
Foothills Campus
Fort Collins, Colorado 80521
Attn: Reading Room, Engr Res Center

1 University of California at San Diego
La Jolla, CA 92038
Attn: Dr. A. T. Ellis
Dept of Applied Math

1 Florida Atlantic University
Ocean Engineering Department
Boca Raton, Fla 33432
Attn: Technical Library

2 Harvard University
Pierce Hall
Cambridge, Mass 02138
Attn: Prof. G. Carrier
Gordon McKay Library

1 University of Hawaii
Department of Ocean Engineering
2565 The Mall
Honolulu, Hawaii 96822
Attn: Dr. C. Bretschneider

1 University of Illinois
Urbana, Illinois 61801
Attn: Dr. J. Robertson

3 Institute of Hydraulic Research
The University of Iowa
Iowa City, Iowa 52240
Attn: Library
Dr. L. Landweber
Dr. J. Kennedy

1 The John Hopkins University
Baltimore, Md 21218
Attn: Prof. O. Phillips
Mechanics Dept

1 Kansas State University
Engineering Experiment Station
Seaton Hall
Manhattan, Kansas 66502
Attn: Prof. D. Nesmith

1 University of Kansas
Chm Civil Engr Dept Library
Lawrence, Kansas 60644

1 Fritz Engr Laboratory Library
Depart of Civil Engr
Lehigh University
Bethlehem, Penna 18015

5 Department of Ocean Engineering
Massachusetts Institute of Technology
Cambridge, Mass 02139
Attn: Department Library
Prof. P. Leehey
Prof. P. Mandel
Prof. M. Abkowitz
Dr. J. Newman

1 Parsons Laboratory
Massachusetts Institute of Technology
Cambridge, Mass 02139
Attn: Prof. A. Ippen

5 St. Anthony Falls Hydraulic Laboratory
University of Minnesota
Mississippi River at 3rd Avenue S.E.
Minneapolis, Minnesota 55414
Attn: Director
Mr. J. Wetzel
Mr. F. Schiebe
Mr. J. Killen
Dr. C. Song

3 Department of Naval Architecture
and Marine Engineering
University of Michigan
Ann Arbor, Michigan 48104
Attn: Library
Dr. T. F. Ogilvie
Prof. F. Hammitt

2 College of Engineering
University of Notre Dame
Notre Dame, Indiana 46556
Attn: Engineering Library
Dr. A. Strandhagen

2 New York University
Courant Inst. of Math. Sciences
251 Mercier Street
New York, New York 10012
Attn: Prof. A. Peters
Prof. J. Stoker

New York University
University Heights
Bronx, New York 10453
Attn: Prof. W. Pierson, Jr.

Department of Aerospace &
Mechanical Sciences
Princeton University
Princeton, N.J. 08540
Attn: Prof. G. Mellor

3 Davidson Laboratory
Stevens Institute of Technology
711 Hudson Street
Hoboken, New Jersey 07030
Attn: Library
Mr. J. Breslin
Mr. S. Tsakonas

1 Department of Mathematics
St. John's University
Jamaica, New York 11432
Attn: Prof. J. Lurye

1 Applied Research Laboratory Library
University of Texas
P.O. Box 8029
Austin, Texas 78712

College of Engineering
Utah State University
Logan, Utah 84321
Attn: Dr. R. Jeppson

2 Stanford University
Stanford, CA 94305
Attn: Engineering Library
Dr. R. Street

3 Webb Institute of Naval Architecture
Crescent Beach Road
Glen Cover, L.I., N.Y. 11542
Attn: Library
Prof. E. V. Lewis
Prof. L. W. Ward

1 National Science Foundation
Engineering Division Library
1800 G Street N. W.
Washington, D. C. 20550

1 University of Connecticut
Box U-37
Storrs, Conn 06268
Attn: Dr. V. Scottron
Hydraulic Research Lab

1 Long Island University
Graduate Department of
Marine Science
40 Merrick Avenue
East Meadow, L.I., N.Y. 11554
Attn: Prof. David Price